NASr-21(07)

UNPUBLISHED PRELIMINARY DATA

MEMORANDUM
RM-3412-NASA
DECEMBER 1964

AUTOMATIC PATTERN RECOGNITION OF METEOROLOGICAL SATELLITE CLOUD PHOTOGRAPHY

Y. H. Katz and W. L. Doyle

GPO PRICE $ _____

OTS PRICE(S) $ _____

Hard copy (HC) _____

Microfiche (MF) _____

FACILITY FORM 602

N65 15379
(ACCESSION NUMBER)

(THRU)

95
(PAGES)

1
(CODE)

CR 60318
(NASA CR OR TMX OR AD NUMBER)

30
(CATEGORY)

PREPARED FOR:

NATIONAL AERONAUTICS AND SPACE ADMINISTRATION

The RAND Corporation
SANTA MONICA • CALIFORNIA

MEMORANDUM
RM-3412-NASA
DECEMBER 1964

AUTOMATIC PATTERN RECOGNITION OF METEOROLOGICAL SATELLITE CLOUD PHOTOGRAPHY

Y. H. Katz and W. L. Doyle

This research is sponsored by the National Aeronautics and Space Administration under Contract No. NASr-21. This report does not necessarily represent the views of the National Aeronautics and Space Administration.

The RAND Corporation
1700 MAIN ST. • SANTA MONICA • CALIFORNIA • 90406

PREFACE

The RAND Corporation is currently engaged in a program of research on satellite meteorology under NASA Contract NASr-21(07). As part of the program studying the scientific utilization of meteorological satellite data and the implications of new techniques and measurements to meteorological satellite development, RAND is examining the information content of satellite-derived cloud photography. This Memorandum describes research performed in automatic pattern recognition of such photography. It constitutes a first step in what is hoped will be a continuation and enlargement of this effort by others with more direct and immediate interests, and with larger capabilities for carrying on investigations of this nature.

While much of the meteorological significance and meaning of specific cloud patterns seen in satellite photography remains to be discovered, it is the consensus of many investigators that these patterns are related to various synoptic-scale weather features, and as such may become increasingly useful as diagnostic tools to supplement conventional weather analysis methods.

SUMMARY

15379

The quantitative characteristics of cloud patterns were studied by determining common attributes of several pattern classes. Some mechanical procedures for automatically recognizing and classifying specific cloud patterns from satellite photography are described and several data reduction transformations that have detected and isolated certain characteristics in which cloud "streets" differ from randomly placed cloud elements are detailed. An approach to the problem of automatically determining global cloud cover from satellite photography is also discussed.

Author

ACKNOWLEDGMENT

Various portions of this research were discussed with Irving S. Reed. For his time spent in our behalf, as well as for the many valuable comments and suggestions that evolved from these discussions, we wish to express our appreciation.

CONTENTS

PREFACE iii

SUMMARY v

ACKNOWLEDGMENT vii

Section

I. INTRODUCTION 1

II. CLOUD PATTERN SAMPLES AND GENERATION OF DIGITAL DATA . . 4

III. GENERAL OUTLINE OF A HYPOTHETICAL PATTERN RECOGNITION SCHEME USING METEOROLOGICAL SATELLITE CLOUD PHOTOGRAPHY 5

IV. CLASS DESCRIPTION 7

V. DATA REDUCTION 8

VI. CONCLUDING REMARKS 79

APPENDIX 81

REFERENCES 89

I. INTRODUCTION

The launch of the first of the highly successful series of TIROS meteorological satellites on April 1, 1960, added a new dimension to the observations and data collection of meteorologists. Never before had they been able to sense and view manifestations of atmospheric processes on such a large, and yet detailed scale as that allowed by the pictorial returns of the earth's cloud cover.

Today, four and one-half years and eight satellites later, more than 300,000 television pictures have been transmitted to ground readout stations. In August, 1964, the Nimbus I experimental satellite was launched, and although operative for less than 4 weeks, it was able to transmit to earth some 27,000 pictures, or about 1,000 a day.

This is only the beginning, for there will be more satellites launched, and within a few years a truly operational meteorological satellite system will become a reality, unleashing a continuous flood of pictures. In addition, the prospect of having more than one satellite in operation at all times, each possessing greater sensory capabilities than are now available, makes it apparent that the acquisition of pictures (as well as other data) may well take place at a rate far exceeding our ability to handle, communicate, and analyze them. So it is that not only have new methods greatly advanced the rates and amounts of data that can be acquired, but at the same time accelerating advances in meteorological research are causing ever increasing demands to be made on the rate at which the accumulated data are converted into usable information.

Improvements in transmission systems arising from increases in the bandwidth of the communication link or from increasing the number of ground readout stations are more than likely to be only minor relief from an inherent weakness in the total system, and may fail to bring about a match among potential rates of data collection, transmission, and digestion by many orders of magnitude. A trained observer operating from a manned satellite would, by virtue of his ability to look over, select, and transmit information, as well as provide a commentary about events, greatly alleviate many of the data problems

just mentioned. However, unmanned vehicles will evidently continue to be available for meteorological purposes much earlier and in greater numbers than manned vehicles. The need for research aimed at providing a capability for alleviating the limitations or inherent constraints on the amount of useful data that a satellite can send to earth is thus clearly indicated.

The large quantity of pictures that results from meteorological satellite operations and the need for rapid analysis of the feature content of the pictures requires a high degree of automation in the interpretation of the photography. While attempts have been made to alleviate some of the data-processing problems (e.g., automatic picture rectification, mapping, and mosaicking), other aspects of data processing, such as the automatic analysis of the information content of the photography itself have received little attention.

Only a small portion of the information contained in the pictures (in fact, only a small fraction of the pictures so far accumulated) has been utilized. The sheer quantity of pictures requiring close "looks" is certainly reason enough for this state of affairs. But it is also true that the information content of the pictures has not been extracted in an objective and synoptically meaningful way to provide a better understanding of the properties of the image that make the field interesting for meteorological purposes.

Our concern at RAND has been with this latter problem, viz., the development of automatic techniques for assessing the information content in the field of view, with the ultimate objective of providing a system that can alleviate the heavy burden of acquiring, transmitting, identifying and interpreting data that are inherent in any meteorological satellite system. The assessment of an image requires the development of techniques for automatically and with little delay detecting and recognizing meteorologically significant cloud patterns. While much of the meteorological meaning and significance of specific cloud patterns remains to be "discovered," it is assumed that cloud patterns as seen from meteorological satellite photography derive from various synoptic-scale weather features, that they are useful as diagnostic tools to supplement conventional weather-analysis methods, and in fact, that these may also be useful as forecasting tools.

A basic problem in automating a cloud pattern is that of eliminating the "noise," or unimportant information, while saving the information that is pertinent. In meteorology, this problem is more complicated than elsewhere, because the pertinent parameters do not lend themselves to easy definition. Since the morphological classification of clouds is qualitative rather than quantitative, and since objective, quantitative information on cloud photography would be of value to meteorologists in their efforts to interpret picture contents, work was undertaken to extract various sets of measurements useful in the description of a given cloud pattern. (It is worth noting that the exact pattern of clouds seen on a given photograph had never occurred before that picture was taken, and will never occur again. However, patterns with the same statistical properties may very well occur whenever the gross synoptic pattern is the same. Thus small pattern features may provide information about conditions over larger areas.)

II. CLOUD PATTERN SAMPLES AND GENERATION OF DIGITAL DATA

Data reduction and testing of the recognition schemes to be described in later sections were made from cloud-pattern samples chosen from the narrow-angle photographs from TIROS I, which offered pictures having resolutions approximately one order of magnitude higher than did the wider-angle camera. Too, we were testing pattern fields that were essentially homogeneous to the eye (i.e., having but one pattern), so that even with the narrow-angle photography, only a portion of the picture was utilized. Several dozen samples of transparencies containing patterns of (1) seemingly randomly spaced and sized cloud cells, and (2) cloud bands or streets were selected (for identification purposes, we arbitrarily called the former CUMULUS CELLS or CUCL, and the latter STRATOCUMULUS STREETS STRAIGHT or SCSS). The only restrictions to sample selection were that the pictures contain no confusing background terrain, that the viewing angle be within approximately 20 degrees of the nadir angle (no distortion problem), and that they display a reasonable degree of contrast, or density range. Each transparency was reduced or enlarged to 0.75 by 0.75 inch, as necessary.

The pictures were then converted to digital data on tape for further processing using the IBM 7090 digital computer. The conversion process was accomplished by generating an electrical analog of the gray tones in the image. A cathode-ray tube used as a flying-spot light source (approximately 2.5 mils in diameter) was successively focused on the transparency and moved incrementally to cover the entire area. Light passing through the transparency impinged on a photomultiplier, generating a signal that was proportional to the transmissivity of the film. Analog to digital conversion reduced the signal brightness values to a 64-shades-of-gray scale. The values were then stored on tape in such an order as to allow each spot to be related to its original position on the image. Each picture input to the data reduction operations that follow is, therefore, a large set of real numbers, namely the image intensities at approximately 100,000 resolvable spots.

III. GENERAL OUTLINE OF A HYPOTHETICAL PATTERN RECOGNITION SCHEME USING METEOROLOGICAL SATELLITE CLOUD PHOTOGRAPHY

Let us imagine that there is a set of cloud-pattern pictures and a collection of sub-classes named in advance, distinguished in such a way that each picture belongs to exactly one class. Further, let us suppose that a consensus of meteorologists can classify any picture from this set correctly. The problem then, is to specify some mechanical procedure for realizing comparable automatic classification.

The mechanical process can be divided into two stages (always conceptually, and usually in practice as well); one process we call the data reduction stage, and the other process we call the decision stage. In the first stage, tests are made or features are extracted that we hope are significant. These reduced data or features are still expected to display the important distinctions between the classes.

In the second stage, the reduced data would become the arguments of a set of decision functions whose values are used to partition the sample space and provide our guess at an unknown's identity. When the data are statistical variables, for example, the decision functions may be likelihood functions for the classes, and the partitioning may be into regions where each likelihood function is a maximum. At the other extreme, the data may be purely qualitative, and the decision functions may be Boolean functions corresponding to a decision tree, as in Ref. (1).

In order to reach a practical solution to the pattern recognition problem, both stages will have to be dealt with, and ideally it might be best to consider them simultaneously, thereby deducing the optimum combination of data reduction and decision.

However, we believe that our most pressing and difficult task is to assemble an appropriate set of measurements or tests, that taken together, are adequate to classify samples with acceptable accuracy. This resembles the main problem confronting researchers

in voice and character recognition, for example. The decision problem itself is often far from trivial however, especially in practical applications where the measurements rarely fit a convenient model. Despite such inconveniences, decision rules can be formulated whose performance, if not optimal, is at least practically useful.

In this report, therefore, we consider only the processes of the data-reduction stage. The contributions presented here are germane to two problem areas in satellite meteorology: the pattern recognition problem associated with attempts to reduce the bulk of data and eliminate redundancy, and the problem of quantitatively describing and characterizing the image in order to aid in the analysis and interpretation of satellite photography.

IV. CLASS DESCRIPTION

A class can be described (at least to a great extent) by a mixture of the following two extreme kinds of information.

On one hand, there may be a list of features guaranteed to separate the classes logically and a set of rules for distinguishing the classes once each feature has been tested for. At a slight remove, the features may be present in some degree, rather than present or not, but again a reasonably direct and reliable classification can be made from a complete set of features.

On the other hand, one can imagine the classes being specified directly in terms of a list (finite or infinite) of all those members (e.g., the names of cloud types) belonging to each one, as in the case of social clubs or political parties. These are connotive--denotive descriptions.

In either of these cases, where the classes are completely specified, the problems of interest in developing the pattern-recognition system become combinatorial choices of speed, convenience, and the error rate of different data-reduction and decision methods, particularly when some of the available information has been relinquished in return for greater speed or ease of mechanization.

Sometimes, and this holds for our problem, one has no complete description in either sense, but only partial information. We have rough theoretical (connotive) contributions to descriptions of our classes and a small number of samples, too few to contribute much to the denotive description. Furthermore, our samples are typical only in the way in which museum specimens of minerals are typical: they embody what are thought to be the important characteristics of the classes in very striking form. One should not be too disappointed if mine-run samples are not as easy to classify accurately.

Although descriptions for our CUCL and SCSS pattern classes remain qualitative, they have been consistently classified by meteorologists at RAND; they do contain clues to features that an automatic system should be designed to extract. The problem is to suggest and investigate mechanical procedures for comparable, automatic classification.

V. DATA REDUCTION

If the machines had unlimited capacity for storing descriptions of the classes to be distinguished, or if unlimited time were available, the data-reduction phase would be unnecessary, and clean, noise-free pictures could be fed directly to the decision mechanism. In our case, however, the number of input pictures is sufficiently large to demand some preliminary data reduction or feature extraction. That is, the very high dimensional sample space is mapped onto a few low dimensional feature spaces with as little information loss as practical. As this language suggests, these reduced data or features are expected to continue to embody the distinctions among the classes. One of the major tasks is that of choosing such operations as will preserve these distinctions while at the same time mapping the images onto a restricted set of outputs in order to minimize any work that may be done later in the decision phase.

The kinds of mapping comprising the data-reduction phase are suggested by qualitative descriptions of the CUCL and SCSS classes, by intuitive notions we get upon looking at the samples, and finally, by some general principles from the theory of detecting random signals. In order to be practically useful, the mappings are usable by analog apparatus, as well as amenable to simple digital simulation. Roughly speaking, this means that the operations treat the elements of the picture en masse in ways that are independent of the local structure of the image. While certain characteristics could be discovered by tracing each cloud in detail and gathering relevant statistics, we rule out such procedures as likely to engender excessively complicated apparatus and consumption of unconscionable lengths of time in digital simulation.

As mentioned earlier, our pictorial input to the data reduction operations is a large set of real numbers -- the image intensities at each of about 100,000 resolvable spots per picture. The product of each operation or feature mapping is another, much smaller set of real numbers. These sets consist of from one to quite a few components, and the components taken all together form a real vector in a multidimensional space.

Although work on the decision process was not undertaken, a brief description of the approach to it is appropriate. The decision process amounts to partitioning the multidimensional space into as many regions as there are classes to be distinguished. Linear equalities may be used, for example, to determine the decision regions, adjusting the boundaries partly through previous knowledge of the properties of the classes and partly through observations on the hopefully typical samples available for experimentation.

PHYSICAL AND SIMULATION DATA FORMATS

When illustrating possible mechanizations of operations, we shall consider, when convenient, either optical or electrical equipment. Thus at times the data may be assumed to take the form of pictures, transparencies, or optical images; at other times we may suppose the data to take the form of video signals. These forms are interconvertible, though at some cost. For the purposes of this report, we shall not worry about suggesting a consistent, efficient processing system, but shall merely indicate various possibilities.

It would be most desirable to work directly from data stored on board the satellite without having to go through the analog-to-picture-to-digital conversion before the information is inserted into the computer. While recognizing the ultimate desirability, in the future, of such an approach to the data reduction problem, we made no attempt to go this route in obtaining our digital simulations.

Since our operations were performed on the IBM 7090 digital computer, much attention was paid to data storage and programming in order to keep time costs at a minimum. Since a picture with a few hundred lines contains a great many bits of information, storage must be efficient, and careful attention must be given to programming those loops that will be executed many times. Mainly for these reasons the input to the simulation was composed of 6-bit positive numbers, which represent the image intensities at every resolvable spot composing an input picture. Depending on how much of a 32 k store is occupied by program instructions, this choice permits a 300- or a 400-line, square picture to be kept in fast storage.

It happens, incidentally, that our input pictures do not contain 32 distinguishable gray levels, let alone the 64 that were available in gray scale, so that no degradation of the image should result from

this degree of fineness of quantization. A choice of 32 gray levels, for example, permits handling some fair quality pictures (if they become available later) and represents at least a fair "ballpark" match to the dynamic range available from analog apparatus.

SCALING AND SMOOTHING

Because the ranges of density and contrast vary from one of our sample patterns to another, we rescaled all of them to a standard range of densities. And because our samples are reproduced from low-grade, low-resolution television signals that are afflicted with scanning jitter and video noise, some spatial averaging seemed beneficial. These two operations are like AGC (automatic gain control) and pre-detection filtering for ordinary electrical signals. Indeed, the scaling could be done electrically by ordinary AGC and clipping circuits while the picture signals are in electrical form, and no further description for this purpose is necessary.

We have retained some flexibility in our digital simulation by using the following scheme for rescaling each input picture to fit the intensity range $0 \leq x \leq 31$. First we find the probability distribution of the original, 6-bit measures of image intensity. We then determine, for a small probability, pc, chosen in advance, what image intensities correspond to the points near opposite ends of the density scale and beyond each of which the corresponding tail of the distribution has the measure pc. We then transform the lower such intensity, and all below it, to zero, and the upper such intensity, and all above it, to 31. The intensities between are transformed linearly. Of course, since there may not be a continuum of intensities, the actual extreme points of the linear range will not encompass exactly the fraction 1 - 2pc of all intensities but rather some fraction approximating this. The original distribution of intensities might look like Fig. 1, which for simplicity is drawn as a smooth curve corresponding to analog data. The digital simulation has the corresponding step-function distribution. The rescaling would look like Fig. 2. The object of this rescaling is to retain a maximum of the contrast of the original image by using the full available scale or dynamic range of the processing machinery for the "significant" part of the density scale. Obviously, the assumption has been made that henceforth all relatively small, extremely light or extremely

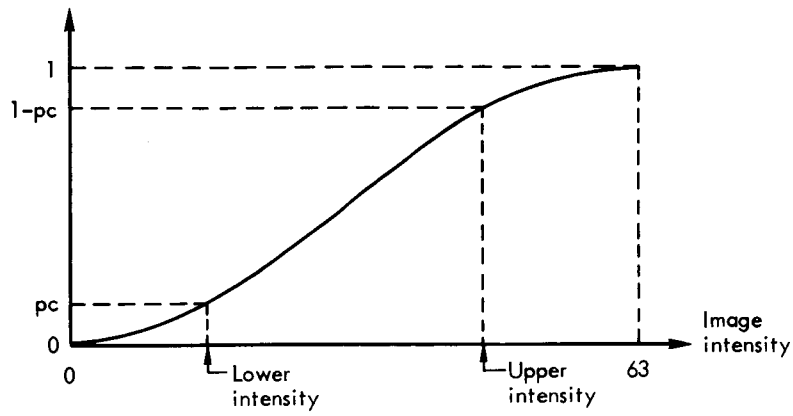

Fig. 1 Typical distribution of image intensities

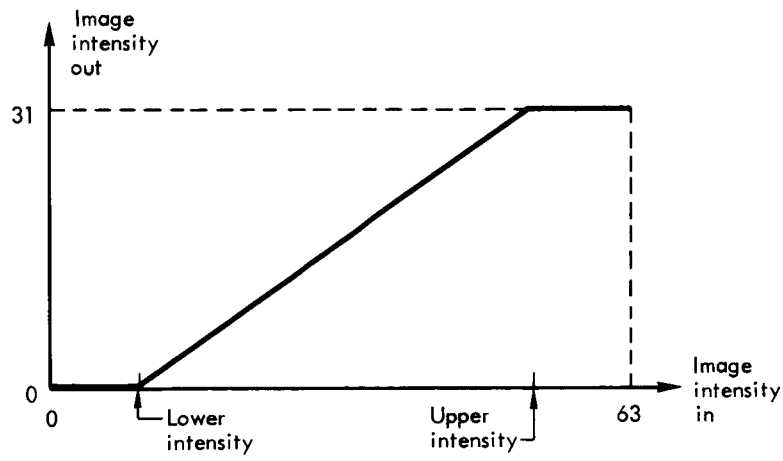

Fig. 2 Typical scale normalization

dark areas may be merged into white and black, respectively, without loss of useful information. This seems likely to be true for such cloud pictures as those we are considering. For a class of unknowns where low-contrast detail at extremes of the range is significant, one could set pc = 0, giving a simple linear transformation of the whole range.

There are several reasons for using some degree of spatial averaging on our data. First, we expect significant detail to vary only over an extent of several resolvable elements, while there is some noise fluctuation from element to element; thus such averaging acts like a low-pass filter to produce a useful increase in signal-to-noise ratio. In addition, if noise results from scanning jitter as the images are reconstituted (as in our samples, which were taken from a cathode-ray tube), averaging the data over several lines should eliminate some of the noise. Finally, at least with our digital simulation, we save processing time by exchanging our original data array for a coarser one corresponding to elements two or three times as far apart as those of the raw data. Likewise, in scanning, using analog apparatus, time could be saved by having fewer lines to scan.

In an analog machine, such as in an optical system, the weighting function for spatial filtering would be smooth and circularly symmetrical; a single parameter would be available to adjust the smoothing. For our digital simulation we are limited to what can be done with a checkerboard array of resolvable elements. Because it could be programmed simply and was fast-running, our basic spatial-smoothing operation was taken as a transformation to a new image having the same number of elements as the original, but of such a nature that each element of the new image is the average of four neighboring elements of the old image. That is, if $x_{i,j}$ and $y_{i,j}$ are the intensities at (i,j) of the old and new images, respectively, then

$$4y_{i,j} = x_{i,j} + x_{i+1,j} + x_{i,j+1} + x_{i+1,j+1} \quad .$$

It is evident that in applying this rule to the limited aperture covered by our image something must be done about the edges. Precisely what is done probably matters little. Because it was the least trouble, we adopted tactics equivalent to covering the border of

the image plane with spots of intensity zero, although an average "gray" might be more appropriate. For the digital simulation, the degree of smoothing is adjusted by varying the number of times this basic operation is iterated. Applying it one, two, or three times corresponds to smoothing by blur functions that are clearly described by the following arrays of weights:

$$\begin{matrix} 1 & 1 \\ 1 & 1 \end{matrix} \qquad \begin{matrix} 1 & 2 & 1 \\ 2 & 4 & 2 \\ 1 & 2 & 1 \end{matrix} \qquad \begin{matrix} 1 & 3 & 3 & 1 \\ 3 & 9 & 9 & 3 \\ 3 & 9 & 9 & 3 \\ 1 & 3 & 3 & 1 \end{matrix}$$

MOTION INVARIANCE

It is a characteristic of our problem, and of many other pattern-recognition problems, that the features we are looking for, if they are local, may be found anywhere in a plane region and do not occur in any particular orientation. They may also, like our cloud-cover patterns, be distributed features and still be independent of translations or rotations of the input-image plane. For example, a feature of cloud cover that may contribute to classification and recognition is the average size, or perhaps the distribution of sizes, of the separate clouds. This characteristic is clearly not localized at any particular place and is not affected by rigid motion of the image in its plane. Also, the frequent occurrence of clouds lying in roughly parallel and evenly spaced rows or bands should be discernible independently of rigid motions of the image.

Now there is a trivially motion-invariant way of extracting features from an image region. It amounts to looking for them everywhere! One provides a template (reference function) for the feature, tries it all over the plane, in all orientations, and notes when a good match occurs. There are cases for which such a search can be readily mechanized and where the method can be practically effective.[2]

We have avoided such searches, taking the view that to ask the three-dimensional array of questions, "Is the configuration present at (x,y) with orientation θ ?" is an undesirable approach to the question, "Is the configuration present somewhere in the plane?" Instead we have attempted to generate data-reduction transformations that retain evidence of important features and whose outputs are independent of rigid motions of the input.

TWO-DIMENSIONAL AUTOCOVARIANCE AS A REDUCED-DATA ITEM

One easily mechanized (both digitally and optically) translation-invariant transformation of the raw input image is its two-dimensional autocovariance function (ACF). Let I (x,y) be the image intensity at the point with rectangular coordinates (x,y). Let m be the average value of I. Then the autocovariance function for displacement (h,k) is

$$C\ (h,k) = \iint [I\ (x,y) - m]\ [I\ (x-h,\ y-k) - m]\ dxdy \quad . \qquad (1)$$

The term C (h,k) is obviously translation-invariant. Its usefulness for pattern recognition has been recognized for at least a dozen years,[3] and it has been applied to some simple examples.[4,5] Any rotation-invariant feature of C (h,k) will be a motion-invariant feature of I (x,y) and should provide useful data. (Several such features will be introduced in the next section.) For example, a noticeable peak in the ACF plot other than the one at the origin evidently corresponds to the presence of well defined rows or bands of clouds in the original image. Even if no peak is apparent, the ACF still contains information about the relative size and spacing of the clouds in the original image.

At first glance, this may not seem to be much of a reduction in data dimensionality. However, for our particular samples, both the sizes of the individual clouds and their spacings are only a fraction of the picture width. Where this fraction is 1/5 to 1/10, for example, one need consider finding the ACF for only 1/25 to 1/100 as many displacements as there are resolvable lines in the original image.

If, in addition, some slight smoothing of the original is allowed, then still more of the data are eliminated for this transformation.

An aspect of our problem that suggests the use of the ACF is the resemblance between pictures of cloud cover and samples from a two-dimensional random process. Since gaussian random processes are completely determined by their means and covariance matrices, we expect the ACF to contribute useful information even if the process is not gaussian, so long as it is random and spatially homogeneous (the two-dimensional equivalent of stationariness).

If the mechanized autocovariance input image is available as a phototransparency, the two-dimensional ACF may be obtained by two simple and ingenious schemes suggested by Kovásznay and Arman[6] and reproduced in Figs. 3 and 4. The scheme of Fig. 3 yields the ACF as an image at the focus of the lens, where it can be photographed, scanned or subjected to further optical transformation. The scheme of Fig. 4 yields the ACF sequentially, in whatever order is specified by the cathode-ray tube (CRT) scan, as an electrical wave form.

When the image is the list of numbers forming the input for digital simulation (as in our case), one simply computes the ACF by doing many sums of products. Since this arithmetic can be expected to take quite a lot of time if done casually, some pains were taken to make the calculation fast by an appropriate combination of data storage and programming, the detailed description of which we defer to pages 24--28. One detail should be mentioned here, however. Since at this point our pictures are smoothed and filtered, it has appeared possible to save time in the ACF calculation, without much information loss, by replacing the original image with a half-resolution image after filtering. That is, we simply throw away all points, for example, whose coordinates are not both odd.

ROTATION-INVARIANT ABSTRACTIONS FROM C (h,k)

In this section we shall discuss a few rotation-invariant features that may be discernible in C (h,k) and note how they can be extracted from the data if present.

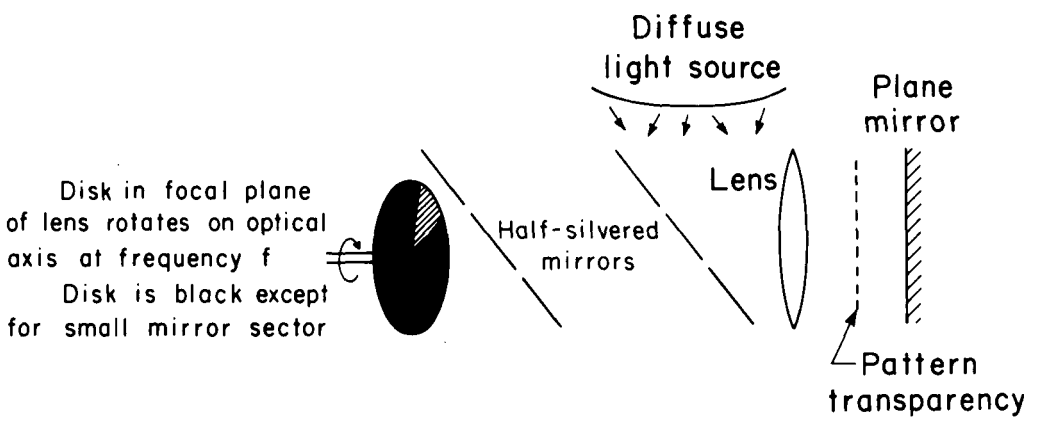

Fig. 3 An optical arrangement for displaying the autocorrelation function as an image at the focus of the lens

Similarity-Insensitive C(h,k) Scan

Doyle[5] has previously reported a way to transform

$$C'(h,k) = \iint I(x,y)\, I(x-h,y-k)\, dxdy \approx C(h,k) - m^2 \iint dxdy$$

into a time function, w(t), which to a close approximation will only be delayed or magnified when the input image, I(x,y), is rotated or magnified. After such a transformation, patterns may be detected by passing w(t) into a set of matched filters whose outputs can be compared with a threshold proportional to the factor by which w(t) may be magnified. In particular, such a variable threshold might be translated into a fixed ratio by which each matched filter output would be required to exceed the rms output of all the filters together, averaged over a scan period.

The transformation amounts to a spiral scan of C' (h,k). We repeat here the short argument leading to this scan. Let (r,θ) be polar coordinates in the (h,k) plane. We wish to describe a scan that will produce an output independent of rotation or dilatation of the (h,k) plane. Independence of rotation evidently requires that $d\theta/dt$ be constant and that a shift in the starting phase of the scan not affect the output wave shape. To see what is required for independence of size, consider the effect of, say, enlarging the picture. In order to get from a portion of the autocorrelation image at one radius to a portion at another radius in the same time interval after enlargement as before, it is evidently necessary that the radial scanning speed be proportional to radius, namely $dr/dt = ar$. A little thought shows that the resulting spiral scan, $h = \exp(at) \cdot \cos bt$, $k = \exp(at) \cdot \sin bt$, cannot be independent of the starting phase in general. However, since there is a finite resolution limit, by keeping the expansion parameter, a, small enough, the output function, w(t), resulting from the scan can be made sufficiently insensitive to variations of the starting phase for practical purposes. The scanning spot size should (probably) also be varied proportionately to r in order to maintain constant relative resolution, a logical concomitant of size-independence. An actual scan would start at, say, one

resolution spot out from $h = k = 0$ and terminate before reaching a boundary of the $C'(h,k)$ image.

Such a scan can be easily produced on an ordinary CRT, so that the mechanism for realizing $w(t)$ has in effect already been sketched in Fig. 4. We have only to subtract from the output in Fig. 4 the easily estimated constant $m^2 \iint dx\, dy$.

Periodic Components

There is an elementary characteristic of $I(x,y)$ that probably will show up readily in $C(h,k)$ if present. It is rough periodicity in some particular direction, corresponding to the presence of a strong component $\cos(ax + by + c)$ in the input pattern. Such a component will be present, for example, if there is a direction along which clouds are fairly uniformly spaced across the field of view. The component will appear as a series of equally spaced peaks lying along a line through $h = k = 0$. The rotation-invariant feature thus determined is the distance between the peaks plus an indication of the strength of the component. Such peaks might reasonably be detected by comparing the value of $C(h,k)$ at each point with a pair of thresholds determined by the rms value of $C(h,k)$ over some annulus with mean radius $\sqrt{h^2+k^2}$. The direction of such a line of peaks should be of no interest in itself, although the angle to any other oriented feature would be.

Path of Minimum Decorrelation

For most cloud-cover pictures, no such obvious peaks as have just been discussed are likely to be present in $C(h,k)$. However, there still may be some related tendencies toward periodicity which can be extracted from $C(h,k)$ in the form of a slightly vaguer piece of rotation-invariant data. It seems easiest to describe what we have in mind by simply giving a data-reduction procedure to be applied to $C(h,k)$.

For each radius, r, in the (h,k) plane we consider an annulus bracketing r. As for the previously discussed feature, we find the rms value, s, of C over this annulus. We also have a threshold

factor, f. Whenever C(h,k) exceeds fs at some point of the annulus we find the maximum such C and its corresponding location (h,k). If we do this as a continuous function of r, we obtain a path, possibly interrupted by gaps where the peak insufficiently exceeds the rms value, and a function defined along this path. The result may be given by a pair of functions, $\theta(r)$ and $z(r)$, describing the path and the ratio by which C exceeds fs, respectively. As given, $\theta(r)$ is not rotation-invariant; however, there are reasonable ways to select a preferred direction, θ_0 -- a weighted average of θ over r is one -- so that a rotation-invariant path, $\theta(r) - \theta_0$, is determined.

The above procedure, as given, contains some vagueness we shall not dispel. Remaining to be decided are such questions as the variation of annulus width with radius, the variation of threshold, f, with radius and the weight function used to determine θ_0 (or some other angle-normalization procedure).

In any case the piece of data just described, which we shall call the path and function of minimum decorrelation, is a rotation-invariant abstraction from the ACF. When there is a strong component, cos (ax + by + c), in I(x,y) then $\theta(r)$ reduces to a constant and $z(r)$ to a succession of equally spaced peaks. Since the feature described by $\theta(r)$, $z(r)$ will include the case where C(h,k) exhibits a prominent periodic component, we need not explicitly hunt peaks of C(h,k) if we decide to extract the path and function of minimum decorrelation.

Part of a mechanization of this feature is readily derivable from Fig. 4 and from the spiral scan used to produce w(t) if the spot size for the spiral scan is about right for the resolution of the image. We may subtract the constant $m^2 \iint dx\, dy$ from the scan output, square the difference and then low-pass filter that difference with a time constant of $2\pi/b$. This will give a reasonable approach to the annular average mentioned earlier. In practice, merely rectifying the difference linearly should be as useful as squaring it. We have still to suggest how the succession of maxima for different annuli may be found.

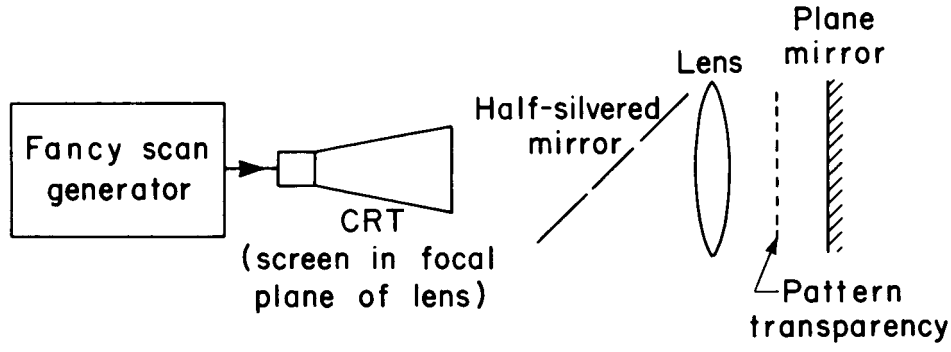

Fig. 4 An optical arrangement for displaying the autocorrelation function as an electrical wave form

An untidy way to discover the annular maxima would be to employ two distinct scans that time-share the CRT beam and the photoreceptor output. The first scan and its output yield the running rms value of C(h,k) over an annulus of growing radius. The second scan, running behind the first, yields the value and location of each annular maximum by an operation requiring two revolutions of the scan. During the first revolution, the value of the maximum is determined, for example, by feeding the output of the scan through a diode to a capacitor. During the second revolution, the location and the maximum are both obtained by discharging the condenser when the signal amplitude coincides with the condenser potential. The timing of this coincidence yields $\theta(r)$, while the size of the discharge yields $z(r)$.

For digital simulation, since this feature is described as an arithmetic calculation, one simply does the calculation. This one is simple enough that it is not necessary to take pains to do it efficiently.

Rotating C(h,k) Into a Reference Position

If C(h,k) contains a strong enough indication of a special, or reference direction, then it may be useful to rotate C(h,k) so that the reference direction falls along the new h-axis and use the resulting, normalized C(h,k) as input to an ordinary cross-correlation detection scheme. This seems unlikely to be as useful for cloud-pattern classification and recognition as for some simpler problems like reading the alphabet.

To find such a reference direction one might consider $\theta(r) - \theta_0$, the path of minimum decorrelation. If its fluctuation as a function of r is small enough, one may choose θ_0 as the reference direction. Otherwise it could be decided that there is insufficient indication of any preferred direction.

If C(h,k) is rotated to a preferred direction, the resulting function is evidently a motion-invariant product of the original image.

Fourier Analysis by Annuli

Another procedure for deriving rotation-invariant products from $C(h,k)$ is based on the fact that if the (h,k) plane is described in polar coordinates (ρ,θ), then $C(\rho,\theta)$ is periodic in θ (the period is π in general). If we divide the plane into a few convenient rings, average $C(\rho,\theta)$ radially over each one, and then Fourier analyze the resulting periodic functions, the strengths of the harmonics (sum of squares of sine and cosine for each frequency) are a rotation-invariant abstraction from $C(h,k)$.

This sort of operation is easily performed by simply adding to the output of Fig. 4 a series of narrow-band filters centered at the frequencies b/π, $2b/\pi$, $3b/\pi$ and so on. Rectifying their outputs and averaging over several cycles of a slowly expanding spiral scan will give the strengths of all the harmonics as functions of ρ.

To do this Fourier analysis digitally is too lengthy to be practical; further it adds nothing to the information already contained in the function $w(t)$ produced by the spiral scan of $C(h,k)$. It has seemed worth pointing out, however, that the harmonic analysis represents another analog scheme to produce rotation-invariant features of $C(h,k)$, hence of $I(x,y)$. A simple form of this, treating the whole (h,k) plane as one ring, has been used to recognize simple line patterns in Doyle's work.[5]

CREEPING UNIFORMITY

An interesting motion-invariant datum useful for classifying black and white patterns has been described by Blum.[7] We imagine the pattern on a plane. At $t = 0$, a wave starts out from the pattern, moving (within the plane) at constant speed in all directions into new territory. It propagates like a wave of chemical destruction: it can advance only into area not already overrun. At each instant, t, we note the area, $a(t)$, of the region enclosed by the wavefront. This function, $a(t)$ is a motion-invariant characteristic of the original pattern. For our purposes area is the easiest to compute; the growing perimeter, $p(t)$, containing the same information could also be used

(the area is evidently the integral of the perimeter). The process clearly need not be limited to plane or two-dimensional patterns, nor specifically to area.

There are at least two ways to apply this idea to continuous-tone patterns. One is to choose a threshold intensity* and change the image to a black and white (no gray) one, turning each spot into black or white according as it originally was darker or lighter than the threshold shade. After this transformation we proceed as described above.

To see how this operation gives information about blob sizes, suppose clouds to be white, background dark. As the dark eats up the cloud areas, clouds begin to disappear. An individual cloud that was entirely convex, for example, would be devoured in the time it takes the wave to traverse half the width of the cloud. Thus a(t) gives some information about the distribution of cloud sizes.

Evidently we could, in the black and white case, permit white to overrun black and measure the area of white at each instant rather than black. Thus by the same operation we can get information related to the distribution of widths of spaces between clouds. Further, it should be noted that the rate of cloud expansion, or overrunning, is a minimum for cloud forms whose pictorial representations are circular.

The second way to apply this idea is to devise a continuous-tone analog of this creeping-wave operation and then derive a(t) for it. At this point the reader is reminded that the earlier filtering of the raw data smears the image points equally in all directions. We could filter many times, producing ever fuzzier and less contrasty images, eventually winding up with a uniform average gray. The end product of this succession of fuzzier and flatter images is the continuous equivalent of the succession of ever more completely blackened images produced in the two-tone version. We now need some measure of the uniformity of the blurred, continuous-tone images corresponding to the function, a(t). One such measure is the fraction of the picture area whose tone is within k levels of the mean tone, where k would be small, say $0 \leq k \leq 4$, but would depend on the tonal range of the original picture.

---

*This problem is discussed in the section dealing with the determination of amount of cloud cover.

Notice that the continuous smear operation, as given, is symmetrical and does not yield the two different kinds of information provided by the creeping white and the creeping black. However, by replacing the symmetrical condition, "within k levels of the mean tone," by the two extreme conditions, "more than k levels above (or below) the mean tone," we again have the two complementary items of data.

For the computer simulation, all these variations are easily tried. For continuous-tone images we alternately filter and recompute the density distribution. For black and white images we add one more operation, hard limiting (described in the section dealing with determination of cloud amount), which forces all grays to black, while only the pure white level is left white. Spatial averaging followed by hard limiting is equivalent to one step of the creeping blackness, and we get a(t) by repeating the sequence: average, limit, and recompute distribution.

It is unfortunately not clear how to implement these functions with fast analog apparatus. While some discussion of the problem appeared in Ref. (7), no useful progress was made. A clumsy solution may be possible if a defocusable image is available that can be scanned over and over, with the intensity distribution being found each time the image is further blurred.

AUTOCORRELATION CALCULATION

People are increasingly busy these days with digital processing of pictorial cloud data, and in particular with the two-dimensional spectral analysis of such data. This section describes a combination of data storage and programming that yields two-dimensional autocorrelation functions in about 1/20th the time of standard procedures that have been reported by Leese and Epstein[8] and that are apparently in use. A trivial change would permit the same program to compute cross-correlation functions.

Let $I(i,j)$ for $i = 1,2,\ldots,m$ and $j = 1,2,\ldots,n$ be pictorial data sampled on a rectangular grid. Then the autocovariance $C(h,k)$ for the two-dimensional displacement (h,k) is calculated for $h \geq 0$ by

$$(m - h)\ (n - k)\ C(h,k) =$$

$$\sum_{p=1}^{m-h} \sum_{q=1}^{n-k} [I(p,q) - \bar{I}]\,[I(p+h,q+k) - \bar{I}] \text{ for } k \geq 0, \text{ and}$$

$$\sum_{p=1}^{m-h} \sum_{q=1-k}^{n} [I(p,q) - \bar{I}]\,[I(p+h,q+k) - \bar{I}] \text{ for } k < 0 \quad , \tag{2}$$

where $\bar{I}$ is the average of all the data. If the displacements are not a great fraction of the picture dimensions, then the sums that are linear in I may be replaced by the appropriate multiples of $\bar{I}$, giving the simpler calculation

$$C(h,k) = \sum_{p=1}^{m-h} \sum_{q=1}^{n-k} I(p,q)\ I(p-h,\ q-k)/(m-h)(n-k) - (\bar{I})^2 \text{ for } K \geq 0 \tag{3}$$

and similarly for $k < 0$.

The program referred to above uses Eq. (2); a greater saving (by about 27 per cent) is possible using Eq. (3). Either of these computations requires that a great many sums of products be taken. The scheme to be described does the task quickly because it takes advantage of the peculiarities of the machine and the form in which the data can be stored.

The nucleus of the calculation is a simple consequence of two facts. The first is that the IBM 7090 has a table-look-up instruction, CAQ, which along with a suitable multiplication table, permits one to augment the high-order end of the accumulator by three sums of products in a single instruction taking 8 machine cycles (garbage is simultaneously accumulated in the lower end). The 6 separate quantities must be integers of 6 bits or less; they are assembled in the multiplier-quotient.

The second fact is that most of the pictorial data that people are processing are more than adequately representable by 6 bits. Leese and Epstein[8] for example, mention 5 gray levels, which is 2^+ bits, and we have been using 5 bits (32 levels).

To expand this idea into a usable program, it is necessary to devise a scheme of storage and an order of processing that would not fritter away time by much data shifting and bookkeeping. Our scheme to mechanize Eq. (2) will be described mainly in words, and should permit any competent programmer to produce his own program easily.

The image is stored in the machine in duplicate, in versions that will be referred to as the fixed and the shifted images, respectively. Each image is a block of contiguous words, composed of sub-blocks that represent individual lines. Each word contains three items of data, each consisting of 5 bits in our case, and is stored in the right end of each third of a machine word. Thus, if we assume that about one-third of the store is used for each image and one-third for program, a 32k machine will accommodate a $30{,}000^+$ sample picture, say a picture about 180 by 180, at any one time. At present, this seems to be more than adequate for a TIROS picture, for example.

With the data stored three to a word, it is evidently easy to take care of all the shifts that are divisible by 3. We therefore consider the entire set of displacements and first get C(h,k) for all h divisible by 3. Incidentally, if there were no other shifts, then the duplicate image could be dispensed with and only a single one used. Next we shift the entire shifted image one datum left (12 bits) and get the ACF for all the h that are congruent to 1 modulo 3. Finally, the shifted image is shifted again and the ACF computed for all the h congruent to 2 modulo 3.

To compute the quantity in Eq. (2) for any particular displacement (h,k) we calculate (in a FORTRAN program) the indices and locations that describe the two overlapping rectangles for which the quantity in Eq. (2) is to be found. The remaining two loops are FAP-coded. The outer FAP loop and the FORTRAN coding can be fairly sloppy, but the innermost loop should be as short as it can be made. This loop which accumulates one line of sums of products is:

```
        ZAC                     SET SUM TO ZERO.
        XCL                     SAVE SUM IN MQ.
        CAL     **,2            GET 3 DATA FROM FIRST IMAGE
        ALS     6
        ORA     **,2            AND 3 FROM SECOND.
        XCL                     SUM TO AC, DATA TO MQ.
        CAQ     MULT,,6         ADD 3 MORE PRODUCTS.
        ANA     LEFT            REMOVE TABLE ADDRESS BITS.
        TIX     *-7,2,1         GO GET 3 MORE PAIRS.

    LEFT SVN    ,,-1            MASK FOR SUM OF PRODUCTS.
```

This loop takes 23 cycles. An obvious 6-cycle loop collects the linear sums for Eq. (2) three at a time. If the formula of Eq. (3) can be used, a considerable saving results. The last short loop is not needed at all, while the shift can be omitted from the first loop and the duplicate arrays all shifted left a further 6 bits when they are first set up. Thus if Eq. (3) were used, the innermost loops would be reduced in length from 29 cycles to 21, for a further 27 per cent reduction in time.

If one has fairly small pictures, say not more than about a 60 by 60 matrix, then the sums might be accumulated a few bits farther left, and the ANA put after the loop for another 3-cycle saving.

The multiplication table can easily be generated in FAP as follows:

```
            TITLE
    T32     MACRO           A
            IRP             A
    D       SET             *
            DUP             1,32
            VFD             18/C**-C*D,18/MULT
    C       SET             C+1
            IRP
    T32     END
            NOCRS
    C       SET             *-*
    MULT    DUP             1,32
            PZE             32**-32*MULT+MULS
    MULS    T32             (,,,,,,,,,,,,,,,,,,,,,,,,,,,,,,,,)
```

This multiplication table occupies (32)(33)=1056 words.

The autocorrelations* that we computed for our TIROS pictures consisted of matrices about 145 by 145 quantized into 32 gray levels. For 20 lags (i.e., 21 x 41 values) the computation takes about 3.5 minutes on the IBM 7090. This includes input of the picture data and output of the autocorrelation function in printed and punched forms, all under control of the FORTRAN monitor.

The saving of time afforded by this combination of data storage and processing can be estimated by comparing the running times of this scheme with a similar calculation made on the same machine (the IBM 7090) and reported in Ref. (8).

They report a time estimate of about 7 minutes to compute the autocorrelation of a 60 by 60 picture for 15 lags in each direction. If E^2 is the number of picture elements and M is the number of lags in each direction, then computation time is roughly proportional to E^2M^2. Our process took 14 minutes for 4 pictures. The pictures were not quite square, but were equivalent in area to a 145 by 145 element picture. The autocorrelations were computed for 20 lags (21 x 41 values). Thus our process would take about

$$\frac{14}{4} \frac{(60)^2}{(145)^2} \frac{(15)^2}{(20)^2} = 0.34 \text{ minutes}$$

for a 60 by 60 picture for 15 lags, which is faster by a factor of about 20. The times given for our autocorrelation calculation include reading the patterns into storage, doing all the incidental computation and printing and punching the autocorrelation. Of course, our process is limited to 5-bit data (32 gray levels); however Leese and Epstein mention 5 gray levels (2^+ bits) and 32 should be plenty for most investigations of this kind.

---

*Up to now we have only mentioned the autocovariance, or ACF, to avoid confusion. The reader is probably aware that the autocorrelation function is defined as the normalized autocovariance (the autocovariance divided by the individual variances). The program that was written calculates and prints out 1,000 times the value of the normalized two-dimensional autocovariance of our sample cloud patterns, which will be shown in the sections to follow.

A FEATURE THAT REVEALS REGULAR ALIGNMENT

The feature that will be discussed in this section is one that was developed ad hoc from the two-dimensional autocorrelation function. It is intended to help separate cloud patterns that occur in more-or-less parallel and equally spaced rows (SCSS) from those that do not (specifically, from CUCL).

Let us first consider the autocorrelation $\rho(h,k)$ for an idealized picture composed of alternate black and white stripes of equal width. As displacements are made along the stripes, $\rho(h,k)$ remains constant, but when displacements are made perpendicular to the stripes, the function alternates regularly between +1 and -1.

In the case of clouds that are roughly aligned in streets or bands, the value of the function $\rho(h,k)$ would be expected to fall off slowly as the displacement is increased parallel to the streets or bands. When displacements are made perpendicular to streets or bands, the oscillation between +1 and -1 would be expected to die away more-or-less rapidly, perhaps even in a single cycle. Even when the alignment of clouds is only vaguely discernible to the eye, it can be expected that the fall-off of the central hump of $\rho(h,k)$ as displacements move away from (0,0) will, by its directionality, indicate the extent to which the cloud elements are aligned.

Figures 5 and 6 are typical patterns of individual cloud cells (CUCL) and their corresponding IBM 7090 computer printouts of the two-dimensional autocorrelations. The +100 (+10%) and +200 (+20%) contours are both roughly drawn, but for this discussion particular attention should be paid to the +200 contour line, which was arbitrarily singled out as one that seemed to be significant in delineating the general degree and direction, if any, of cloud alignment, as well as serving visually to separate SCSS printouts from CUCL printouts. Figures 7 and 8 represent typical patterns of cloud streets (SCSS) and their corresponding two-dimensional autocorrelation printouts. The general agreement between the original patterns and their autocorrelation transformations with regard to the direction and degree of elongation of the +200 contour

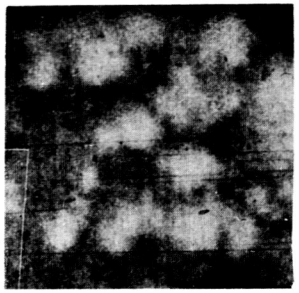

FR 01
AXRAT 0.82

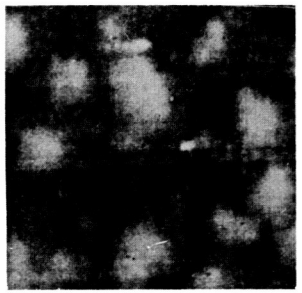

FR 02
AXRAT 0.83

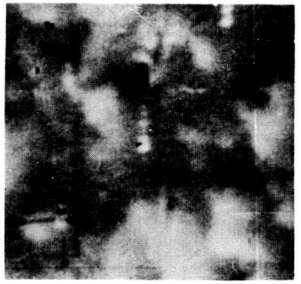

FR 04
AXRAT 0.78

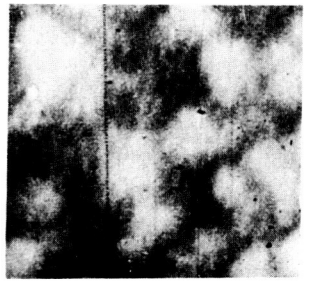

FR 32
AXRAT 0.82

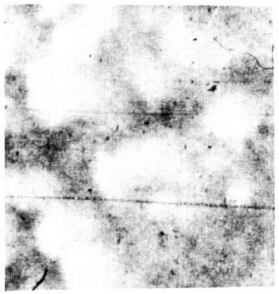

FR 33
AXRAT 0.81

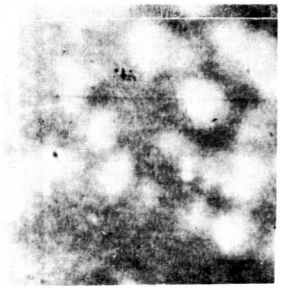

FR 35
AXRAT 0.89

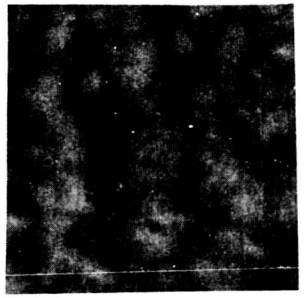

FR 40
AXRAT 0.85

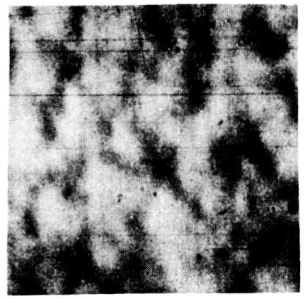

FR 42
AXRAT 0.90

Fig. 5 Samples of pattern CUCL

Legend indicates frame number (FR) and axes ratio (AXRAT)

C(H,K) FOR CHECK= 4 CIOUCL CUMULUS CELLS FR 01

-59	-90	-86	-35	-26	-21	-13	-25	-38	-56	-56	-53	-29	-22	-16	-6	-1	4	-3	0	1
-68	-96	-98	-17	-6	-0	9	-4	-16	-36	-37	-34	-1	8	16	23	27	30	24	26	25
-67	-91	-76	13	25	31	32	18	7	-11	-11	-9	23	33	40	38	37	39	35	36	35
-61	-79	-58	41	53	53	53	36	25	10	12	14	38	42	45	35	34	33	28	29	28
-41	-59	-37	58	68	72	61	42	31	23	27	29	41	39	38	19	18	17	12	14	13
-6	-27	-10	59	69	69	53	35	23	27	34	38	43	35	28	-1	-4	-5	-4	-0	-2
22	-7	1	37	41	38	27	12	2	20	32	40	45	34	23	-14	-16	-18	-15	-13	-16
38	-2	-5	-7	-7	-12	-12	-23	-26	10	25	36	45	36	28	-7	-10	-12	-15	-15	-19
44	-8	-20	-52	-54	-60	-47	-53	-51	2	20	31	49	47	46	13	10	8	1	-2	-9
58	-3	-24	-75	-78	-84	-63	-64	-57	4	24	35	59	59	62	42	39	37	30	26	15
68	-3	-27	-81	-94	-93	-63	-64	-54	9	25	36	60	60	66	60	59	59	51	45	33
55	-20	-46	-74	-72	-77	-54	-55	-47	-3	10	20	44	45	52	54	57	59	48	41	29
20	-54	-76	-73	-67	-73	-43	-45	-39	-23	-14	-6	18	20	28	32	38	42	31	25	14
-19	-86	-103	-82	-73	-73	-38	-39	-36	-40	-34	-30	-3	-0	7	14	20	23	10	8	1
-33	-91	-102	-73	-69	-70	-27	-28	-26	-43	-38	-37	-8	-5	2	10	13	14	-2	-0	-2
-0	-49	-56	-47	-45	-52	-23	-24	-22	-33	-27	-23	4	5	11	14	15	13	-4	-1	-1
100	104	53	45	15	5	-9	-6	-13	-10	-6	3	9	27	24	28	23	28	26	8	10	9
200																				
287	234	21[illegible]	11[illegible]	[illegible]	62	29	20	21	38	48	54	54	49	53	55	56	56	38	40	39
530	463	423	3[illegible]	191	14[illegible]	79	67	70	84	90	91	80	73	76	86	91	94	79	78	76
785	697	619	323	254	21[illegible]	135	122	119	120	118	113	[illegible]	83	87	110	119	126	117	113	105
999	946	731	359	292	23[illegible]	173	163	162	142	133	122	94	88	94	124	135	144	140	135	126
785	679	532	246	[illegible]	144	118	115	11[illegible]	97	87	74	54	54	64	101	114	124	118	113	105
530	435	36[illegible]	[illegible]	72	42	55	52	72	63	53	41	28	33	45	83	95	101	81	75	71
297	199	14[illegible]	-17	-35	-43	15	30	45	43	35	27	20	25	39	66	73	75	47	42	38
200																				
100	26	-17	-32	-99	-92	-2	16	35	32	24	17	16	20	32	43	44	40	9	6	6
-0	-61	-91	-116	-107	-94	-2	11	25	16	7	-0	4	6	15	9	6	-0	-36	-35	-31
-33	-79	-95	-15	-75	-61	0	9	17	-4	-13	-23	-22	-21	-13	-30	-36	-46	-79	-76	-67
-19	-48	-52	-32	-23	-14	12	13	13	-23	-33	-42	-47	-50	-46	-66	-75	-83	-108	-102	-88
20	4	9	19	21	24	22	16	8	-43	-52	-60	-65	-70	-70	-90	-99	-107	-121	-112	-98
55	45	49	49	45	44	25	16	5	-47	-54	-59	-68	-77	-81	-103	-110	-116	-121	-112	-97
68	58	63	48	42	36	18	9	0	-30	-34	-38	-55	-67	-73	-99	-104	-108	-107	-100	-87
58	46	51	34	18	11	5	1	-3	-8	-9	-10	-29	-42	-50	-77	-81	-82	-80	-76	-69
44	27	23	-12	-18	-23	-5	-3	-2	8	10	10	-2	-12	-18	-50	-54	-56	-58	-55	-50
38	14	7	-17	-53	-55	-14	-10	-4	19	21	20	12	4	1	-30	-36	-38	-42	-41	-38
22	-9	-23	-40	-82	-73	-33	-22	-15	13	14	11	-2	-7	-7	-29	-33	-33	-39	-39	-38
-6	-38	-52	-37	-94	-87	-44	-36	-29	-6	-6	-10	-27	-28	-25	-34	-37	-37	-47	-48	-49
-41	-69	-76	-36	-91	-14	-47	-42	-36	-28	-30	-34	-45	-45	-41	-42	-43	-43	-53	-53	-51
-61	-82	-79	-58	-58	-31	-27	-25	-24	-32	-35	-39	-45	-44	-41	-42	-44	-45	-52	-51	-49
-67	-80	-71	-31	-10	-13	-4	-6	-9	-28	-30	-33	-36	-36	-34	-38	-42	-43	-51	-48	-44
-68	-75	-60	3	15	13	9	1	-5	-26	-24	-22	-26	-25	-23	-30	-37	-40	-43	-40	-34
-59	-61	-39	28	34	33	3	-6	-14	-26	-20	-14	13	-12	-10	-19	-25	-29	-30	-26	-20

Fig. 6 Computer printouts of the autocorrelation for cumulus patterns Frame 01

C(H,K) FOR DH=DK= 4 O2SUCL CUMULUS CELLS FR 02

-24	-32	-29	-18	-13	-9	-7	-5	-6	-25	-28	-30	-24	-12	-1	53	65	73	81	77	73
-24	-33	-31	-23	-21	-19	-27	-26	-28	-41	-41	-40	-29	-17	-5	49	59	66	68	62	57
-11	-23	-23	-17	-17	-17	-27	-27	-29	-38	-35	-33	-24	-11	-0	53	63	68	66	58	52
-16	-29	-28	-17	-16	-15	-24	-24	-26	-35	-34	-33	-30	-19	-10	42	51	55	47	38	31
-18	-33	-31	-8	-3	-0	-8	-9	-9	-23	-23	-24	-28	-19	-12	26	34	36	20	10	4
-27	-45	-45	-10	-4	0	-5	-5	-5	-15	-16	-18	-24	-17	-13	5	6	3	-17	-27	-30
-47	-68	-63	-33	-25	-13	-20	-20	-21	-23	-21	-20	-25	-22	-23	-27	-31	-38	-59	-65	-64
-58	-80	-82	-53	-46	-40	-39	-37	-35	-28	-22	-19	-24	-24	-30	-53	-61	-70	-88	-89	-83
-61	-85	-98	-71	-68	-63	-59	-55	-52	-34	-27	-23	-27	-28	-36	-69	-78	-89	-101	-100	-92
-51	-79	-96	-68	-37	-86	-75	-58	-54	-42	-35	-29	-31	-33	-40	-71	-91	-91	-96	-98	-91
-36	-58	-70	-72	-93	-94	-65	-80	-75	-56	-49	-42	-38	-39	-44	-67	-74	-83	-90	-91	-86
-27	-66	-73	-47	-89	-91	-80	-85	-83	-69	-62	-56	-44	-41	-44	-58	-65	-73	-82	-86	-85
-12	-47	-59	-73	-75	-76	-77	-77	-76	-71	-67	-62	-42	-37	-38	-45	-51	-59	-73	-79	-81
3	-32	-45	-57	-62	-62	-65	-64	-64	-65	-63	-59	-35	-27	-25	-25	-32	-39	-59	-68	-73
47	10	-4	-34	-41	-45	-54	-54	-53	-46	-44	-37	-14	-5	-2	1	-4	-11	-33	-46	-54
124	39	73	6	-11	-25	-59	-57	-54	-31	-23	-15	12	21	25	29	24	17	-5	-19	-27
253	217	26	70	33	3	-75	-76	-71	-28	-15	-2	29	37	37	42	37	29	4	-9	-19
419	378	347	139	91	28	-95	-96	-90	-24	-4	11	49	57	57	57	52	44	18	2	-8
615	548	529	21	133	69	-110	-113	-107	-25	-1	20	65	74	74	72	68	59	27	10	-3
904	748	670	279	73	[illegible]	-116	-121	-115	-24	-3	13	68	89	94	87	82	74	41	20	3
999	934	814	363	255	123	-41	-70	-65	11	32	50	96	110	117	124	117	107	72	49	30
804	740	632	279	84	13	-98	-105	-101	-34	-16	-0	45	61	72	88	82	72	41	19	0
615	572	526	21	149	71	-88	-93	-90	-39	-25	-11	32	48	58	83	80	73	42	19	1
419	336	354	142	54	35	-86	-86	-82	-46	-35	-24	14	30	40	73	74	72	46	27	10
253	227	[illegible]	12	42	7	-70	-70	-67	-36	-26	-19	3	18	28	70	77	79	66	46	30
124	103	97	35	8	-13	-62	-62	-58	-32	-26	-21	-16	-4	5	61	72	80	88	71	56
47	31	30	13	-1	-16	-47	-47	-45	-32	-30	-30	-35	-20	-7	66	82	96	124	114	99
3	-10	-5	1	-5	-13	-38	-40	-41	-49	-52	-56	-52	-45	-30	66	88	107	159	147	132
-12	-23	-17	11	9	4	-16	-20	-27	-60	-66	-73	-75	-58	-40	72	98	121	182	172	160
-27	-37	-29	13	13	14	-4	-12	-21	-73	-82	-89	-85	-66	-46	75	101	124	183	174	163
-36	-45	-36	15	18	23	9	-1	-14	-77	-94	-90	-75	-54	-31	96	109	130	177	167	156
-51	-61	-50	7	14	21	5	-6	-19	-80	-87	-89	-61	-39	-18	87	104	120	151	140	130
-61	-70	-59	4	12	20	1	-13	-23	-71	-73	-71	-31	-11	8	87	98	108	127	117	107
-58	-54	-57	5	12	13	-5	-16	-27	-58	-54	-48	-4	14	30	81	86	91	95	89	79
-47	-57	-43	4	9	11	-19	-28	-37	-44	-35	-27	14	29	39	72	72	73	77	70	62
-27	-40	-35	1	2	0	-13	-38	-41	-26	-15	-7	19	27	32	50	49	48	60	55	50
-18	-33	-32	-15	-19	-23	-51	-51	-48	-19	-6	0	10	12	10	15	13	14	42	41	42
-16	-32	-35	-37	-45	-50	-68	-63	-55	-15	-7	-1	-5	-11	-19	-23	-23	-19	24	29	35
-11	-29	-37	-57	-65	-63	-74	-64	-52	-6	-0	0	-15	-24	-36	-49	-47	-41	12	20	30
-24	-44	-54	-31	-87	-87	-77	-65	-52	-5	-3	-4	-33	-43	-55	-74	-72	-66	-7	3	17
-24	-43	-53	-32	-95	-87	-64	-50	-37	1	0	-3	-40	-49	-61	-86	-87	-82	-22	-10	4

Fig. 6 (Continued)

Frame 02

C(H,K) FOR DH=DK= 4 04CUCL CUMULUS CELLS FR 04

-80	-86	-89	-93	-91	-89	-98	-99	-99	-91	-88	-83	-37	-24	-15	11	8	5	11	10	11
-68	-72	-75	-80	-81	-80	-87	-98	-86	-75	-71	-64	-17	-6	2	30	29	28	39	37	36
-58	-59	-60	-63	-64	-62	-61	-61	-60	-51	-46	-38	3	13	20	47	47	47	61	59	57
-56	-57	-56	-49	-47	-43	-35	-34	-34	-31	-25	-16	18	26	33	53	52	52	67	66	64
-58	-60	-60	-45	-39	-31	-21	-20	-19	-16	-11	-3	22	29	36	48	46	44	57	58	57
-60	-64	-66	-47	-38	-29	-21	-20	-19	-12	-7	-1	16	22	28	35	31	29	39	42	43
-60	-64	-67	-52	-43	-35	-33	-31	-29	-18	-11	-4	0	4	9	12	9	9	16	20	22
-63	-64	-67	-58	-51	-44	-37	-35	-32	-22	-15	-6	-11	-10	-8	-6	-8	-8	-5	-0	-0
-78	-75	-74	-62	-54	-46	-25	-23	-18	-16	-9	-1	-8	-10	-11	-16	-18	-18	-24	-22	-23
-110	-102	-95	-70	-57	-44	-7	-1	1	-4	0	9	10	6	0	-17	-20	-22	-40	-38	-39
-142	-131	-119	-77	-59	-41	10	17	19	7	11	20	27	25	19	-11	-15	-21	-44	-42	-42
-154	-142	-128	-74	-52	-31	25	31	32	18	21	30	43	43	40	8	1	-5	-30	-28	-28
-130	-122	-110	-58	-35	-15	40	46	46	32	34	40	57	60	62	40	30	20	-9	-10	-11
-71	-67	-59	-17	1	17	62	68	67	51	49	50	67	73	78	69	60	50	16	12	8
16	14	20	45	56	64	91	96	94	71	65	62	76	84	93	94	85	77	45	38	30
127	119	116	115	115	114	123	126	125	100	89	84	89	98	108	111	104	97	72	60	47
267	249	233	186	174	163	156	159	157	132	121	112	102	109	119	122	116	109	83	71	55
442	413	378	262	234	21[illegible]	182	183	183	157	148	141	112	114	119	115	109	103	81	62	45
641	598	541	341	295	258	200	199	199	172	164	157	111	106	104	90	87	81	52	34	19
840	787	708	428	365	314	215	208	204	182	175	167	107	96	88	67	63	57	24	8	-4
999	921	821	491	419	358	230	217	210	191	185	177	102	84	72	41	38	33	0	-13	-24
840	804	735	463	394	338	208	194	186	158	152	144	69	48	31	-8	-11	-13	-35	-42	-48
641	623	583	396	340	290	175	162	154	121	116	109	41	19	0	-48	-51	-53	-59	-60	-62
442	435	415	306	263	22[illegible]	132	123	116	[illegible]8	73	66	7	-11	-28	-80	-82	-79	-73	-69	-66
267	268	261	20[illegible]	180	154	87	79	71	29	23	16	-34	-50	-63	-104	-102	-95	-75	-67	-61
127	131	132	120	10[illegible]	90	48	38	26	-19	-24	-32	-73	-82	-90	-109	-102	-92	-62	-53	-47
16	21	27	44	42	39	16	4	-11	-62	-69	-76	-109	-113	-113	-101	-88	-75	-45	-37	-33
-71	-65	-56	-23	-14	-6	-12	-25	-43	-96	-102	-109	-134	-132	-127	-90	-74	-58	-34	-28	-25
-130	-127	-119	-70	-54	-39	-35	-47	-63	-109	-113	-119	-140	-133	-123	-72	-56	-41	-21	-15	-12
-154	-154	-147	-38	-69	-52	-40	-47	-59	-99	-104	-111	-126	-116	-103	-46	-31	-18	1	6	6
-142	-145	-139	-86	-67	-51	-27	-29	-38	-71	-78	-86	-95	-86	-73	-14	-0	12	25	25	23
-110	-114	-112	-74	-58	-43	-7	-6	-10	-35	-43	-51	-56	-48	-37	20	34	46	49	45	39
-78	-83	-83	-58	-43	-28	13	17	15	-2	-11	-18	-19	-13	-5	49	62	72	69	60	50
-63	-67	-68	-50	-36	-21	23	28	27	13	8	5	9	11	16	61	73	82	75	64	54
-60	-65	-66	-53	-38	-22	23	29	30	21	19	20	27	27	28	61	72	80	75	64	55
-60	-66	-69	-59	-45	-31	9	18	22	27	27	30	38	35	32	54	61	67	65	59	51
-58	-66	-71	-64	-53	-42	-9	0	8	30	32	34	38	34	30	42	45	48	52	48	43
-56	-65	-69	-62	-54	-48	-25	-16	-6	26	28	29	25	21	17	22	23	23	32	30	28
-58	-61	-60	-53	-51	-50	-38	-30	-21	18	21	22	10	4	-0	-3	-4	-4	8	9	10
-68	-65	-58	-45	-46	-47	-48	-44	-36	4	8	12	-1	-9	-17	-31	-33	-34	-20	-16	-13
-80	-72	-61	-40	-40	-42	-47	-46	-42	-8	-2	2	-9	-20	-30	-51	-55	-58	-52	-47	-43

Fig. 6 (Continued)

Frame 04

:(H,K) FOR DH=DK= 4 32CUCL CUMULUS CELLS FR 32

-107	-106	-101	-79	-63	-45	14	35	55	103	108	108	62	46	30	-10	-17	-22	-28	-30	-32
-109	-111	-110	-100	-84	-64	3	26	47	95	101	102	64	49	33	-8	-16	-21	-27	-29	-30
-108	-113	-114	-118	-102	-82	-11	10	31	74	81	84	60	48	35	-4	-12	-18	-24	-26	-26
-101	-107	-110	-126	-112	-95	-33	-12	5	45	55	62	57	49	38	4	-4	-13	-17	-18	-19
-83	-91	-94	-122	-113	-100	-57	-40	-24	17	31	42	56	51	44	14	2	-7	-11	-12	-13
-59	-65	-71	-108	-104	-97	-77	-64	-50	-1	17	32	64	63	57	26	12	1	-5	-6	-6
-37	-45	-51	-93	-92	-90	-92	-81	-69	-16	4	22	71	73	70	37	22	9	1	0	0
-28	-38	-44	-80	-80	-80	-93	-85	-75	-26	-6	12	71	77	76	47	32	19	10	9	8
-33	-44	-49	-69	-68	-66	-83	-79	-73	-35	-16	1	64	72	76	56	42	31	18	15	12
-42	-52	-55	-52	-47	-45	-67	-68	-67	-42	-24	-6	56	66	72	62	51	42	26	20	14
-40	-50	-53	-34	-27	-24	-56	-61	-65	-48	-31	-13	49	58	65	61	54	48	31	23	16
-19	-31	-36	-19	-14	-14	-53	-62	-68	-50	-33	-14	42	50	55	55	52	50	36	27	19
19	1	-10	-15	-16	-19	-56	-65	-71	-47	-31	-15	29	34	38	44	46	46	40	32	24
73	49	28	-12	-18	-25	-56	-62	-67	-45	-31	-19	6	9	12	30	36	42	46	41	31
148	118	89	12	-0	-13	-43	-49	-53	-45	-37	-32	-25	-23	-20	10	23	34	55	52	43
241	201	173	67	47	29	-15	-25	-33	-49	-50	-53	-60	-60	-55	-14	4	22	63	63	56
359	326	287	149	121	95	21	4	-13	-59	-69	-79	-93	-99	-93	-45	-21	2	65	69	67
510	477	434	247	204	168	56	27	-0	-74	-90	-105	-135	-136	-133	-79	-54	-24	59	70	72
693	659	605	347	287	23[illegible]	[illegible]3	45	9	-88	-109	-130	-168	-171	-163	-113	-86	-56	43	60	70
873	833	760	422	345	280	[illegible]	58	19	-92	-119	-144	-189	-190	-182	-133	-107	-78	25	49	66
999	929	841	462	377	304	109	70	31	-36	-116	-143	-191	-192	-183	-135	-112	-96	11	38	60
873	834	770	442	363	294	113	75	37	-77	-107	-135	-182	-182	-174	-129	-110	-86	-1	25	48
693	672	634	405	343	285	120	93	44	-68	-97	-123	-159	-159	-152	-111	-96	-77	-3	20	41
510	506	488	357	314	269	128	91	52	-58	-84	-107	-124	-122	-115	-83	-72	-59	1	21	40
359	367	366	303	275	241	129	96	61	-39	-61	-81	-78	-74	-68	-48	-43	-37	7	23	39
241	255	262	243	224	20[illegible]	117	90	62	-18	-37	-51	-35	-31	-27	-17	-20	-18	6	18	32
148	163	172	181	171	156	101	79	56	-3	-17	-27	-4	-1	2	0	-5	-7	1	11	21
73	84	[illegible]	125	123	117	87	70	52	9	-1	-10	9	12	14	6	-0	-5	-2	4	13
19	26	35	83	90	93	85	73	59	21	9	-0	10	11	11	2	-3	-7	2	9	18
-19	-13	-5	57	70	79	86	79	70	33	19	7	3	2	0	-3	-6	-7	16	25	32
-40	-35	-25	37	54	66	87	84	78	45	31	16	1	-1	-5	-5	-6	-5	39	40	49
-42	-35	-27	21	36	49	81	82	81	59	47	33	10	6	1	-1	-5	-6	32	43	51
-33	-26	-21	5	17	29	72	80	86	81	71	59	29	24	17	6	-0	-5	21	31	40
-28	-24	-22	-9	0	10	66	81	95	110	102	91	53	45	36	15	5	-3	0	7	13
-37	-34	-32	-25	-16	-7	61	81	102	137	132	125	80	69	56	24	10	-4	-24	-22	-19
-59	-54	-50	-42	-35	-27	51	77	102	154	152	147	101	88	72	24	4	-15	-53	-54	-51
-83	-77	-71	-62	-56	-49	35	64	94	157	159	155	110	96	78	14	-9	-32	-82	-85	-83
-101	-94	-88	-79	-75	-68	14	43	74	144	148	146	103	98	71	0	-24	-51	-107	-111	-109
-108	-103	-98	-93	-90	-84	-10	16	45	115	119	118	82	70	55	-13	-37	-62	-122	-126	-124
-109	-106	-103	-103	-101	-97	-40	-18	6	72	79	80	54	45	34	-25	-46	-68	-128	-131	-130
107	-107	-107	-111	-110	-108	-69	-53	-33	25	34	38	23	18	11	-35	-51	-69	-121	-124	-124

Fig. 6 (Continued)

Frame 32

C(H,K) FOR THETAK= 4 33CUCL CUMULUS CELLS FR 33

62	42	22	-33	-47	-52	-51	-47	-44	-30	-30	-34	-33	-31	-25	10	21	32	74	75	72
59	41	25	-15	-23	-28	-29	-28	-29	-27	-33	-40	-47	-45	-40	-10	-0	10	57	63	66
54	40	29	9	1	-4	-6	-8	-12	-21	-29	-39	-55	-53	-49	-31	-23	-12	33	43	50
40	34	33	26	21	15	12	9	5	-9	-18	-28	-53	-57	-55	-50	-42	-33	9	20	29
11	13	17	36	34	33	30	26	21	3	-4	-14	-53	-56	-57	-66	-60	-51	-15	-3	6
-26	-17	-7	37	45	51	54	49	43	19	9	-1	-50	-55	-60	-80	-75	-69	-36	-25	-16
-66	-50	-34	35	52	66	91	75	67	30	18	5	-46	-54	-61	-88	-85	-81	-56	-46	-39
-94	-73	-52	37	60	80	105	39	91	42	27	11	-42	-52	-59	-87	-87	-97	-75	-68	-63
-101	-78	-55	41	65	86	119	116	108	56	39	22	-28	-39	-48	-78	-82	-97	-92	-87	-84
-85	-67	-47	37	58	75	111	111	106	63	49	34	-11	-20	-29	-60	-68	-77	-99	-99	-98
-57	-44	-33	29	41	53	86	89	98	61	53	45	13	6	0	-26	-36	-47	-87	-93	-95
-25	-20	-15	8	10	15	44	53	58	53	53	51	40	39	37	22	14	2	-52	-63	-70
0	-1	-3	-11	-15	-15	3	22	34	50	58	64	74	79	83	80	71	59	-6	-22	-34
14	7	1	-22	-28	-29	-5	10	23	51	63	74	104	113	121	125	115	103	35	14	-3
35	24	13	-7	-14	-13	3	16	29	59	73	86	130	142	150	151	141	127	60	37	14
100 [illegible]	[illegible]	[illegible]	[illegible]	[illegible]	[illegible]	29	36	44	72	85	97	147	157	162	154	142	126	62	38	14
200 207	[illegible]	130	123	115	[illegible]	62	60	59	76	88	99	146	151	153	136	121	103	43	22	1
390	377	356	242	210	[illegible]	[illegible]	76	64	68	76	85	123	125	123	98	81	63	10	-5	-21
620	601	565	354	299	343	[illegible]	76	51	40	45	49	74	74	71	47	33	18	-24	-33	-41
834	806	749	427	349	281	[illegible]	57	25	-6	-9	-1	9	11	10	-0	-9	-18	-42	-45	-46
[illegible]	926	844	456	366	[illegible]	82	41	7	-33	-39	-44	-47	-43	-49	-34	-35	-38	-39	-36	-32
834	736	732	389	306	[illegible]	38	1	-30	-73	-81	-89	-99	-93	-86	-61	-53	-47	-25	-20	-13
620	593	551	307	243	[illegible]	16	-14	-42	-78	-89	-97	-115	-112	-105	-66	-52	-40	-6	0	5
390	378	360	[illegible]	179	136	10	-15	-38	-62	-71	-77	-95	-97	-94	-62	-46	-34	-0	4	8
200 207	207	[illegible]	156	133	104	17	-2	-19	-29	-35	-40	-59	-67	-71	-58	-48	-39	-12	-8	-4
100 [illegible]	[illegible]	107	114	107	[illegible]	37	22	5	9	5	-2	-25	-38	-50	-58	-55	-52	-30	-24	-19
35	40	50	83	86	81	61	50	41	46	39	32	0	-16	-33	-61	-62	-61	-39	-32	-26
14	13	17	54	62	64	81	77	74	75	63	53	10	-7	-23	-55	-55	-53	-27	-18	-10
0	-8	-12	19	31	41	85	89	92	87	72	57	6	-7	-21	-40	-38	-33	0	10	19
-25	-40	-46	-26	-14	-1	65	76	84	83	69	53	4	-4	-12	-16	-12	-4	33	45	53
-57	-75	-87	-44	-72	-58	18	35	50	65	56	46	8	4	0	11	16	26	64	73	79
-85	-105	-121	-137	-127	-115	-36	-14	4	50	50	47	21	20	21	36	44	51	85	90	93
-101	-122	-139	-171	-164	-152	-79	-55	-32	38	47	52	40	41	42	61	67	73	100	100	97
-94	-113	-131	-177	-173	-163	-95	-72	-51	29	43	52	52	54	54	72	77	80	94	90	83
-66	-83	-100	-150	-140	-142	-84	-66	-49	14	20	39	50	53	53	74	75	74	79	73	65
-26	-41	-56	-97	-97	-94	-49	-38	-30	-0	9	19	38	42	43	67	66	63	59	51	41
11	-0	-11	-35	-37	-36	-10	-8	-8	-13	-7	0	24	30	32	55	52	48	36	28	18
40	35	31	26	22	19	25	20	14	-15	-12	-7	14	22	26	40	34	27	8	0	-6
54	56	60	73	68	60	42	34	25	-13	-14	-11	3	9	13	19	11	4	-15	-21	-26
59	69	79	99	92	82	46	35	25	-11	-14	-14	-9	-4	-2	-1	-7	-14	-35	-40	-44
62	74	87	107	97	88	42	30	19	-13	-18	-20	-24	-21	-19	-25	-30	-35	-53	-56	-60

Fig. 6 (Continued)

Frame 33

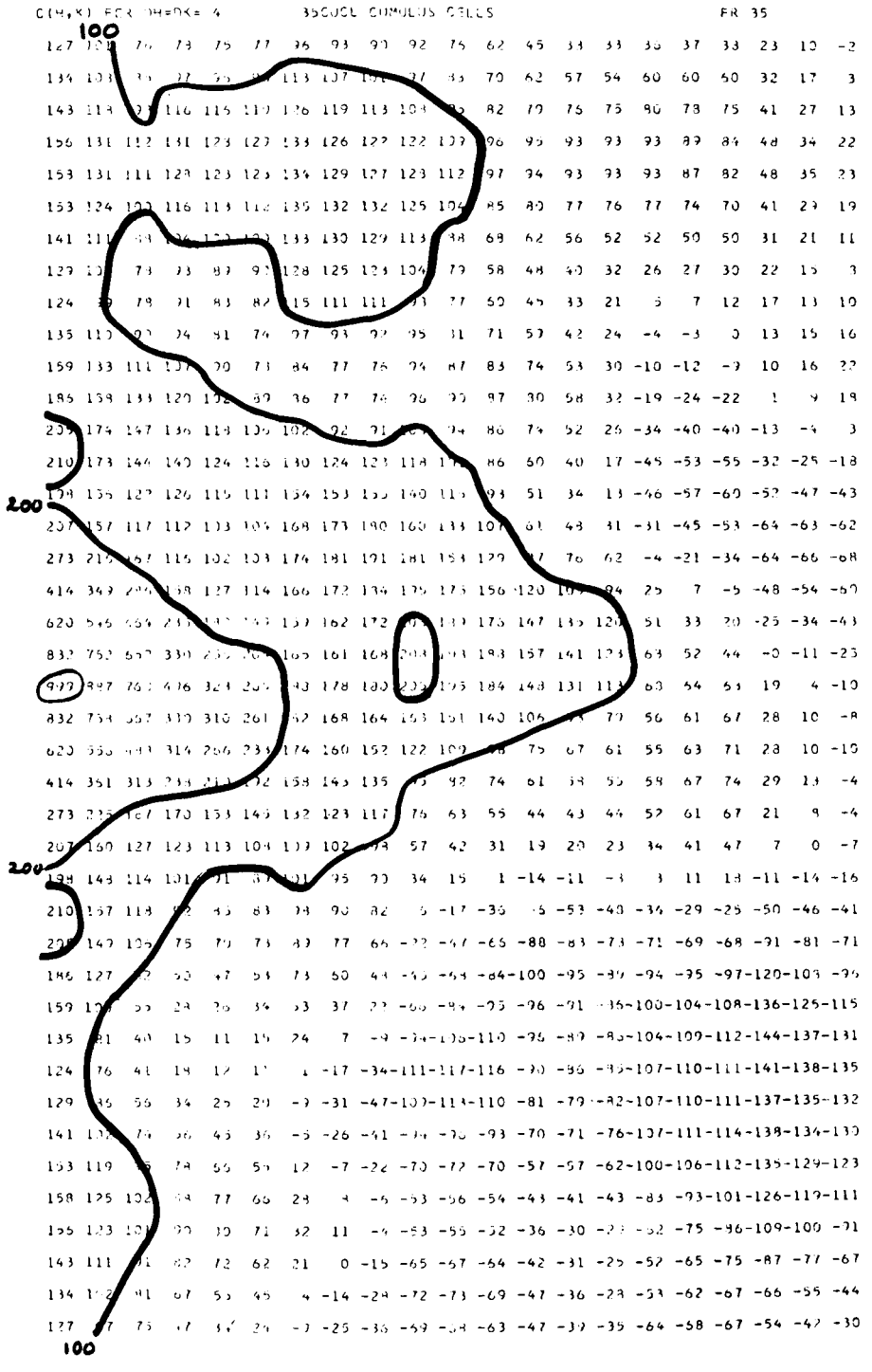

Fig. 6 (Continued)

Frame 35

C(H,K) FOR DH=DK= 4 40 FRAME 40

-17	-72	-102	-115	-103	-81	-5	15	28	46	39	32	-22	-39	-47	-41	-39	-29	0	5	8
-10	-66	-97	-117	-105	-85	-17	7	27	64	57	48	-23	-41	-48	-48	-45	-39	-13	-5	-0
8	-40	-65	-89	-82	-68	-17	6	24	70	61	47	-21	-41	-50	-55	-52	-45	-19	-10	-3
27	-11	-29	-58	-59	-54	-27	-4	11	54	42	24	-39	-55	-61	-68	-65	-51	-16	-4	3
57	25	13	-36	-43	-46	-35	-13	4	40	27	7	-47	-59	-61	-61	-59	-45	-2	9	15
86	55	41	-30	-47	-50	-33	-12	2	32	17	-3	-58	-68	-67	-52	-48	-35	8	19	22
99	66	50	-31	-50	-57	-42	-23	-11	23	13	-7	-61	-73	-70	-43	-36	-25	8	18	24
98	66	49	-28	-48	-60	-58	-37	-22	31	28	11	-51	-69	-71	-51	-46	-36	-1	7	15
101	71	56	-17	-39	-51	-66	-43	-23	53	57	41	-37	-62	-73	-64	-60	-51	-13	1	15
108	77	62	8	-15	-30	-62	-36	-14	80	85	70	-18	-46	-60	-75	-73	-66	-24	-4	16
129	95	78	20	-5	-23	-54	-27	-0	91	99	86	0	-27	-49	-93	-92	-80	-28	-7	14
164	126	10[illegible]	17	-12	-35	-48	-19	6	101	111	101	15	-11	-34	-104	-107	-93	-16	8	28
181	144	122	7	-27	-53	-52	-24	2	104	121	117	44	13	-13	-96	-106	-94	-4	23	45
179	139	114	-1	-34	-57	-65	-38	-14	93	112	117	81	50	22	-74	-88	-80	0	25	46
173	127	103	-15	-47	-65	-79	-51	-27	71	91	97	98	73	46	-48	-60	-52	16	37	51
170	125	103	-29	-66	-83	-73	-44	-19	53	70	74	94	75	51	-34	-45	-36	29	47	55
21[illegible]	178	154	4	-41	-69	-66	-30	-3	68	85	87	117	101	75	-20	-35	-28	40	62	76
287	248	21[illegible]	20	-25	-57	-76	-48	-24	63	83	93	134	115	88	-29	-48	-46	24	49	70
425	370	310	22	-35	-70	-99	-78	-63	24	54	77	133	114	88	-44	-65	-67	-8	14	33
651	564	460	8	-45	-84	-125	-109	-96	-3	36	69	142	124	99	-28	-55	-60	-16	3	20
999	804	655	12[illegible]	37	-13	-87	-77	-67	18	64	96	163	146	122	11	-18	-32	-15	-0	10
651	587	499	[illegible]0	5	-40	-132	-128	-125	-40	4	38	106	94	77	-2	-28	-46	-42	-30	-21
425	380	337	80	30	-8	-94	-92	-100	-24	19	46	99	83	66	4	-18	-34	-40	-26	-15
287	245	21[illegible]	41	1	-24	-80	-70	-68	14	50	71	96	71	43	-26	-45	-57	-47	-24	-5
217	183	166	23	-16	-47	-91	-71	-56	43	78	96	98	69	36	-59	-80	-91	-71	-42	-15
170	146	135	27	-14	-48	-114	-97	-83	33	75	100	99	70	38	-59	-79	-90	-83	-55	-23
173	154	147	67	27	-6	-100	-91	-82	21	66	98	113	89	60	-29	-47	-58	-65	-46	-18
179	159	150	80	45	12	-105	-104	-99	-10	34	65	97	78	53	-24	-38	-45	-49	-34	-15
181	158	153	86	51	18	-122	-124	-124	-49	-6	27	79	68	48	-20	-36	-42	-38	-26	-12
164	147	149	10[illegible]	67	27	-127	-132	-133	-66	-28	1	68	60	47	-23	-41	-50	-47	-38	-26
129	116	122	10[illegible]	67	27	-125	-127	-126	-56	-17	10	69	60	47	-24	-45	-56	-55	-48	-40
108	[illegible]	[illegible]	74	44	8	-123	-127	-129	-67	-24	7	71	62	44	-31	-55	-71	-74	-66	-56
101	89	92	59	32	1	-121	-126	-127	-80	-38	-1	79	71	53	-28	-56	-75	-83	-72	-57
98	89	89	48	23	-5	-123	-132	-136	-85	-45	-13	63	60	46	-25	-56	-77	-93	-81	-61
99	88	88	43	18	-10	-124	-132	-130	-76	-37	-11	49	48	40	-10	-38	-58	-80	-68	-47
86	79	81	42	15	-15	-128	-130	-124	-65	-31	-10	35	37	36	2	-20	-40	-59	-47	-29
57	56	67	34	10	-18	-131	-134	-128	-72	-41	-25	23	30	36	14	-7	-23	-45	-35	-21
27	38	61	46	22	-8	-118	-125	-124	-89	-61	-45	16	28	39	27	6	-10	-37	-29	-15
8	31	62	65	36	6	-101	-109	-111	-102	-81	-68	-3	11	27	31	11	-5	-38	-28	-15
-10	19	54	74	45	13	-79	-85	-88	-107	-92	-82	-25	-8	7	25	6	-11	-43	-34	-22
-17	11	49	81	54	23	-53	-58	-62	-96	-88	-82	-34	-16	-0	18	1	-16	-45	-38	-27

Fig. 6 (Continued)

Frame 40

C(H,K) FOR DH=DK= 4 42 FRAME 42

-52	-66	-62	-72	-67	-67	-94	-99	-105	-96	-85	-79	-74	-70	-73	-81	-75	-71	-67	-67	-67
-44	-57	-52	-55	-47	-46	-83	-89	-96	-101	-90	-82	-60	-52	-53	-74	-73	-72	-77	-77	-76
-26	-41	-38	-44	-31	-28	-70	-77	-86	-100	-91	-83	-48	-35	-34	-61	-64	-68	-85	-84	-81
-7	-21	-19	-31	-18	-15	-57	-64	-73	-94	-88	-82	-36	-18	-15	-48	-53	-62	-89	-87	-80
5	-4	1	-14	-5	-5	-52	-57	-64	-87	-85	-81	-33	-11	-4	-39	-47	-59	-89	-85	-76
13	7	18	6	8	1	-53	-55	-59	-84	-83	-80	-40	-15	-4	-34	-43	-55	-83	-79	-71
20	17	33	27	24	9	-49	-47	-47	-80	-81	-81	-52	-25	-11	-27	-35	-45	-75	-73	-66
20	20	40	41	33	13	-44	-36	-34	-75	-78	-81	-66	-40	-23	-16	-20	-29	-65	-64	-60
24	26	50	57	47	23	-33	-22	-17	-56	-58	-62	-69	-46	-30	0	2	-2	-48	-49	-44
34	37	64	72	60	39	-21	-12	-7	-32	-32	-38	-63	-44	-31	8	17	16	-27	-32	-29
54	56	84	95	84	63	-4	-1	2	-2	0	-5	-48	-35	-27	6	20	26	-6	-13	-12
81	81	108	129	119	[illegible]	21	20	20	29	36	32	-23	-17	-16	-1	13	22	11	5	3
116	111	135	162	153	132	47	42	39	59	71	70	2	2	-4	-15	-3	8	27	22	17
169	156	173	190	183	162	71	65	62	89	[illegible]	[illegible]	38	31	16	-27	-19	-7	42	40	35
234	215	222	207	198	178	[illegible]	88	83	110	130	137	79	65	42	-33	-29	-18	58	61	60
311	283	280	216	201	183	125	119	114	126	147	159	117	[illegible]	68	-33	-32	-23	67	77	81
397	359	339	212	191	172	150	152	151	148	161	172	148	128	94	-27	-28	-22	68	81	90
512	458	413	207	179	158	163	177	184	176	183	187	169	151	11[illegible]	-10	-16	-14	62	75	86
668	597	519	212	175	151	169	192	[illegible]	210	211	207	173	161	137	18	5	0	55	66	74
839	755	644	228	187	161	180	[illegible]	231	240	235	222	166	162	149	54	36	22	50	55	60
999	874	743	263	21[illegible]	186	212	243	266	266	254	234	155	158	154	95	75	55	46	44	46
839	776	675	246	1[illegible]7	166	202	235	257	240	224	20[illegible]	112	119	122	104	87	65	19	11	10
668	623	560	241	[illegible]96	166	[illegible]01	229	249	222	20[illegible]	176	[illegible]	[illegible]	104	112	10[illegible]	86	11	-4	-11
512	476	443	239	20[illegible]	176	19[illegible]	219	236	1[illegible]	179	155	[illegible]76	84	[illegible]	114	111	[illegible]7	4	-20	-33
397	365	344	236	215	[illegible]93	183	1[illegible]	20[illegible]	172	156	137	[illegible]63	73	8[illegible]	110	111	[illegible]9	-9	-39	-54
311	278	264	227	221	20[illegible]	171	175	175	141	133	12[illegible]	51	59	65	[illegible]	10[illegible]	88	-25	-54	-67
234	20[illegible]	191	205	215	215	165	155	143	109	110	10[illegible]	40	43	45	77	78	67	-33	-59	-71
169	135	129	180	[illegible]02	212	[illegible]55	135	113	76	84	91	36	35	32	47	50	44	-29	-52	-64
116	81	7[illegible]	149	179	196	134	10[illegible]	82	41	53	64	34	33	26	16	19	18	-24	-41	-52
81	45	39	[illegible]16	146	167	10[illegible]	76	49	10	23	37	33	34	23	-9	-8	-8	-22	-33	-40
54	15	8	71	[illegible]01	122	[illegible]71	45	21	-14	-1	14	28	30	18	-38	-40	-40	-28	-32	-33
34	-4	-16	23	50	71	40	20	4	-20	-5	11	26	26	10	-67	-74	-75	-40	-36	-30
24	-14	-29	-15	6	24	11	-0	-7	-8	6	22	25	22	3	-89	-100	-103	-54	-45	-31
20	-16	-32	-41	-27	-17	-26	-27	-26	0	16	32	22	15	-2	-101	-114	-119	-68	-56	-40
20	-12	-26	-55	-50	-47	-63	-60	-51	1	18	33	8	3	-11	-102	-117	-124	-79	-66	-49
13	-14	-26	-60	-61	-65	-94	-92	-82	-6	12	25	-13	-18	-29	-103	-116	-122	-84	-73	-58
5	-20	-28	-62	-66	-72	-107	-106	-99	-12	5	15	-33	-37	-47	-105	-114	-117	-80	-72	-59
-7	-27	-32	-64	-74	-83	-114	-110	-100	-18	-3	5	-43	-50	-61	-107	-111	-111	-74	-67	-58
-26	-40	-39	-62	-75	-90	-120	-111	-95	-22	-10	-2	-42	-51	-64	-105	-106	-103	-67	-64	-58
-44	-54	-48	-54	-68	-86	-121	-109	-91	-26	-19	-13	-37	-45	-57	-96	-95	-92	-59	-59	-56
-52	-62	-56	-50	-61	-77	-113	-101	-83	-28	-24	-20	-33	-37	-45	-78	-77	-74	-51	-52	-51

Fig. 6 (Continued)

Frame 42

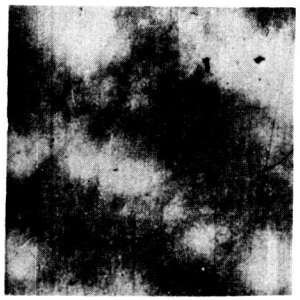

FR 14
AXRAT 0.45
DIRAX 125°—305°

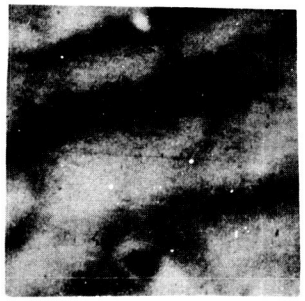

FR 16
AXRAT 0.31
DIRAX 64°—244°

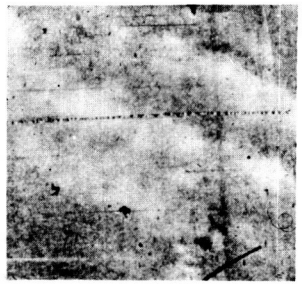

FR 30
AXRAT 0.26
DIRAX 114°—294°

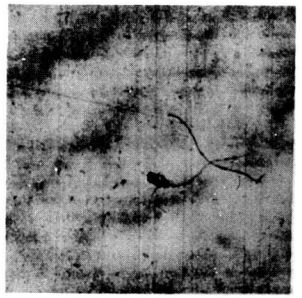

FR 47
AXRAT 0.44
DIRAX 55°—235°

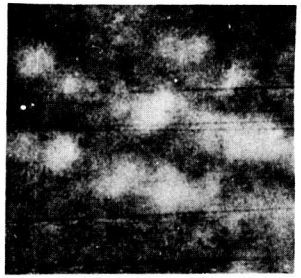

FR 50
AXRAT 0.21
DIRAX 108°—288°

FR 63
AXRAT 0.30
DIRAX 119°—299°

FR 64
AXRAT 0.36
DIRAX 115°—295°

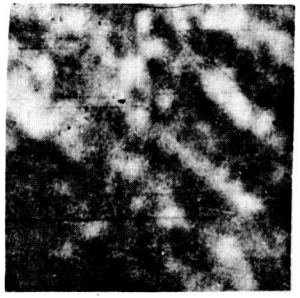

FR 66
AXRAT 0.44
DIRAX 131°—311°

Fig. 7 Samples of pattern SCSS. Legend indicates frame number (FR), axes ratio (AXRAT) and direction of major axis (DIRAX)

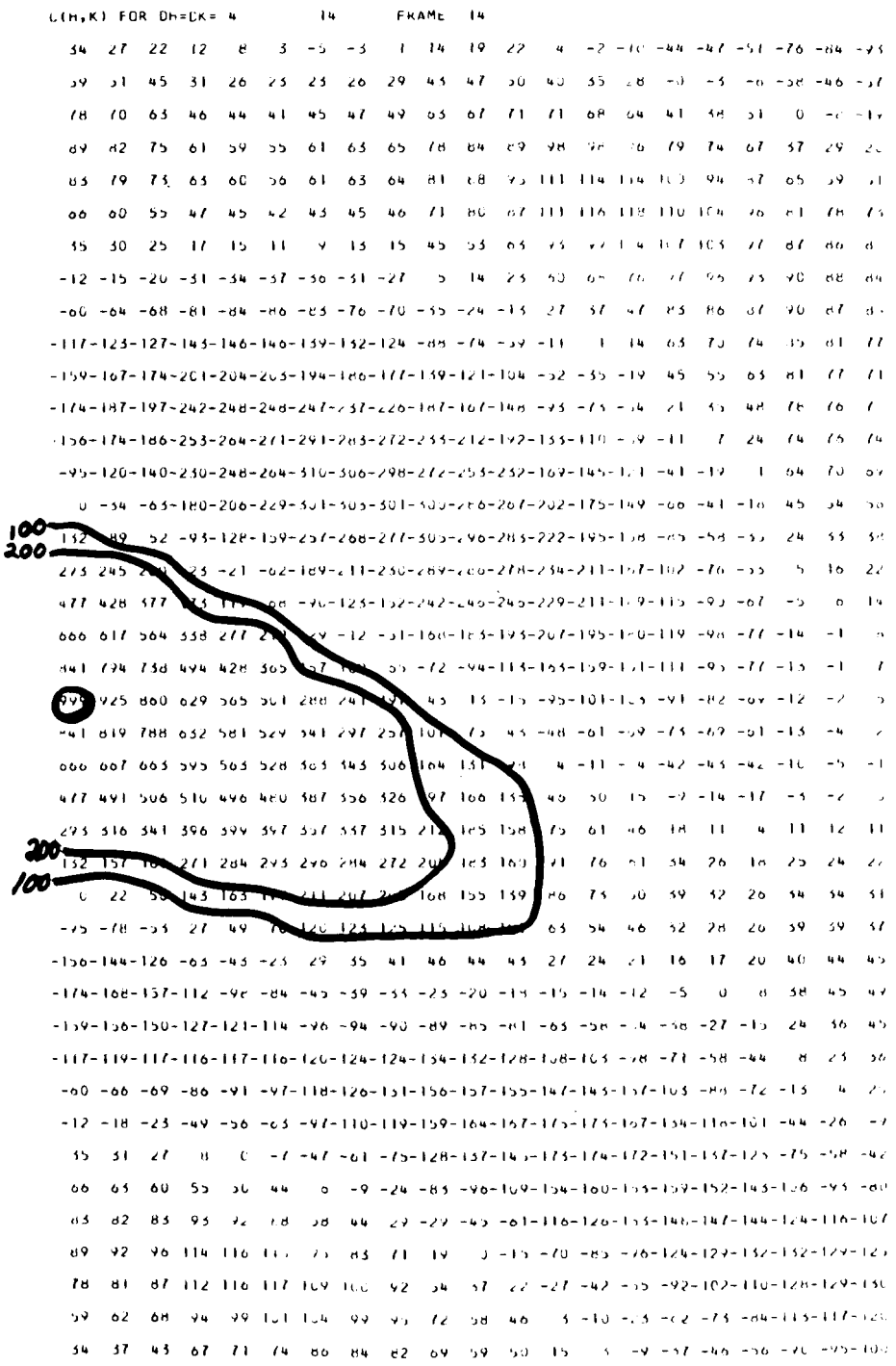

Fig. 8 Computer printouts of the autocorrelation for stratocumulus street patterns

Frame 14

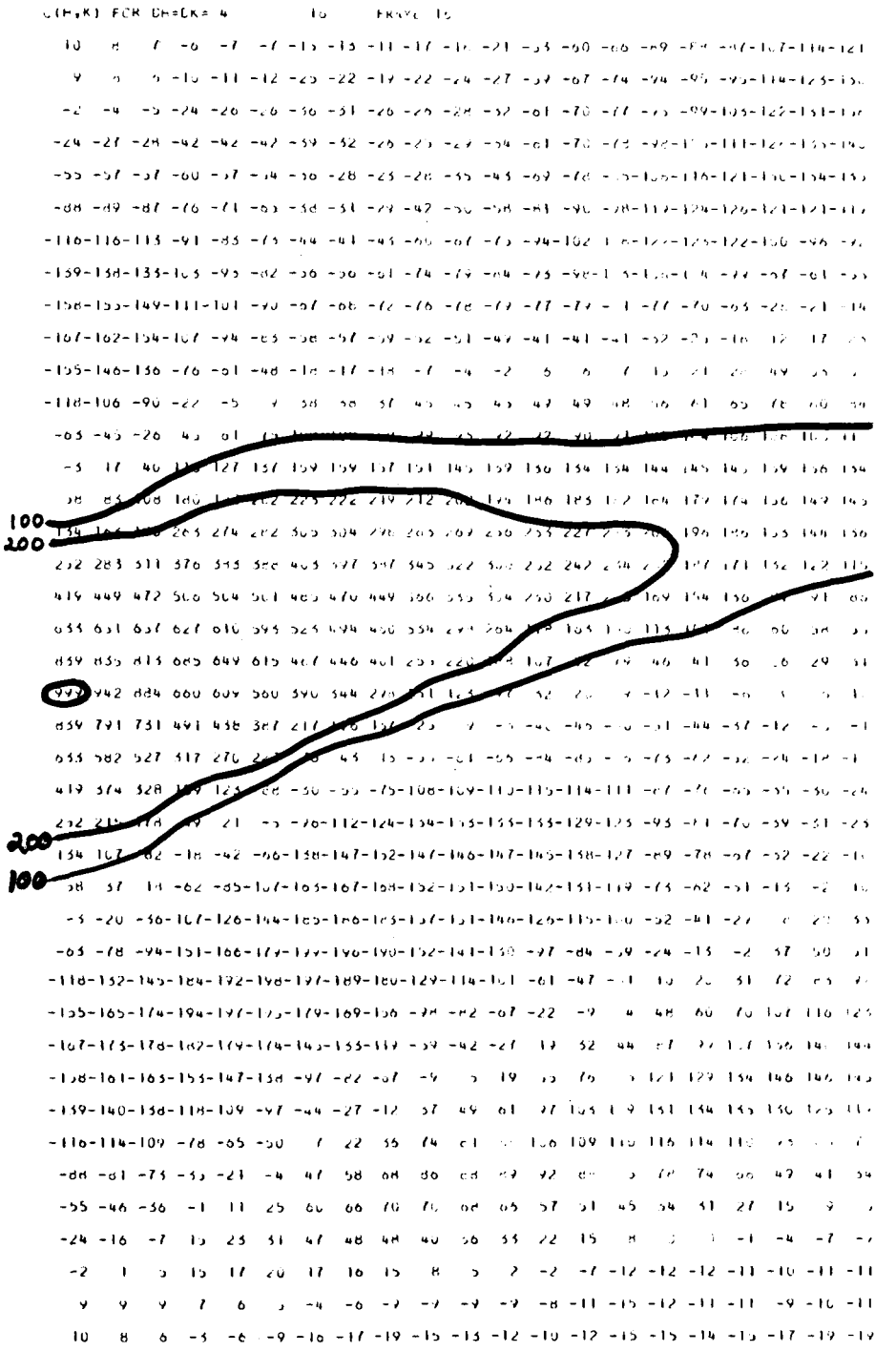

Fig. 8 (Continued)

Frame 16

C(H,K) FOR DH=DK= 4 30SCSS STRATOCUMULUS STREETS, STRAIGHT FR 30

-165	-158	-158	-154	-151	-143	-129	-120	-114	-99	-93	-85	-70	-59	-52	-41	-44	-49	-59	-62	-63
-164	-159	-158	-163	-158	-149	-129	-119	-114	-101	-97	-91	-82	-73	-67	-58	-61	-63	-66	-67	-68
-167	-162	-164	-174	-170	-160	-136	-125	-117	-96	-89	-81	-79	-72	-69	-65	-68	-70	-70	-68	-67
-170	-164	-165	-180	-175	-163	-131	-118	-107	-86	-76	-65	-56	-52	-51	-62	-64	-65	-66	-65	-65
-183	-179	-183	-194	-189	-177	-134	-121	-109	-84	-73	-59	-39	-35	-35	-49	-51	-51	-52	-52	-57
-192	-193	-198	-212	-204	-192	-145	-132	-120	-94	-82	-65	-32	-24	-24	-36	-36	-33	-26	-28	-33
-176	-185	-194	-219	-214	-203	-165	-151	-138	-104	-89	-72	-29	-19	-18	-28	-23	-17	-3	-4	-9
-136	-154	-168	-206	-206	-204	-193	-182	-167	-126	-111	-92	-44	-35	-34	-35	-25	-14	8	8	5
-67	-89	-107	-161	-170	-176	-193	-190	-179	-136	-118	-100	-57	-49	-48	-40	-27	-11	20	23	25
19	-5	-23	-84	-95	-109	-158	-164	-160	-134	-122	-107	-74	-69	-67	-56	-41	-23	23	28	31
96	71	57	11	1	-13	-82	-97	-103	-102	-93	-84	-74	-73	-76	-70	-56	-38	10	17	25
117	101	89	83	79	66	10	-7	-18	-31	-28	-26	-30	-37	-45	-54	-48	-36	2	9	15
94	87	9[illegible]	113	111	10[illegible]	70	55	51	43	43	44	26	20	10	-9	-8	-5	6	9	12
73	67	79	104	102	93	92	89	92	102	104	102	86	79	70	49	45	42	27	26	25
73	60	62	68	65	56	76	80	93	124	129	127	129	127	124	119	116	114	90	82	77
116	87	76	47	37	24	44	53	66	109	115	115	144	150	157	181	183	182	163	157	151
196	151	124	54	39	19	25	28	35	66	73	76	118	129	142	196	206	213	216	215	213
329	272	22[illegible]	109	83	56	32	28	28	40	40	37	85	94	107	165	178	189	225	236	245
524	455	394	213	176	136	80	66	56	30	20	13	46	48	55	104	119	132	194	210	227
737	665	594	350	300	25[illegible]	167	137	111	45	27	10	19	17	16	42	54	68	145	168	189
999	864	772	526	473	423	304	268	228	114	82	56	26	10	-5	-4	2	12	79	101	121
737	714	683	558	520	485	399	366	325	194	155	122	59	33	6	-27	-26	-23	26	41	53
524	524	521	520	505	491	465	442	408	295	255	219	128	91	57	-11	-18	-21	0	6	10
329	335	341	404	407	409	443	435	417	358	325	296	208	168	131	42	26	15	6	4	-0
196	197	19[illegible]	268	272	281	343	346	338	350	334	317	256	223	192	101	81	66	34	25	15
116	111	105	148	152	156	213	218	216	274	267	263	249	227	203	142	124	108	69	58	47
73	61	51	71	71	71	9[illegible]	102	102	174	176	175	184	170	157	133	125	116	86	78	70
73	62	49	45	37	31	26	26	21	79	79	77	86	78	70	78	78	79	78	72	66
94	89	78	49	35	24	-6	-11	-20	6	2	-2	0	-7	-13	15	22	31	46	46	45
117	121	117	75	57	41	-4	-14	-26	-22	-33	-47	-63	-70	-74	-46	-39	-32	-6	-4	-3
9[illegible]	111	119	96	80	66	21	12	0	-16	-33	-52	-82	-92	-101	-92	-90	-87	-64	-60	-56
19	44	64	81	73	64	44	40	34	11	-2	-24	-77	-90	-102	-115	-119	-124	-113	-109	-104
-67	-39	-13	33	33	34	45	50	52	36	24	4	-60	-75	-90	-115	-121	-127	-131	-130	-127
-136	-113	-91	-43	-35	-26	11	24	35	41	35	25	-30	-47	-60	-92	-99	-107	-124	-125	-124
-176	-161	-146	-116	-110	-103	-52	-35	-19	16	20	19	-17	-31	-40	-73	-83	-93	-113	-116	-115
-192	-183	-172	-162	-158	-154	-118	-100	-82	-29	-15	-8	-11	-17	-21	-55	-65	-76	-95	-98	-98
-183	-176	-166	-170	-167	-165	-152	-141	-129	-86	-69	-56	-32	-31	-30	-56	-65	-76	-87	-88	-86
-170	-164	-155	-160	-154	-151	-158	-152	-147	-124	-109	-98	-67	-65	-62	-74	-77	-82	-85	-87	-83
-167	-161	-151	-152	-144	-139	-146	-142	-139	-131	-119	-110	-93	-91	-89	-96	-95	-96	-93	-89	-84
-164	-156	-144	-138	-130	-123	-125	-122	-118	-114	-104	-96	-95	-92	-90	-103	-104	-107	-103	-100	-95
-165	-156	-144	-131	-120	-111	-114	-110	-105	-95	-82	-75	-79	-77	-74	-88	-91	-96	-105	-104	-100

30SCS053

Fig. 8 (Continued)

Frame 30

C(H,K) FOR DH=DK= 4 47 FR 47

-44	-43	-44	-36	-37	-40	-46	-46	-48	-56	-70	-72	-75	-72	-67	-64	-65	-64	-56	-48	-39
-40	-38	-37	-24	-23	-24	-32	-36	-42	-67	-72	-72	-72	-68	-64	-58	-56	-53	-35	-26	-18
-56	-54	-50	-33	-28	-26	-35	-43	-51	-73	-76	-74	-65	-63	-58	-40	-34	-29	-2	6	13
-38	-33	-29	-12	-7	-2	-17	-27	-35	-62	-64	-61	-49	-44	-40	-18	-13	-10	15	20	25
-21	-16	-12	0	4	4	-22	-33	-42	-74	-73	-70	-62	-58	-54	-36	-32	-26	-5	-0	2
0	2	4	16	16	15	-16	-26	-37	-61	-60	-58	-53	-49	-49	-43	-39	-37	-19	-12	-7
41	35	33	30	27	21	-19	-31	-41	-68	-69	-69	-61	-61	-62	-64	-65	-61	-49	-42	-36
32	21	18	-2	-5	-10	-55	-53	-69	-82	-80	-77	-61	-59	-60	-65	-68	-70	-65	-58	-52
44	28	17	-11	-18	-25	-70	-78	-83	-78	-74	-67	-43	-45	-50	-59	-64	-68	-72	-68	-63
12	-9	-23	-52	-56	-60	-96	-102	-107	-87	-79	-71	-38	-40	-46	-50	-53	-56	-62	-62	-57
-24	-44	-54	-71	-71	-72	-89	-92	-96	-57	-49	-42	-17	-20	-27	-27	-30	-32	-40	-42	-39
-76	-90	-95	-90	-85	-81	-78	-78	-78	-28	-19	-15	-6	-13	-20	-13	-14	-16	-33	-39	-37
-135	-139	-133	-90	-76	-63	-40	-38	-35	19	27	31	31	27	24	22	20	15	-9	-17	-17
-147	-140	-122	-46	-27	-11	21	25	26	67	69	69	62	57	52	32	25	21	-1	-4	-4
-145	-122	-91	14	36	50	73	80	83	107	103	[illegible]	84	79	71	43	37	36	24	23	24
-54	-25	10	125	145	159	165	160	154	155	147	136	10[illegible]	93	84	47	43	42	39	39	42
66	96	127	221	233	237	210	198	184	161	151	140	[illegible]3	85	78	50	47	48	49	50	54
263	289	314	351	344	330	267	248	230	175	162	149	[illegible]0	91	86	65	61	58	54	57	64
505	515	518	444	412	378	261	234	21[illegible]	138	121	[illegible]	57	50	46	39	37	33	34	39	47
710	692	661	471	423	372	219	[illegible]0	165	[illegible]2	72	62	31	32	33	34	34	34	52	57	65
999	876	784	475	404	341	[illegible]8	138	11[illegible]	32	23	18	3	8	14	18	23	26	48	54	61
710	644	571	269	20[illegible]	148	[illegible]	3	-15	-26	-60	-57	-51	-27	-15	-8	15	22	27	52	56	60
505	435	366	[illegible]	56	14	-83	-90	-89	-80	-66	-49	-0	12	18	32	36	39	54	57	59
263	20[illegible]	[illegible]	-69	-106	-132	-170	-162	-148	-93	-69	-47	15	25	30	36	37	41	52	53	52
66	13	-32	-173	-189	-196	-176	-154	-129	-37	-9	13	70	75	76	67	63	66	63	60	58
-54	-09	-133	-215	-213	-203	-134	-106	-78	29	54	72	98	91	82	58	54	54	45	40	35
-145	-179	-1[illegible]	-218	-1[illegible]8	-170	-55	-24	2	99	117	127	121	103	86	55	50	48	32	26	20
-147	-166	-174	-136	-107	-70	53	80	102	169	173	168	114	90	66	27	21	18	0	-5	-12
-135	-140	-137	-60	-27	9	116	134	147	179	173	159	73	43	18	-11	-13	-14	-28	-31	-37
-76	-73	-64	28	56	89	164	172	174	158	144	125	29	3	-19	-40	-38	-36	-45	-45	-45
-24	-13	-2	76	95	116	157	156	151	95	73	50	-36	-55	-70	-77	-71	-64	-64	-60	-56
12	27	39	103	112	121	126	120	109	38	15	-5	-81	-90	-96	-84	-73	-64	-52	-46	-41
44	57	65	99	100	99	76	52	47	-37	-59	-77	-124	-124	-121	-92	-82	-71	-51	-45	-40
32	40	44	49	44	40	7	-8	-26	-101	-114	-124	-133	-124	-111	-61	-50	-39	-14	-9	-4
41	41	36	19	8	-0	-49	-65	-80	-135	-139	-139	-126	-110	-94	-29	-17	-8	6	9	11
0	-4	-13	-39	-48	-57	-102	-113	-124	-144	-138	-130	-93	-75	-56	13	22	30	43	41	39
-21	-34	-46	-65	-70	-77	-102	-105	-106	-102	-94	-85	-38	-21	-5	44	49	54	54	50	47
-38	-54	-70	-91	-94	-96	-100	-97	-92	-63	-54	-46	-3	8	19	49	49	50	36	30	26
-56	-71	-84	-96	-95	-91	-71	-62	-53	-14	-6	2	35	40	43	46	43	38	12	6	1
-40	-54	-66	-73	-69	-63	-31	-20	-9	18	21	25	36	33	29	8	0	-6	-38	-45	-46
-44	-53	-61	-59	-54	-47	-13	-1	9	24	22	20	6	-0	-8	-37	-43	-51	-83	-88	-86

Fig. 8 (Continued)

Frame 47

C(H,K) FOR DH=DK= 4 50SCSS STRATOCUMULUS STREETS, STRAIGHT FR 50

-86	-94	-95	-97	-102	-104	-120	-127	-129	-126	-127	-127	-134	-135	-134	-127	-125	-122	-100	-92	-82
-98	-106	-106	-107	-112	-117	-133	-138	-138	-132	-134	-134	-146	-150	-149	-144	-143	-140	-121	-113	-104
-122	-129	-129	-125	-129	-132	-141	-143	-141	-134	-137	-140	-158	-162	-162	-155	-155	-153	-141	-134	-125
-143	-152	-152	-143	-144	-144	-141	-141	-137	-130	-135	-140	-165	-170	-171	-162	-161	-160	-153	-147	-140
-156	-167	-169	-158	-157	-152	-138	-135	-128	-125	-133	-141	-168	-172	-171	-162	-162	-160	-155	-151	-146
-152	-166	-170	-167	-167	-164	-144	-140	-132	-129	-140	-148	-167	-169	-167	-150	-150	-148	-144	-142	-140
-130	-149	-157	-164	-169	-169	-152	-149	-142	-140	-150	-157	-163	-163	-159	-139	-139	-137	-134	-133	-131
-81	-106	-117	-144	-155	-162	-154	-154	-151	-155	-163	-168	-166	-165	-160	-142	-142	-141	-135	-133	-129
-19	-44	-60	-101	-118	-130	-136	-140	-141	-158	-168	-174	-174	-173	-168	-156	-157	-155	-145	-141	-136
51	27	10	-35	-54	-70	-92	-104	-112	-145	-160	-169	-180	-182	-179	-172	-175	-175	-163	-157	-150
114	96	80	43	26	13	-21	-38	-52	-103	-121	-135	-158	-163	-165	-173	-177	-178	-171	-166	-156
150	136	128	115	102	93	59	39	19	-37	-56	-70	-95	-105	-112	-137	-144	-149	-155	-153	-147
146	138	136	144	136	130	115	97	79	34	19	8	-1	-13	-25	-66	-78	-89	-114	-117	-117
103	95	91	120	117	114	122	115	107	92	83	81	95	84	73	17	0	-14	-52	-61	-68
55	46	46	67	66	67	94	93	92	119	122	128	158	150	139	89	70	54	12	1	-10
47	32	28	37	34	33	52	55	62	113	121	130	164	156	145	116	105	93	63	51	40
121	101	90	70	58	46	40	38	41	83	87	96	116	106	96	95	92	88	77	69	63
294	270	249	181	153	125	86	63	54	58	53	51	45	35	25	44	46	48	58	57	58
543	513	479	343	299	258	160	133	108	63	46	30	-5	-18	-27	-7	-4	-0	25	30	35
784	749	703	508	455	405	282	244	204	114	87	61	-1	-17	-28	-27	-27	-26	-5	-0	6
999	916	854	643	593	547	434	393	351	236	205	171	93	71	53	20	9	1	-0	0	3
784	760	723	599	567	539	478	448	414	318	287	257	181	158	136	77	60	43	7	2	2
543	532	516	501	493	486	488	471	450	389	363	338	280	259	237	173	149	129	60	49	40
294	289	288	349	363	373	423	419	409	388	373	357	325	311	295	244	222	199	123	105	94
121	121	123	206	226	243	309	313	310	323	318	312	316	309	301	281	264	243	174	159	142
47	43	42	99	113	125	179	185	186	219	223	223	249	249	248	262	252	238	185	172	156
55	45	37	48	54	56	78	82	84	113	118	119	148	152	154	189	186	178	145	135	122
103	89	77	56	53	48	42	40	37	38	36	34	49	52	54	82	81	76	65	62	57
146	133	121	94	89	81	62	56	47	17	6	-5	-20	-19	-19	-14	-17	-21	-17	-13	-10
150	144	135	130	128	120	94	84	72	20	3	-16	-61	-66	-72	-90	-93	-97	-85	-77	-70
114	114	113	140	141	136	108	98	83	33	17	-2	-61	-71	-80	-115	-119	-122	-115	-104	-96
51	58	64	119	124	120	94	85	74	38	27	12	-35	-45	-55	-99	-104	-109	-110	-102	-97
-19	-6	5	69	74	70	52	47	39	27	22	14	-11	-18	-26	-61	-68	-74	-90	-87	-85
-81	-70	-57	-6	-2	-4	-7	-6	-9	-1	0	-0	-0	-3	-8	-32	-35	-40	-66	-67	-71
-130	-121	-113	-82	-77	-77	-63	-58	-56	-35	-30	-27	-12	-12	-14	-19	-19	-20	-44	-49	-58
-152	-146	-142	-131	-129	-128	-103	-94	-89	-65	-60	-57	-40	-37	-36	-27	-24	-21	-32	-37	-45
-156	-151	-149	-148	-146	-146	-123	-112	-104	-88	-85	-83	-68	-65	-62	-43	-37	-32	-27	-29	-35
-143	-139	-137	-141	-140	-141	-125	-115	-108	-100	-99	-100	-85	-80	-75	-52	-47	-43	-30	-31	-35
-122	-122	-123	-132	-133	-134	-123	-114	-109	-106	-106	-106	-89	-84	-79	-62	-56	-52	-43	-42	-43
-98	-101	-105	-117	-116	-116	-107	-101	-98	-99	-98	-98	-81	-78	-77	-69	-63	-60	-57	-57	-57
-86	-89	-93	-102	-101	-99	-90	-86	-85	-89	-89	-89	-79	-78	-78	-77	-72	-68	-73	-73	-71

Fig. 8 (Continued)

Frame 50

C(H,K) FOR DH=DK= 4 63SCSS STRATOCUMULUS STREETS, STRAIGHT FR 63

27	22	27	57	59	57	11	-13	-37	-88	-91	-88	-51	-45	-39	-3	1	6	22	19	21
6	-2	-3	31	41	52	72	59	41	-35	-52	-65	-67	-60	-51	-10	-8	-7	-6	-10	-8
2	-11	-11	8	14	23	66	69	68	39	22	4	-52	-59	-61	-28	-21	-17	-13	-19	-20
28	12	10	11	16	12	36	41	49	76	71	62	2	-14	-28	-40	-37	-32	-8	-9	-8
73	53	48	35	29	24	16	18	21	56	62	65	46	35	22	-22	-31	-36	-16	-12	-6
100	78	70	56	50	45	22	14	6	5	9	15	41	41	39	4	-9	-23	-38	-38	-32
100	88	85	78	75	72	64	52	39	-9	-17	-22	-3	4	9	13	7	-3	-28	-35	-38
50	49	59	89	90	92	106	100	91	34	15	-3	-43	-43	-41	-21	-13	-9	-16	-23	-29
-19	-15	3	77	85	90	111	115	110	91	75	56	-25	-40	-51	-54	-46	-38	-34	-40	-43
-32	-44	-35	45	58	70	100	102	103	107	102	96	43	25	7	-32	-36	-40	-70	-76	-78
36	4	-8	3	10	19	70	77	83	96	98	99	92	86	77	30	17	2	-67	-78	-84
100	79	60	8	-4	-14	8	21	35	78	81	84	91	92	92	73	62	46	-32	-48	-50
134	112	104	61	38	16	-16	-14	-7	42	50	56	70	72	75	80	76	68	9	-7	-18
100	92	94	95	82	66	17	7	1	3	5	7	33	39	45	64	54	63	31	20	11
56	41	47	85	84	83	75	67	59	19	5	-2	1	8	14	36	36	34	21	16	14
16	-0	1	30	35	40	77	83	86	57	40	25	-6	-8	-9	0	-1	-5	-19	-21	-19
-3	-26	-27	-19	-22	-22	7	18	30	53	46	39	2	-6	-14	-34	-38	-42	-57	-60	-60
50	6	-9	-26	-35	-44	-60	-61	-56	-11	-4	3	11	8	3	-34	-45	-54	-59	-72	-71
100	192	135	-3	-25	-43	-90	-131	-138	-75	-85	-72	-10	4	13	2	-9	-22	-50	-52	-49
200	551	448	[illegible]	29	-12	-87	-100	-112	-150	-154	-150	-88	-62	-36	23	24	19	-14	-21	-23
[illegible]	907	815	360	266	[illegible]	13	-7	-25	-93	-111	-124	-121	-102	-77	20	40	54	58	51	45
659	676	681	487	405	325	[illegible]	23	-15	-109	-127	-142	-179	-175	-167	-100	-75	-50	21	28	32
200	305	352	457	443	417	[illegible]	155	[illegible]	-48	-60	-87	-146	-152	-156	-150	-137	-120	-45	-28	-12
100	53	[illegible]	365	287	311	286	251	[illegible]	67	35	6	-87	-99	-109	-133	-136	-136	-111	-97	-80
-3	-20	-13	64	[illegible]	[illegible]	[illegible]	218	220	172	145	[illegible]	-6	-28	-47	-101	-110	-118	-140	-134	-124
16	-6	-10	-17	-13	-4	[illegible]	162	126	182	180	171	[illegible]	54	25	-68	-81	-92	-120	-119	-117
56	34	29	-11	-22	-28	-6	3	16	[illegible]	102	117	138	91	66	-52	-71	-85	-101	-100	-98
100	85	82	38	22	8	-5	-9	-14	-16	-6	7	51	56	51	-26	-44	-60	-85	-84	-82
134	119	118	86	69	55	34	28	21	-36	-48	-53	-44	-30	-19	-13	-17	-25	-58	-63	-66
100	104	138	[illegible]	85	75	48	44	40	-5	-21	-36	-84	-81	-77	-43	-32	-25	-32	-38	-43
36	34	48	79	75	70	42	34	28	4	0	-2	-38	-45	-53	-70	-64	-58	-42	-40	-38
-32	-48	-41	14	22	26	21	11	-0	-26	-21	-12	5	5	0	-50	-57	-62	-65	-60	-54
-19	-51	-61	-48	-44	-37	-22	-26	-32	-48	-43	-34	-2	6	10	-10	-15	-22	-54	-56	-56
50	18	2	-45	-57	-68	-75	-73	-70	-51	-46	-41	-26	-17	-11	6	14	18	-5	-13	-22
100	81	72	15	-7	-30	-94	-98	-97	-66	-60	-55	-47	-41	-36	-10	2	14	27	25	20
131	89	90	70	53	32	-50	-65	-77	-86	-85	-81	-67	-60	-55	-40	-32	-22	11	21	27
73	62	68	90	84	75	23	5	-13	-72	-81	-85	-80	-69	-60	-53	-51	-49	-25	-13	-0
28	14	15	49	53	56	49	43	33	-35	-54	-69	-85	-73	-62	-48	-47	-49	-51	-44	-35
2	-12	-14	-2	-0	2	10	13	14	-9	-24	-39	-76	-69	-61	-38	-33	-31	-42	-43	-44
6	-8	-14	-28	-32	-35	-44	-43	-41	-30	-30	-31	-46	-43	-42	-35	-29	-25	-20	-20	-22
27	9	-1	-42	-53	-62	-90	-96	-100	-90	-82	-72	-45	-36	-31	-33	-30	-27	-15	-12	-10

Fig. 8 (Continued)

Frame 63

C(H,K) FOR DH=DK= 4 G4SCSS STRATOCUMULUS STREETS, STRAIGHT FR 64

47	47	41	19	9	6	-9	-8	-1	25	28	27	17	12	10	-5	-7	-6	-0	3	7
52	52	51	40	34	35	12	7	6	23	24	26	36	34	33	15	11	6	-8	-10	-9
31	35	34	33	37	46	16	8	0	10	8	9	31	37	41	42	40	37	8	1	-2
2	6	3	-2	11	22	27	23	14	0	-5	-10	10	13	16	45	51	54	36	26	17
2	1	-8	-30	-21	-17	8	16	24	14	2	-5	-4	-4	-6	13	23	34	38	36	33
26	16	3	-31	-30	-42	-42	-31	-15	4	9	-2	-9	-13	-17	-17	-16	-10	0	7	9
50	39	32	4	-6	-21	-53	-52	-46	-27	-22	-15	-4	-11	-16	-20	-25	-39	-38	-30	-24
33	32	34	23	3	-0	-32	-37	-44	-51	-45	-38	-11	-19	-20	-19	-23	-32	-59	-58	-57
9	13	22	25	11	2	-12	-16	-22	-62	-59	-51	-32	-37	-39	-31	-33	-39	-67	-70	-74
-11	-5	8	25	17	11	-1	0	-1	-39	-37	-31	-23	-37	-44	-57	-56	-57	-66	-69	-72
-57	-50	-34	-8	-8	-11	-7	-1	-0	-12	-14	-14	-9	-15	-25	-65	-71	-77	-82	-79	-78
-77	-75	-61	-24	-28	-31	-17	-13	-9	-4	-1	1	-0	-0	-5	-55	-66	-77	-92	-90	-86
-39	-48	-44	-14	-14	-13	-17	-18	-13	14	26	25	16	12	5	-37	-51	-67	-86	-86	-83
28	10	1	-11	-9	-2	-9	-14	-14	20	27	26	17	7	-3	-31	-41	-50	-71	-74	-77
34	80	81	23	15	13	4	13	13	28	21	21	8	-1	-11	-36	-44	-45	-43	-49	-54
95	104	121	95	78	68	39	32	30	55	57	54	35	29	17	-33	-42	-42	-31	-35	-42
88	102	109	117	116	114	35	39	26	39	45	55	73	78	75	19	6	0	-14	-18	-24
117	120	99	102	112	122	78	65	50	15	16	20	55	75	85	52	90	74	30	28	17
222	120	131	67	73	84	72	56	64	33	21	8	4	10	17	55	66	73	73	53	47
561	468	355	12	40	81	49	48	54	63	54	39	12	3	-7	-1	9	17	59	60	50
999	821	670	313	275	91	9	47	81	82	77	72	72	64	51	11	4	-0	22	26	23
561	563	550	399	343	294	140	119	10	44	33	25	37	36	34	-4	-14	-27	-34	-35	-37
222	237	263	314	403	295	172	175	158	75	50	37	35	34	35	14	5	-3	-29	-34	-38
117	102	100	145	120	170	136	137	182	120	94	76	35	30	31	20	14	9	5	2	-2
88	69	57	33	40	44	34	112	121	121	139	80	15	6	2	3	-2	-8	-3	3	7
95	92	70	15	7	-4	12	10	29	58	57	52	-5	-18	-28	-37	-39	-39	-32	-26	-17
84	77	69	22	4	-8	-20	-23	-24	-11	-4	-5	-35	-40	-48	-72	-77	-80	-74	-58	-58
28	33	37	23	9	0	-29	-36	-44	-53	-50	-48	-54	-68	-59	-66	-71	-77	-98	-99	-94
-39	-30	-13	16	7	5	-19	-25	-36	-58	-57	-55	-73	-77	-75	-57	-51	-46	-62	-69	-78
-77	-73	-72	-34	-12	-20	-20	-30	-19	-27	-30	-24	-72	-81	-85	-72	-59	-46	-25	-29	-34
-57	-66	-66	-53	-51	-45	-37	-43	-26	5	3	9	-44	-62	-71	-77	-73	-54	-23	-15	-10
-11	-17	-23	-41	-44	-38	-35	-39	-41	1	14	25	-17	-35	-49	-72	-72	-59	-45	-38	-28
9	5	0	-13	-21	-20	-24	-32	-39	-33	-26	-18	-23	-35	-47	-67	-64	-50	-46	-44	-40
33	26	21	-1	-0	-2	-13	-17	-20	-25	-30	-33	-44	-49	-57	-66	-64	-56	-21	-16	-15
50	51	51	26	27	28	6	1	-3	-13	-13	-16	-39	-46	-52	-57	-52	-45	-4	1	4
26	28	34	55	61	63	50	46	44	5	0	-2	-18	-24	-31	-41	-36	-29	7	13	16
2	0	5	50	55	77	92	93	94	47	29	15	-5	-5	-7	-13	-15	-11	29	31	30
2	-8	-16	9	22	34	80	84	87	57	51	34	-1	-2	-5	1	-1	-2	21	27	28
31	16	2	-11	-8	-3	40	51	59	55	50	41	25	21	17	15	13	11	17	22	25
52	43	36	5	-3	-9	13	22	30	35	35	33	39	40	40	41	39	35	31	35	39
47	39	36	19	7	1	5	13	18	27	25	24	39	44	47	50	48	47	47	50	50

Fig. 8 (Continued)

Frame 64

C(H,K) FOR DH=DK= 4 66SCSS STRATOCUMULUS STREETS, STRAIGHT FR 66

-82	-73	-68	-100	-105	-106	-101	-100	-99	-85	-78	-74	-64	-58	-51	-44	-47	-53	-62	-64	-63
-99	-85	-74	-92	-95	-97	-92	-92	-91	-82	-77	-73	-57	-52	-47	-34	-33	-35	-45	-49	-50
-107	-98	-90	-90	-89	-88	-81	-78	-75	-73	-72	-74	-64	-58	-53	-34	-28	-25	-24	-27	-28
-103	-101	-98	-93	-89	-83	-69	-64	-59	-54	-58	-66	-75	-72	-66	-38	-31	-25	-2	-0	0
-85	-88	-88	-94	-89	-81	-57	-50	-44	-35	-40	-49	-72	-71	-67	-41	-36	-31	11	19	25
-52	-61	-66	-89	-85	-76	-47	-38	-30	-16	-19	-27	-52	-54	-53	-43	-41	-37	14	26	37
-1	-19	-33	-72	-70	-62	-35	-24	-16	4	3	-4	-22	-24	-27	-36	-36	-35	5	19	34
61	40	19	-48	-50	-48	-24	-13	-3	24	24	19	5	3	-1	-27	-30	-31	-5	6	21
105	93	76	-13	-27	-30	-9	2	13	44	46	42	30	27	21	-6	-12	-16	-8	-2	6
117	117	112	42	19	5	12	22	33	63	65	61	54	54	52	31	23	16	-0	-3	-3
94	105	113	93	72	58	36	42	52	77	77	73	78	85	89	70	60	50	17	6	-1
79	93	106	118	109	103	74	71	74	86	87	87	112	122	127	102	88	75	46	34	23
88	99	108	114	115	121	124	114	108	96	99	106	142	150	153	123	105	89	70	61	53
90	101	109	105	110	122	162	155	146	115	114	118	159	167	168	135	120	106	86	80	73
86	92	100	104	108	120	169	171	170	153	145	141	156	163	167	134	125	118	100	91	83
100	94	95	98	101	106	140	155	170	188	182	176	154	155	154	124	120	115	109	100	89
148	125	112	89	86	85	95	116	140	190	194	196	171	164	155	117	112	108	105	98	88
260	215	181	101	88	77	62	77	91	155	168	184	201	193	181	132	121	108	89	83	75
475	408	337	140	111	88	45	55	68	112	129	149	219	221	210	148	130	111	72	68	64
769	686	569	211	162	12	46	49	61	92	103	118	212	221	216	147	130	111	69	64	64
999	897	769	331	260	20	77	72	77	94	98	108	185	195	194	140	124	108	62	54	51
769	770	722	429	356	294	120	101	94	89	92	100	147	154	154	125	118	108	50	36	25
475	512	533	468	416	365	76	145	125	97	100	104	124	131	129	108	106	103	50	30	13
260	296	333	405	389	366	222	187	162	115	114	113	110	118	117	95	94	92	57	39	21
148	165	18	281	290	294	237	21	196	124	113	105	95	100	104	97	93	89	59	50	39
100	100	102	166	183	199	216	212	207	125	103	90	76	79	84	98	92	85	57	55	51
86	74	64	8	101	116	161	168	174	127	102	85	62	62	64	76	76	73	54	50	48
90	67	48	45	52	62	101	108	117	120	106	94	61	55	50	46	51	55	52	45	38
88	65	42	29	36	45	62	64	67	89	88	89	70	58	47	26	28	31	45	39	32
79	58	38	19	26	32	45	45	41	41	49	59	69	61	50	12	8	5	25	26	27
94	75	52	8	9	13	28	33	34	9	13	23	58	57	52	6	-4	-13	-2	7	16
117	102	79	2	-5	-7	2	12	21	8	6	7	37	40	40	1	-8	-17	-23	-12	1
105	101	86	11	-3	-14	-24	-12	0	4	3	3	18	19	18	-5	-8	-15	-34	-27	-13
61	69	69	32	16	0	-32	-23	-13	-10	-9	-5	8	5	1	-11	-11	-14	-38	-35	-27
-1	10	20	38	28	12	-33	-32	-28	-32	-28	-21	0	-1	-6	-14	-13	-15	-35	-39	-38
-52	-43	-33	14	12	2	-43	-45	-42	-44	-43	-39	-15	-14	-18	-18	-14	-13	-30	-37	-39
-85	-80	-74	-27	-24	-26	-53	-57	-58	-53	-53	-53	-35	-30	-28	-19	-14	-11	-31	-36	-37
-103	-103	-104	-75	-68	-64	-61	-66	-69	-66	-65	-64	-50	-44	-39	-26	-21	-17	-30	-34	-32
-107	-115	-122	-114	-103	-92	-70	-72	-74	-74	-73	-70	-59	-55	-51	-37	-33	-28	-25	-26	-25
-99	-111	-124	-139	-129	-118	-81	-78	-77	-75	-75	-73	-61	-58	-54	-45	-43	-42	-29	-25	-21
-82	-91	-103	-147	-145	-140	-101	-93	-88	-80	-79	-76	-60	-54	-49	-45	-48	-50	-39	-30	-21

Fig. 8 (Continued)

Frame 66

is obvious, and looking at the printouts alone, one could easily recognize them as derivatives of either SCSS or CUCL photographs.

However, the printouts of $\rho(h,k)$ do not help us to separate the two pattern classes in any quantitative way, a necessary step in the development of an automatic recognition scheme. What we seek, therefore, is a simple measure of the amount and direction, if any, of the central hump of $\rho(h,k)$.

Such a measure is readily available in the form of the <u>ellipse of concentration</u>[9] if the central hump of $\rho(h,k)$ is considered to be terminated along some positive contour (e.g., where $\rho(h,k) = 0.2$) and then is regarded as a distribution over two variables. Essentially, one finds a curve enclosing the center-of-gravity point of the hump in such a way that if a mass unit is uniformly distributed over the area bounded by the curve, the distribution will have the same first and second moments as the original distribution. Then an ellipse having the required property is found. The direction of the major axis of the ellipse is given by

$$\tan 2\theta = \frac{2\mu_{11}}{\mu_{20} - \mu_{02}} ,$$

where μ_{ij} are central moments. The ratio of axes is

$$r = \sqrt{\lambda_1/\lambda_2} ,$$

where λ_1 and λ_2 are the roots of

$$(\mu_{20}\mu_{02}-\mu_{11}^2)\,\lambda^2 - (\mu_{02} + \mu_{20})\lambda + 1 = 0 .$$

The ratio of axes may be used as a measure of the degree of alignment of the clouds into streets or bands. A value near unity implies no

alignment, while ratios far from unity indicate striation. The direction of the major axis of the ellipse gives the direction of the streets.

The ratio of the semi-minor axis* to the semi-major axis for each of a number of samples from our two pattern classes have been calculated; these are given in Figs. 5 and 7 in conjunction with the corresponding pattern picture. The directions of the streets derive from computed values of the x and y components of the major axes. The correspondence within and the distinction between the two classes can be seen from the photography, and despite the small sample covered by each picture, the ratio of the axes seems to be quite meaningful as a distinctive and important cloud-pattern feature for use in an automatic pattern-recognition system. Of further importance, this parameter should also permit quantitative description of the degree and direction of alignment of the ever-changing cloud scene as it is presented to the sensor on board the satellite.

DETERMINATION OF AMOUNT OF CLOUD COVER

A problem of some importance in the analysis of meteorological satellite photography is that of determining total cloud cover over the entire earth -- an important consideration in studies of atmospheric motions, cloud physics, radiation balance, and climatology, for example. However, the manual task of counting and sizing, or of subjectively estimating cloud cover from pictures is immense and unrewarding.

Briefly stated, the problem is one of developing and using a method that automatically distinguishes clouds from clear areas regardless of background (i.e., terrain features, water, ice, snow), and then simply performs an areal count of the total cloud content in the photograph. An exploratory step towards the eventual solution of this problem will be described.

---

*Because the procedure for displacing the images in the autocorrelation calculation results in only one-half of an ellipse (when computed), we deal only with the semi-minor and the semi-major axes.

Consider a picture containing a random assortment of clouds plus clear areas. It is assumed that the general exposure was uniform, or that any simple brightness trend was removed.* The problem is to choose a reasonable intensity threshold that separates cloud from noncloud. This threshold is to be adjusted automatically to different picture exposures and contrasts. This differs from the approach taken by Arking[10] in that the brightness or intensity threshold is determined automatically and objectively, rather than by human observers and subjective means.

Explanation of the rule that follows is based on a simple intuition that seems to be borne out in the samples that we examined, i.e., that the gradient of intensity at the edges of clouds is likely to be higher than elsewhere in the picture. The threshold is therefore taken to be the average intensity over regions of the picture where the gradient is high. Mechanization of this rule on a digital representation proceeds by the following steps:

1. Starting with the original image, a new image is produced whose value at each point is the absolute value of the brightness gradient surrounding that point in the old image. The new image is called the gradient image.

2. The distribution of intensities for the gradient image is then found. (See Table 1 for example.) For an arbitrary fraction, p, of the gradient image's distribution (e.g., where p = the upper 1/8), let g be the gradient level for which p = probability that the gradient level is $\geq$ g.

3. Form a third image, called a "mask," whose value is 1 where gradient level is $\geq$ g, and whose value is 0 elsewhere.

4. Form another image whose intensity at each point is the product of the original image and the mask. This image consists of those points of the original where the gradient was high, namely the upper p of the gradient image distribution. Let c be the average intensity over the nonzero portions of this product image.

---

*For a discussion of pre-whitening, the reader is referred to Leese and Epstein,[8] p. 637.

Table 1

DISTRIBUTION OF INTENSITIES FOR GRADIENT (FRAME 02 CUCL)

Gradient Level (g)	% Frequency	Accumulated Total	Gradient Level (g)	% Frequency	Accumulated Total
0	10.4	10.4	16	0.0	99.8
1	23.9	34.3	17	0.0	99.8
2	17.4	51.7	18	0.0	99.9
		← p=upper 1/4			
3	24.3	76.0	19	0.0	99.9
4	7.1	83.0	20	0.0	99.9
		← p=upper 1/8			
5	9.2	92.3	21	0.0	99.9
		← p=upper 1/16			
6	3.1	95.3	22	0.0	99.9
7	2.0	97.3	23	0.0	99.9
8	1.0	98.3	24	0.	99.9
9	0.6	99.0	25	0.0	100.0
10	0.3	99.2	26	0.0	100.0
11	0.2	99.4	27	0.0	100.0
12	0.1	99.6	28	0.0	100.0
13	0.1	99.7	29	0.0	100.0
14	0.1	99.8	30	0.0	100.0
15	0.0	99.8	31	0.0	100.0

5. Use c as the threshold above which one calls a point "cloud." It is then a simple matter to determine the amount of cloud cover by finding the fraction of picture bits that are white.

The part of the program that produces the gradient image may be of interest to those readers who are or who may become engaged in this kind of programming. The gradient, in rectangular coordinates, is $G = (\partial I/\partial x, \partial I/\partial y)$, where I denotes the original image value, and the quantity being sought is $||G|| = \sqrt{(\partial I/\partial x)^2 + (\partial I/\partial y)^2}$. Because there may be some tens of thousands of image points, there would be many square roots to take; hence, in order to speed up computation, the rough approximation

$$||G|| = \max \{|\partial I/\partial x|, |\partial I, \partial y|\} + 1/2 \min \{|\partial I/\partial x|, |\partial I, \partial y|\}$$

was used instead. This makes little practical difference, especially for data which like ours, are given only to 5 bits anyway. It makes it easy to keep to our philosophy of handling the pictorial data in packed form, 6 per machine word, and doing the necessary operations en masse without unpacking the data, a procedure that saves much machine time. In order to retain the extra bit, the quantity actually adopted for our computations was 2(max) + (min).

The steps above were programmed and the computations were then displayed on the SC 4020, which is capable of both displaying and photographing computer-generated data. (Output tapes from the IBM 7090 contain the necessary codes for displaying such things as halftone information, vectors, graphs, and alphanumeric characters.) Figures 9 and 10 are reproduced from the SC 4020 display as a series of two-level images; they show the cloud pictures that result (right-hand side of each pair) for p = upper 1/16 (.937), p = upper 1/8 (.875), and p = upper 1/4 (.750). The legend indicates the brightness or intensity level c at which each image was clipped on a 32-level gray scale. (An example of the original intensity distribution copied from a similar SC 4020 display for frame 02 CUCL is shown in Fig. 11.) The left-hand side of each figure is the mask, and the legend indicates the gradient level, g, for each p as "gradient over...".

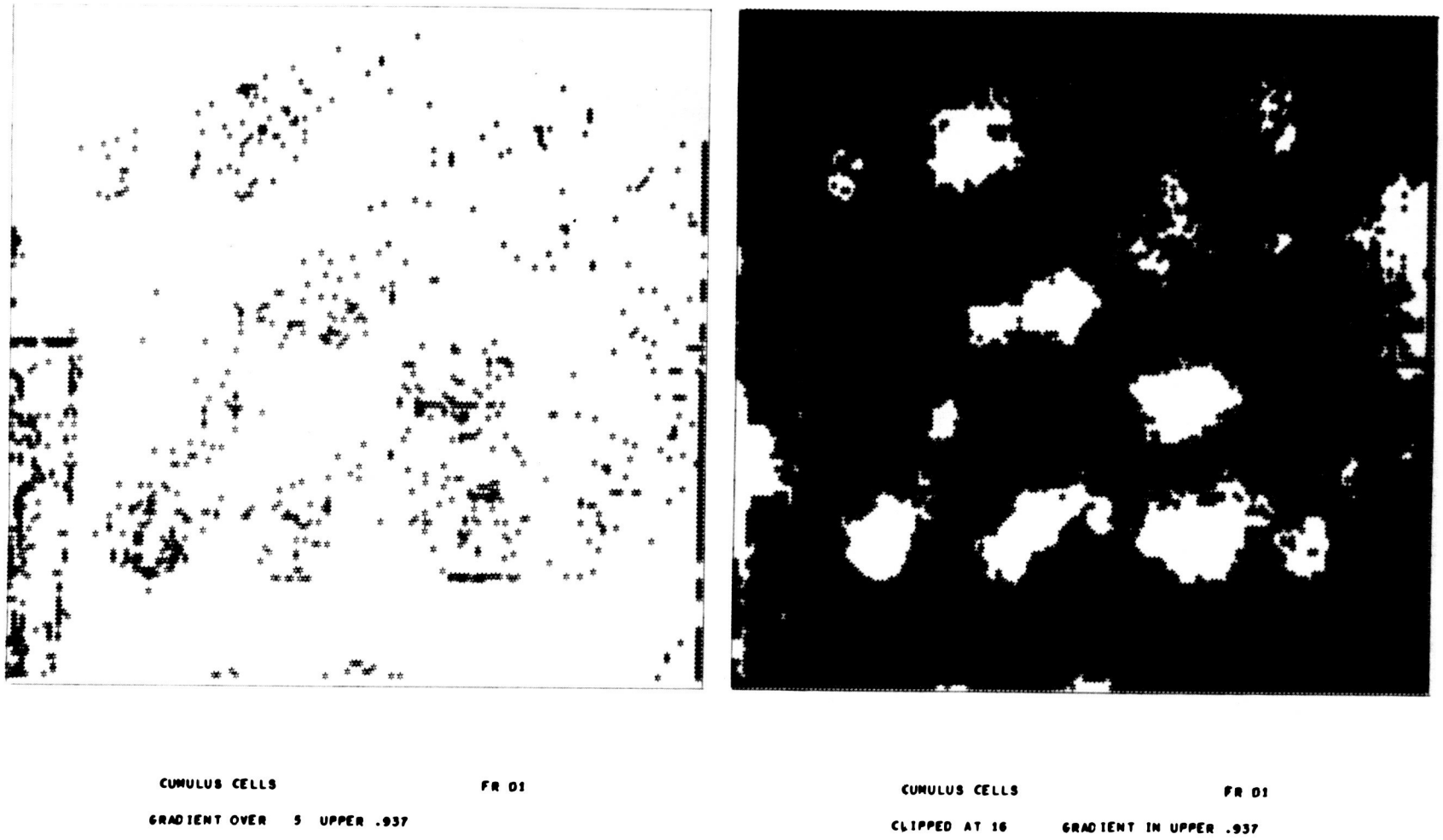

Fig. 9 SC 4020 representation of cloud vs. no-cloud (right) and corresponding mask (left) for cumulus patterns

Frame:	01
Gradient:	over .937
Clipped:	at 16

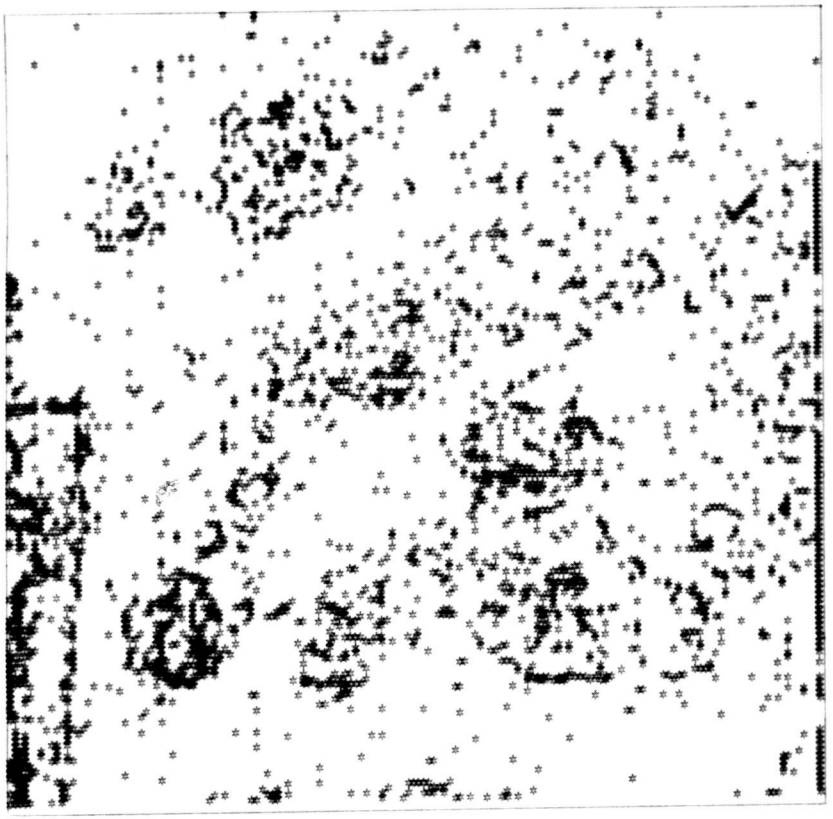

CUMULUS CELLS FR 01

GRADIENT OVER 4 UPPER .875

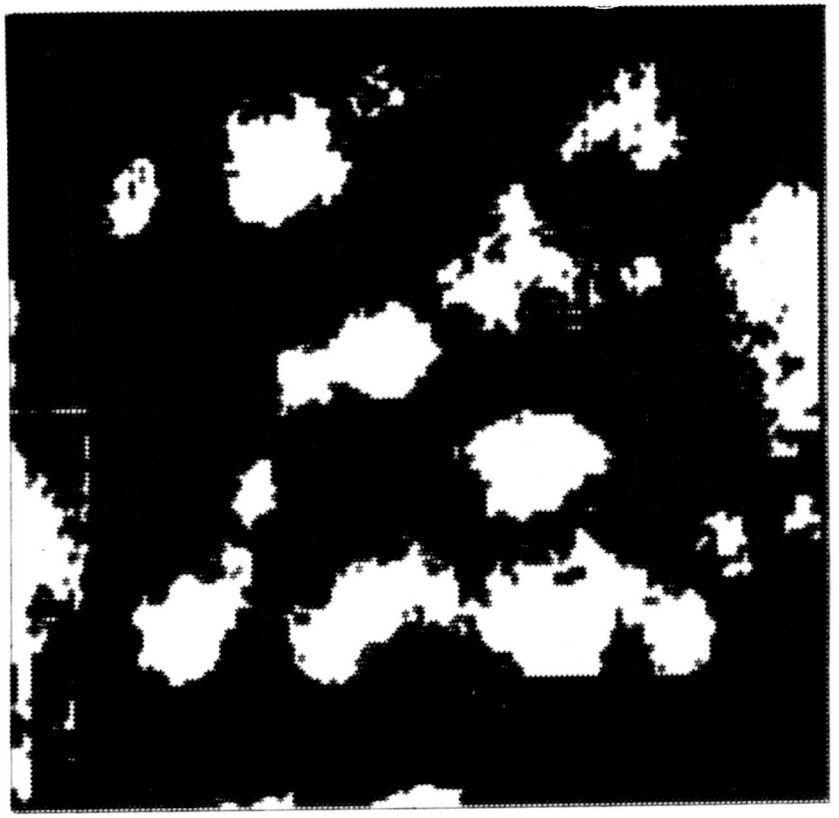

CUMULUS CELLS FR 01

CLIPPED AT 14 GRADIENT IN UPPER .875

Fig. 9 (continued)

Frame:	01
Gradient:	over .875
Clipped:	at 14

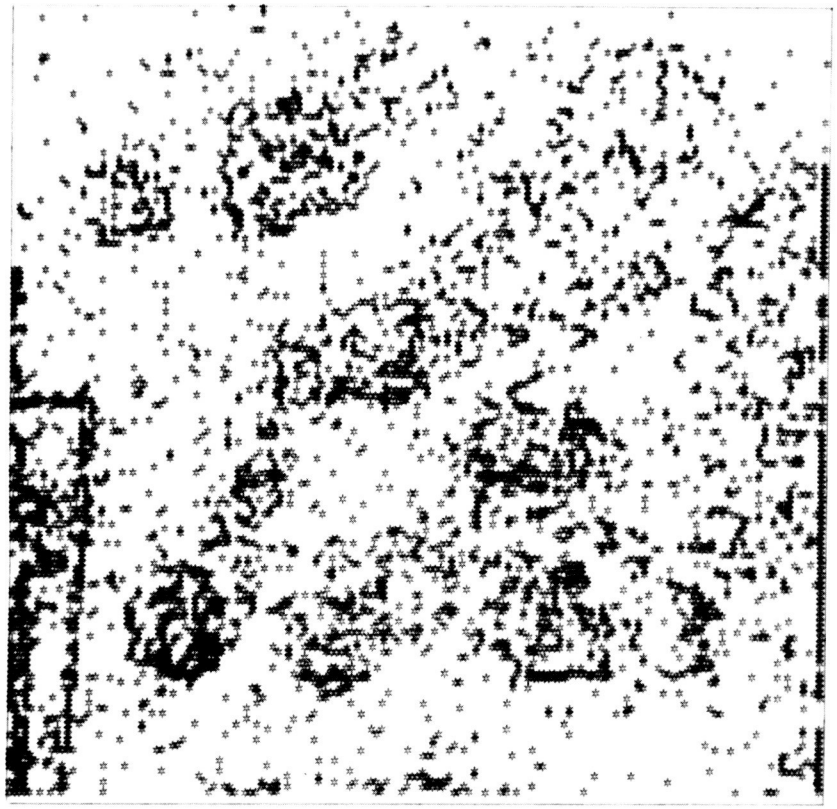

CUMULUS CELLS FR 01

GRADIENT OVER 3 UPPER .750

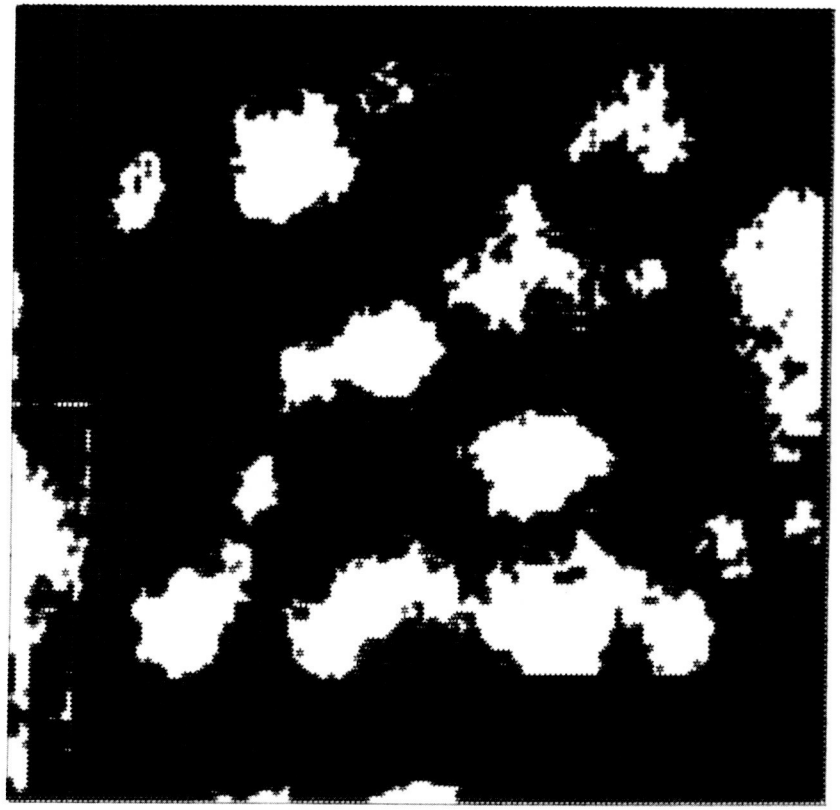

CUMULUS CELLS FR 01

CLIPPED AT 14 GRADIENT IN UPPER .750

Fig. 9 (Continued)

Frame:	01
Gradient:	over .750
Clipped:	at 14

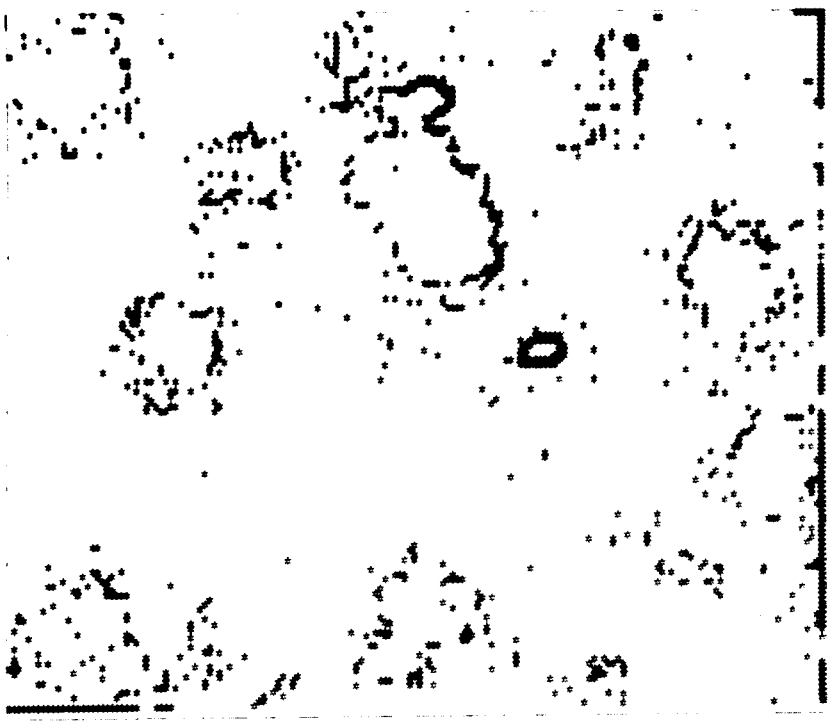

CUMULUS CELLS FR 02

GRADIENT OVER 6 UPPER .937

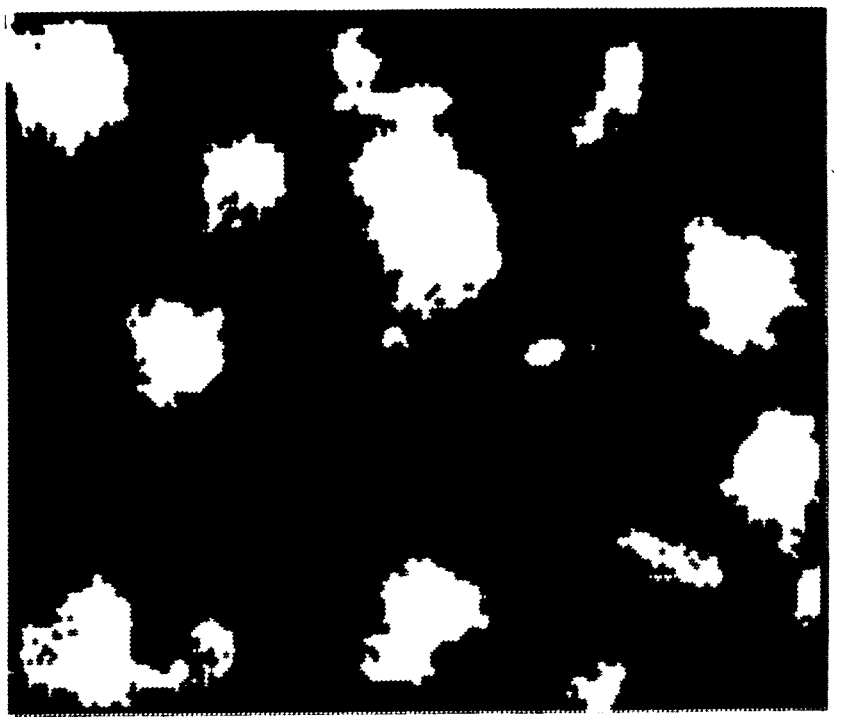

CUMULUS CELLS FR 02

CLIPPED AT 20 GRADIENT IN UPPER .937

Fig. 9 (Continued)

Frame:		02
Gradient:	over	.937
Clipped:	at	20

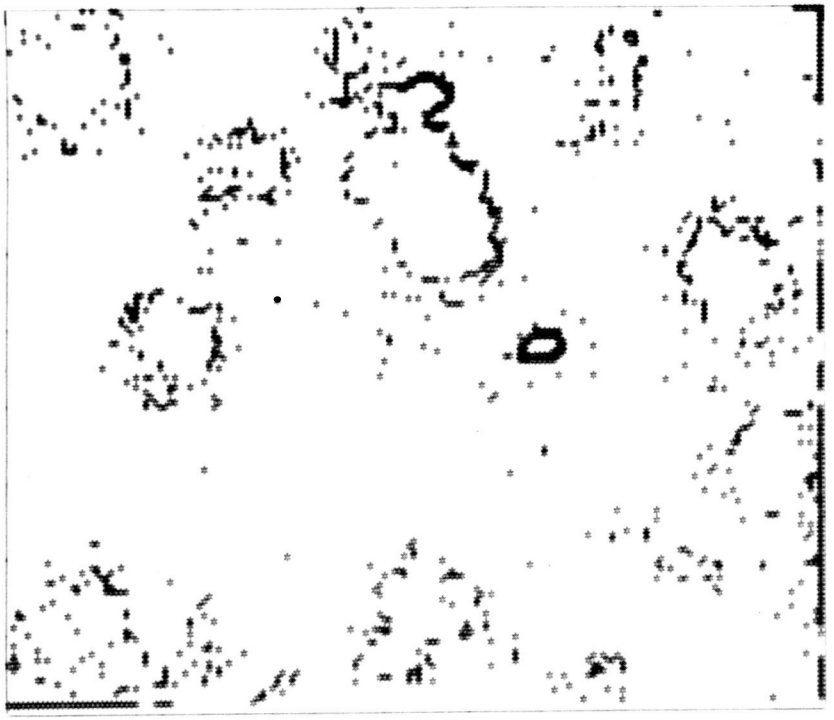

CUMULUS CELLS FR 02

GRADIENT OVER 6 UPPER .937

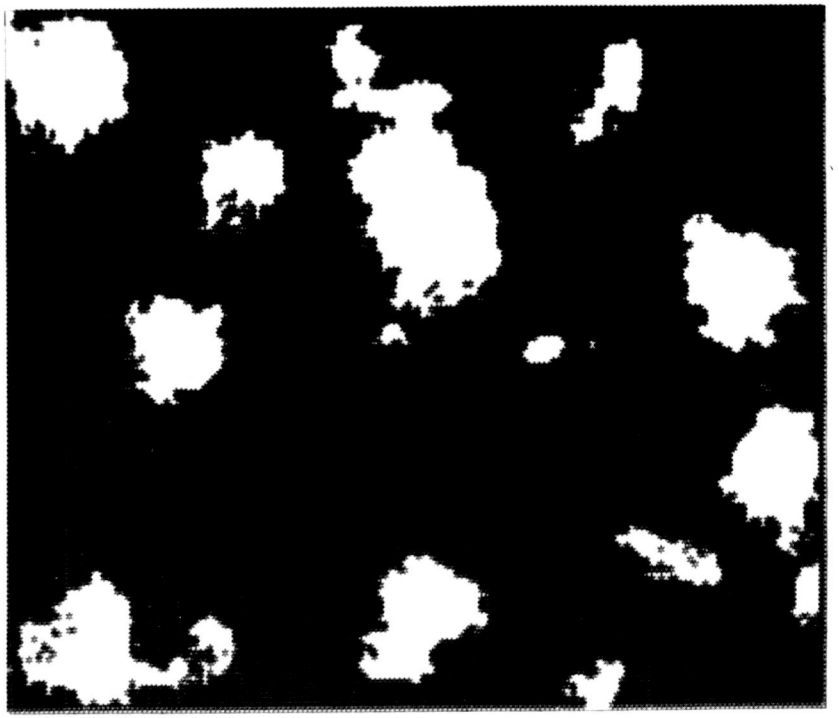

CUMULUS CELLS FR 02

CLIPPED AT 20 GRADIENT IN UPPER .937

Fig. 9 (Continued)

Frame:		02
Gradient:	over	.937
Clipped:	at	20

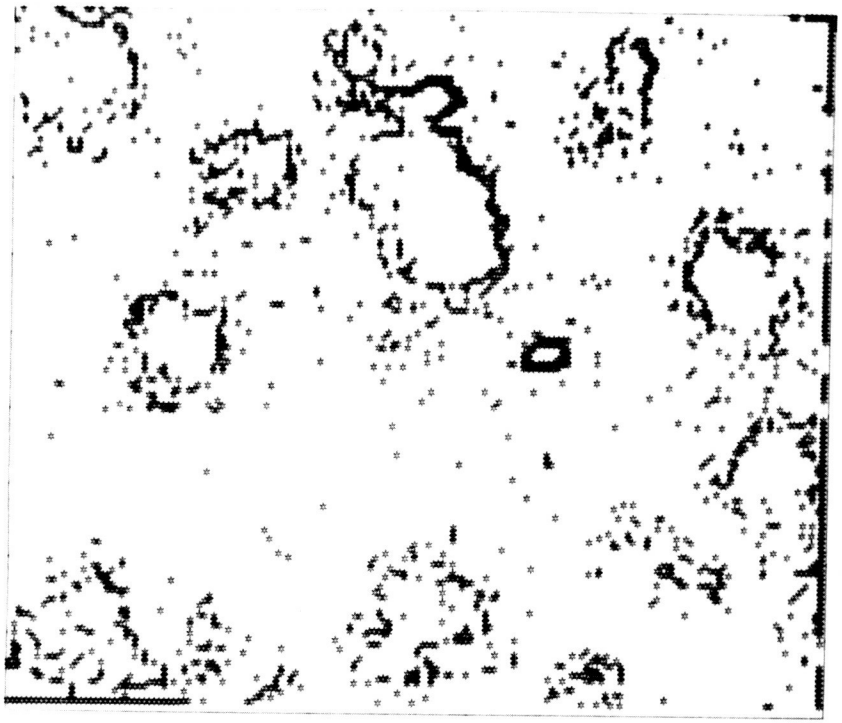

CUMULUS CELLS FR 02

GRADIENT OVER 5 UPPER .875

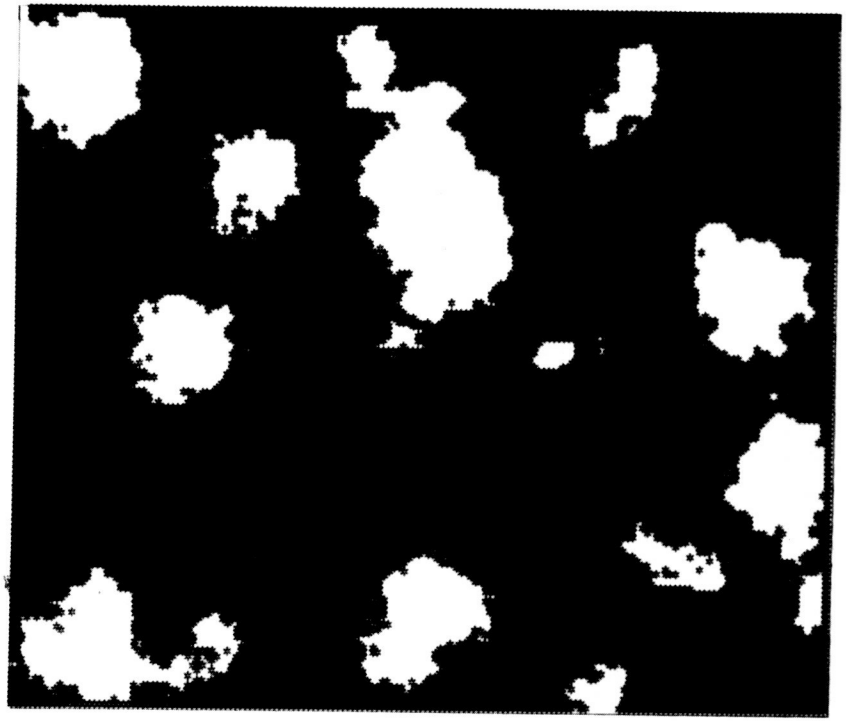

CUMULUS CELLS FR 02

CLIPPED AT 19 GRADIENT IN UPPER .875

Fig. 9 (Continued)

Frame:	02
Gradient:	over .875
Clipped:	at 19

CUMULUS CELLS FR 02

GRADIENT OVER 3 UPPER .750

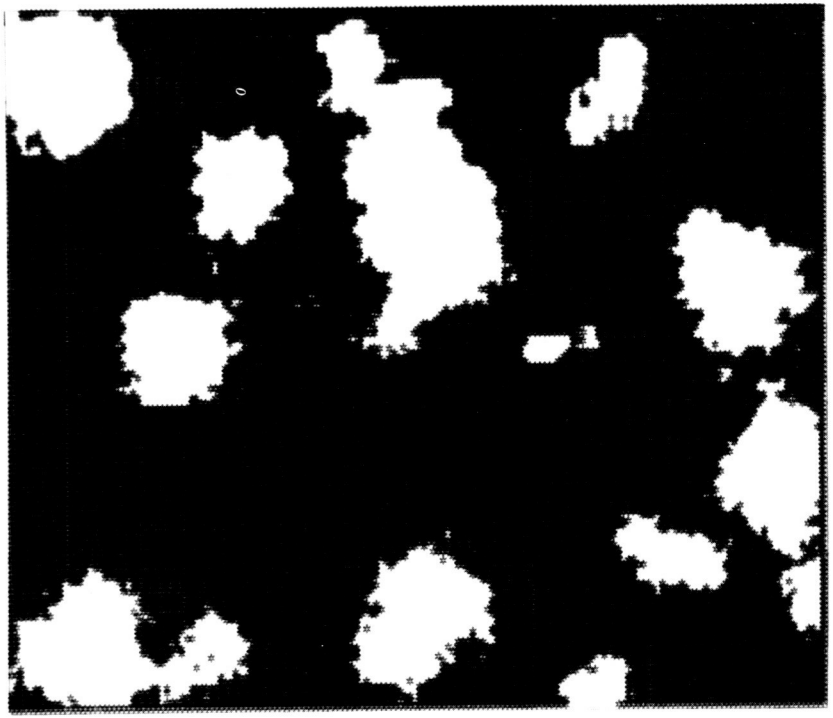

CUMULUS CELLS FR 02

CLIPPED AT 17 GRADIENT IN UPPER .750

Fig. 9 (Continued)

Frame:	02
Gradient:	over .750
Clipped:	at 17

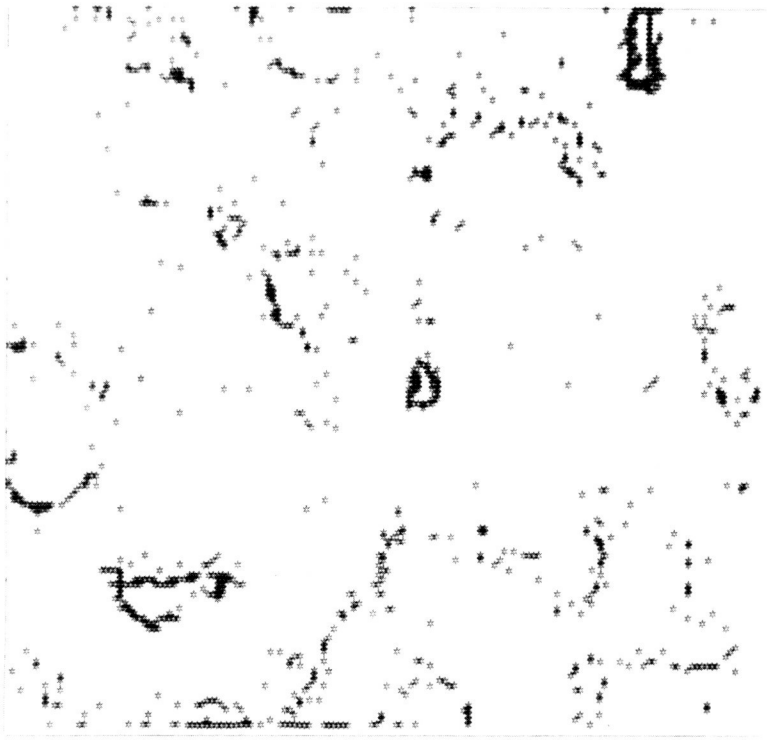

CUMULUS CELLS FR 04

GRADIENT OVER 6 UPPER .937

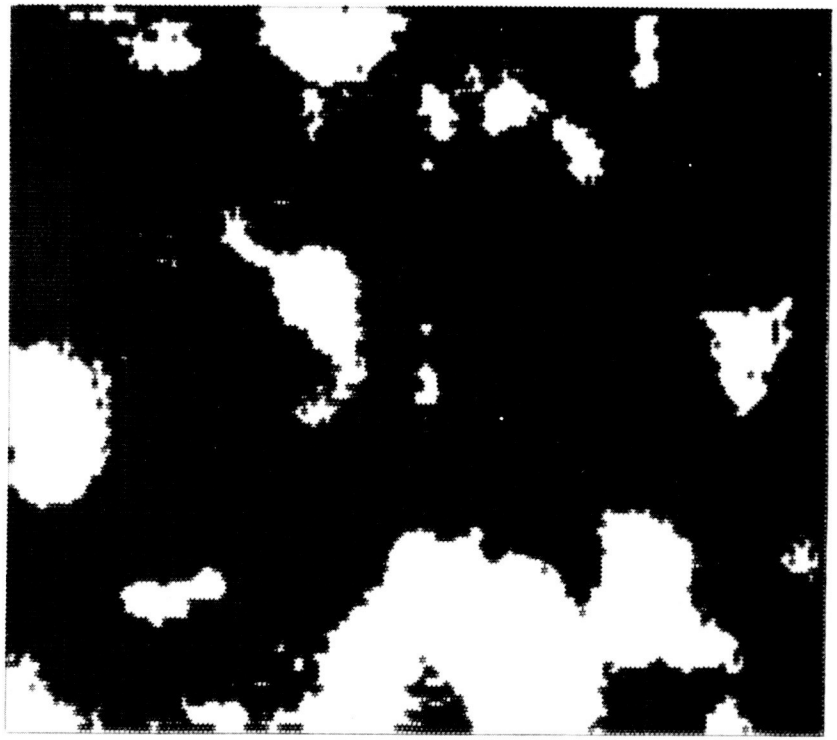

CUMULUS CELLS FR 04

CLIPPED AT 20 GRADIENT IN UPPER .937

Fig. 9 (Continued)

Frame: 04
Gradient: over .937
Clipped: at 20

CUMULUS CELLS FR 04

GRADIENT OVER 3 UPPER .750

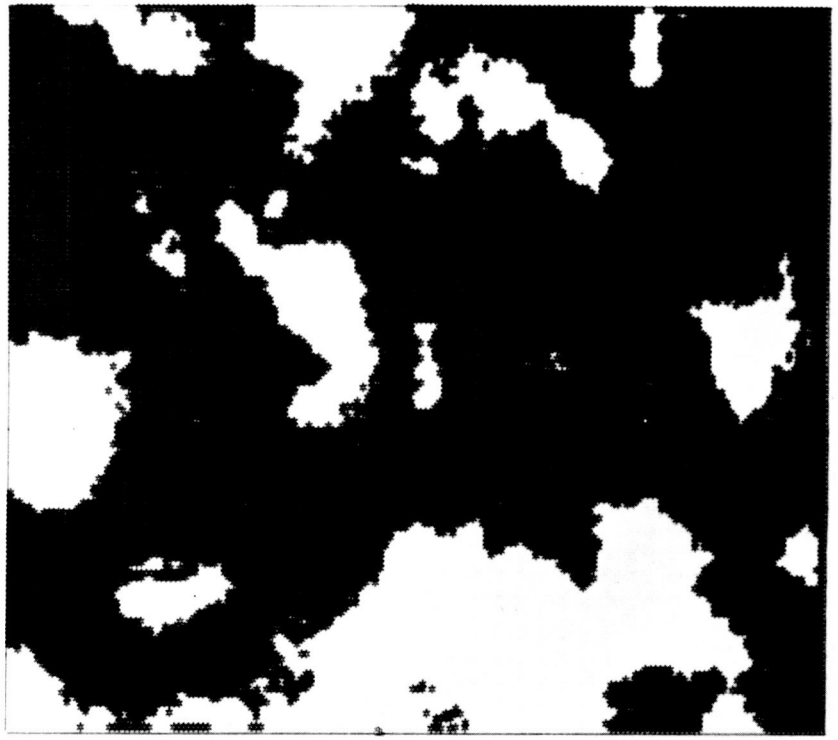

CUMULUS CELLS FR 04

CLIPPED AT 17 GRADIENT IN UPPER .750

Fig. 9 (Continued)

Frame:	04
Gradient:	over .750
Clipped:	at 17

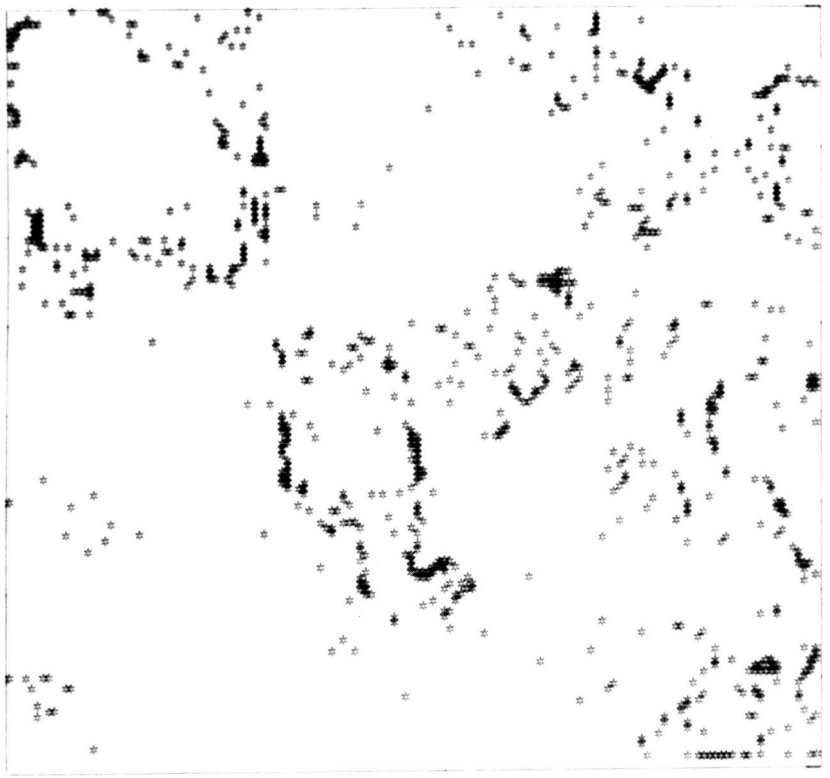

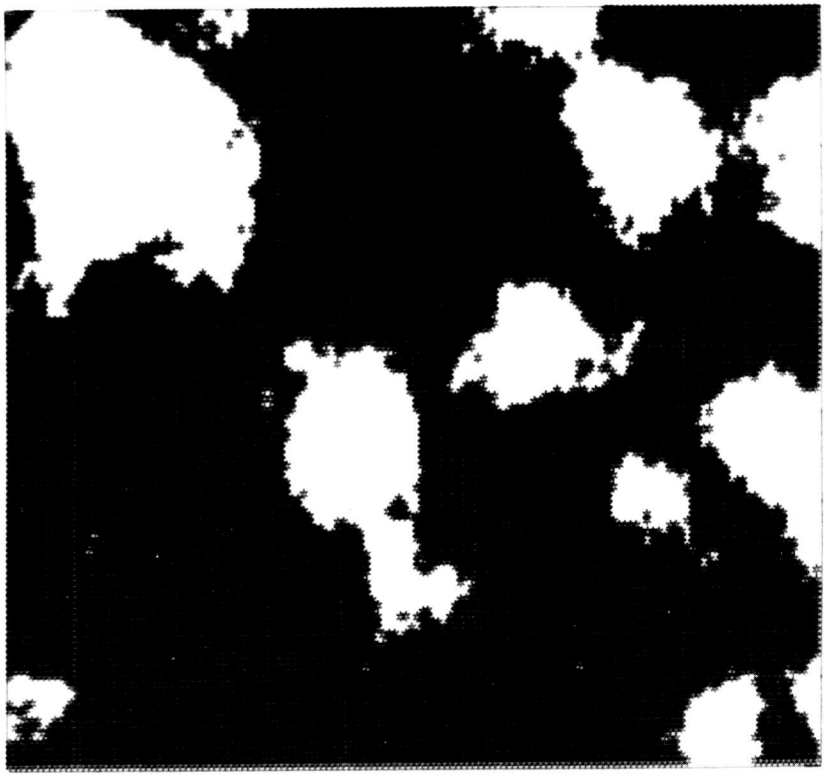

Fig. 9 (Continued)

Frame:		32
Gradient:	over	.937
Clipped:	at	19

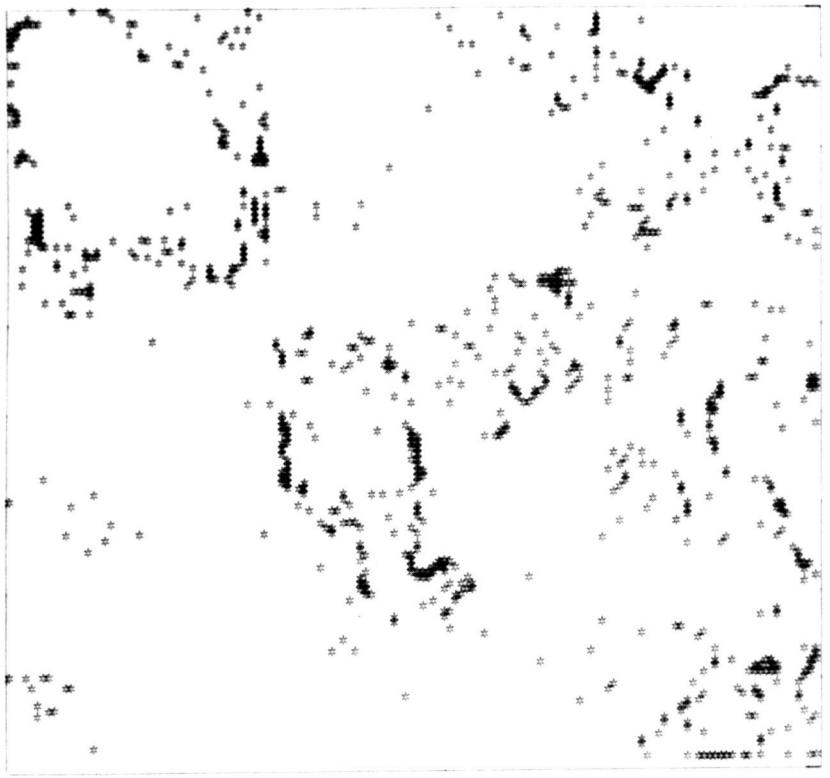

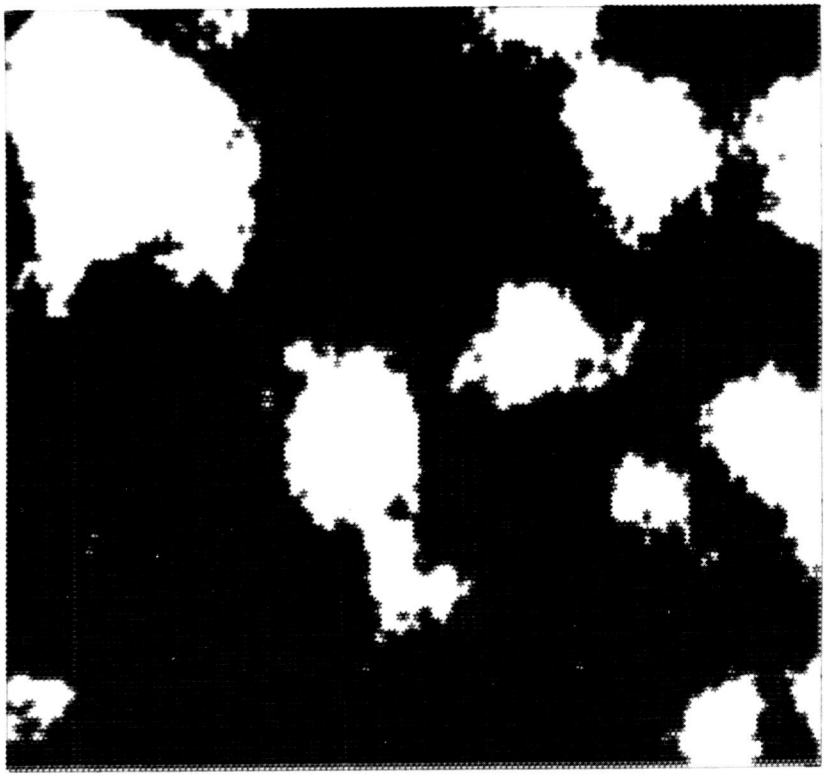

Fig. 9 (Continued)

Frame:		32
Gradient:	over	.937
Clipped:	at	19

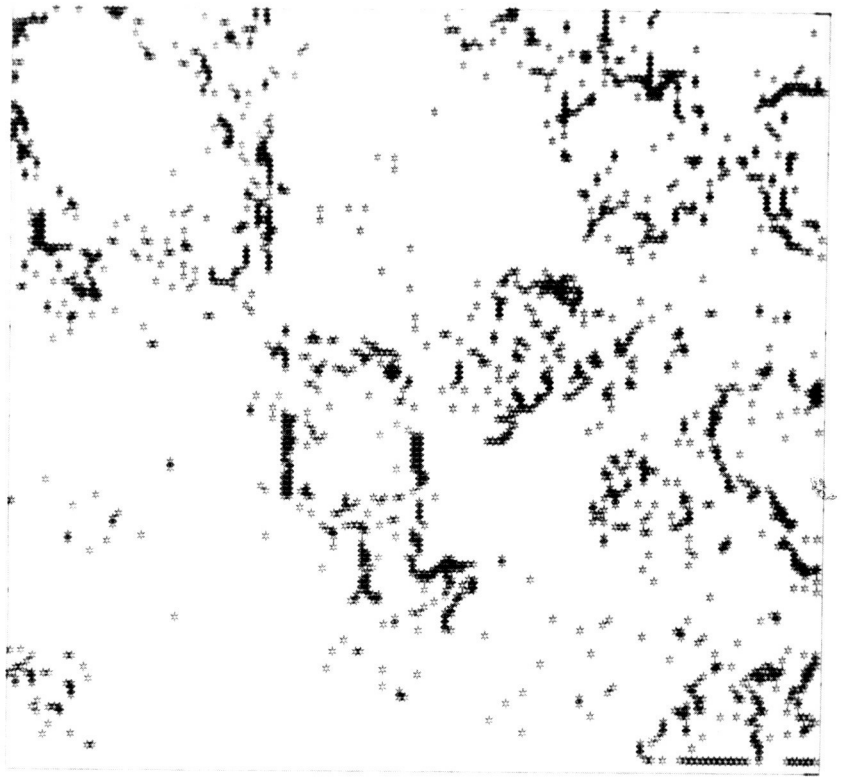

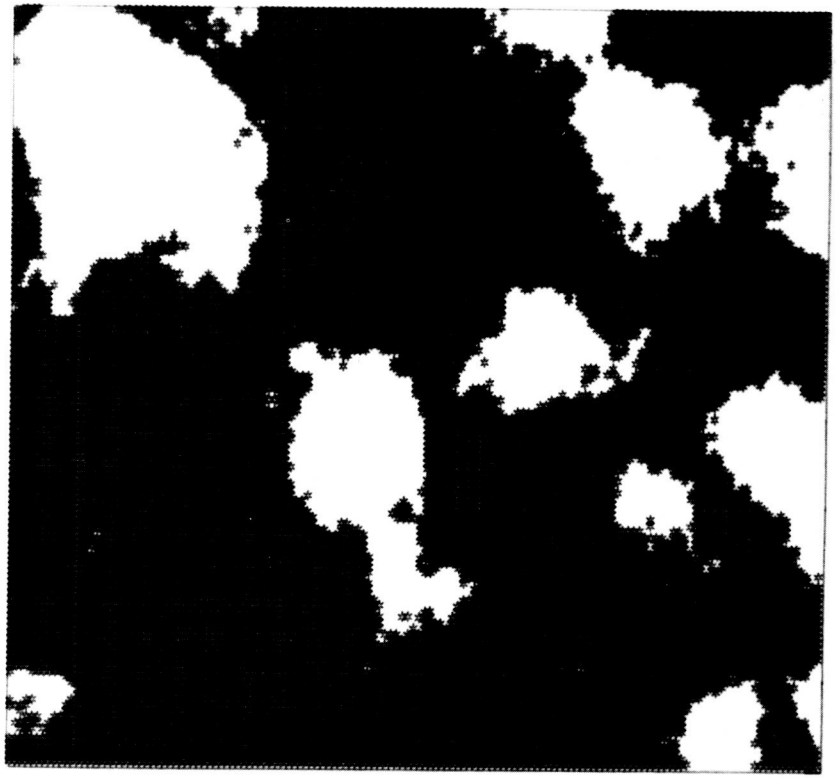

Fig. 9 (Continued)

Frame:	32
Gradient:	over .875
Clipped:	at 19

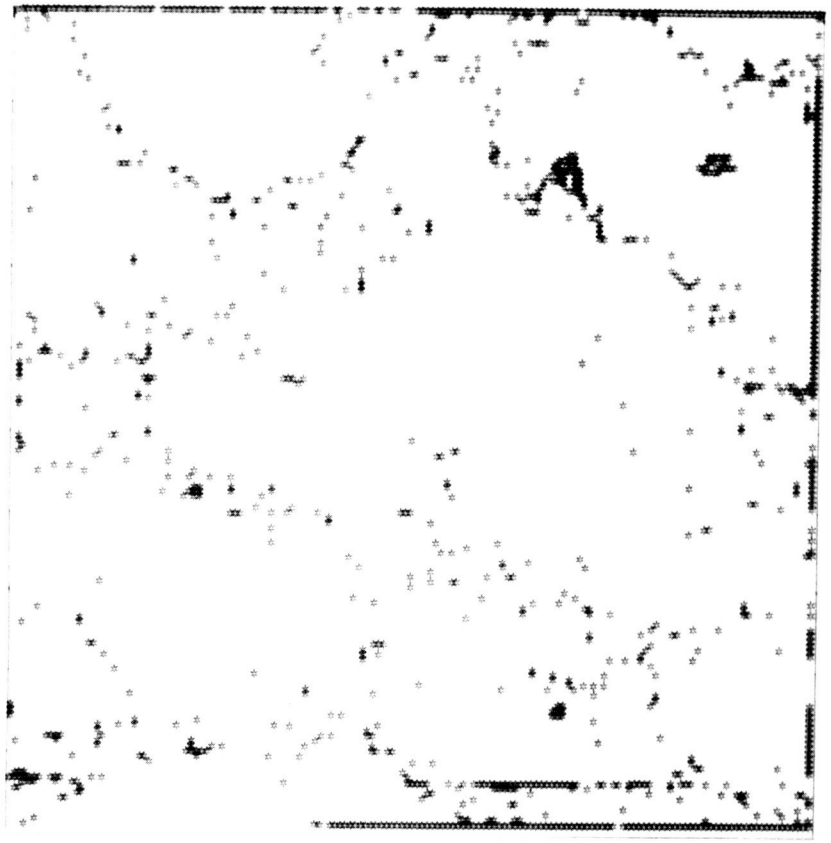

FRAME 14

GRADIENT OVER 7 UPPER .937

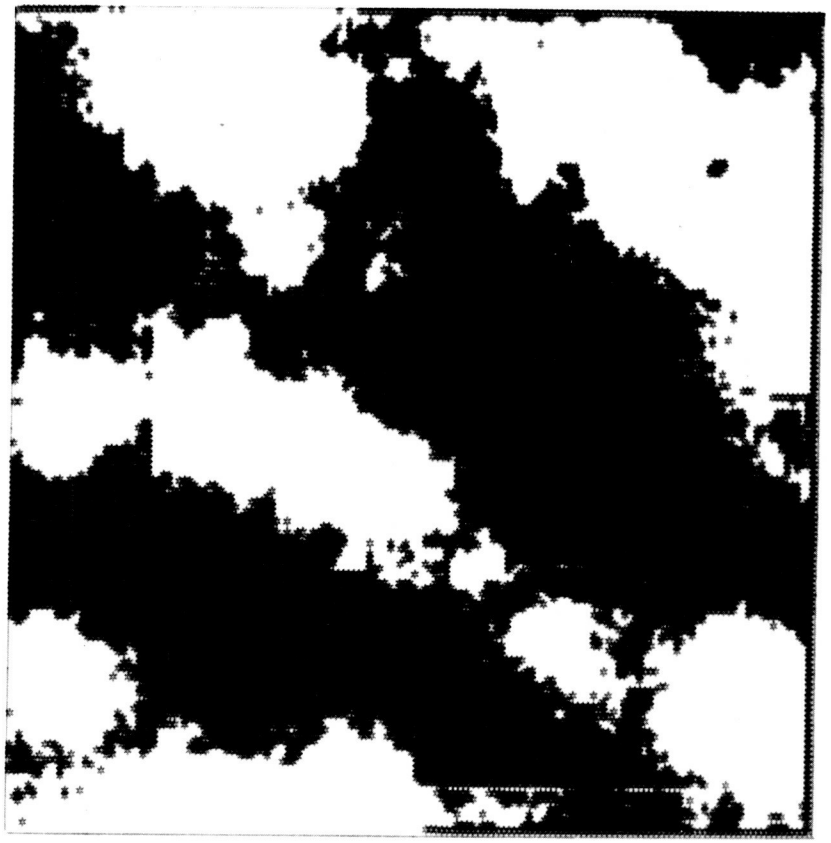

FRAME 14

CLIPPED AT 20 GRADIENT IN UPPER .937

Fig. 10 SC 4020 representations of cloud vs. no-cloud (right) and corresponding mask (left) for stratocumulus street patterns

Frame:	14
Gradient:	over .937
Clipped:	at 20

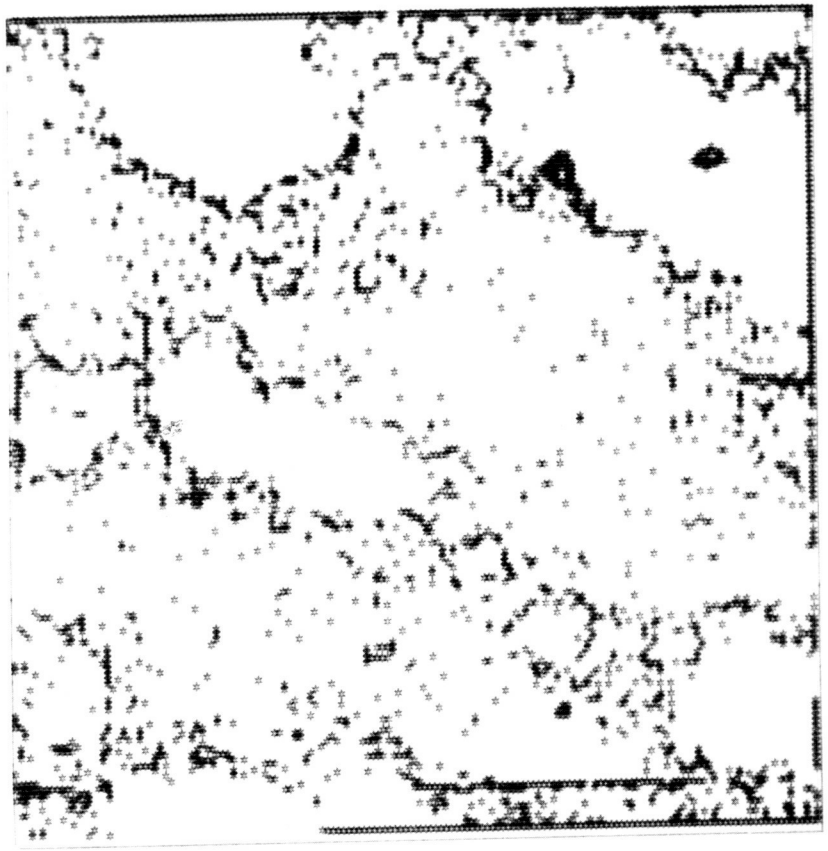

FRAME 14

GRADIENT OVER 5 UPPER .875

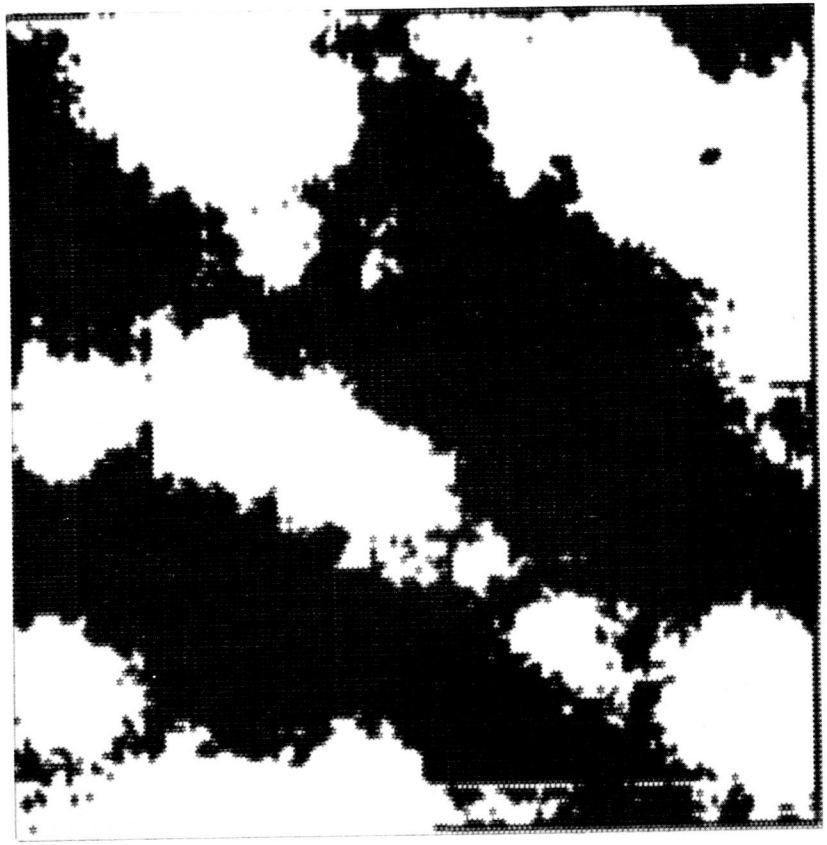

FRAME 14

CLIPPED AT 20 GRADIENT IN UPPER .875

Fig. 10 (Continued)

Frame:	14
Gradient:	over .875
Clipped:	at 20

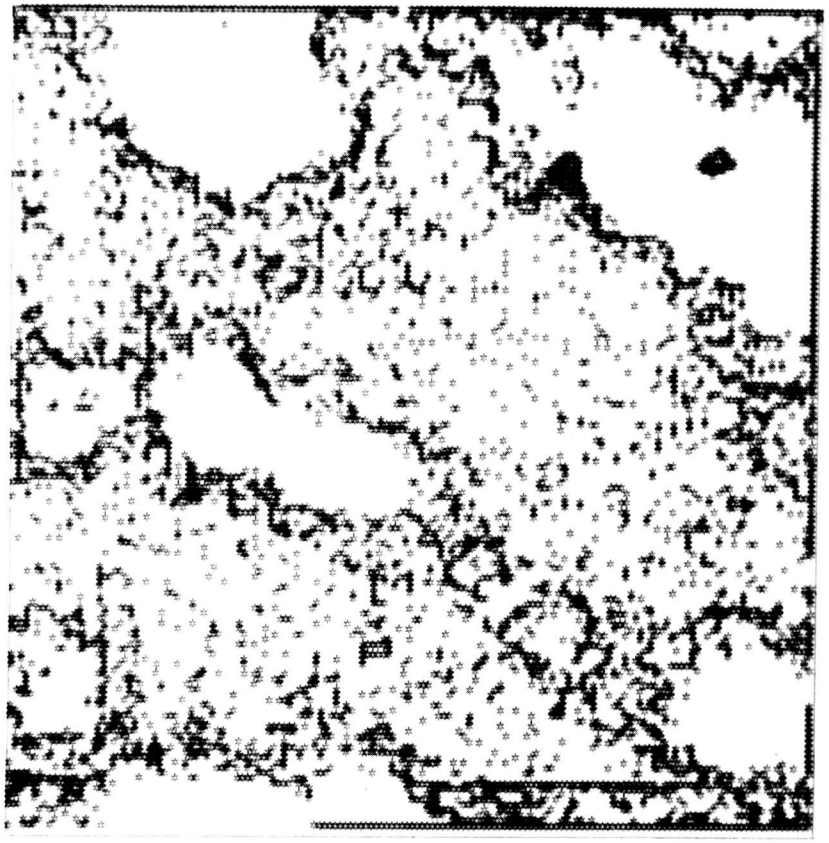

FRAME 14

GRADIENT OVER 4 UPPER .750

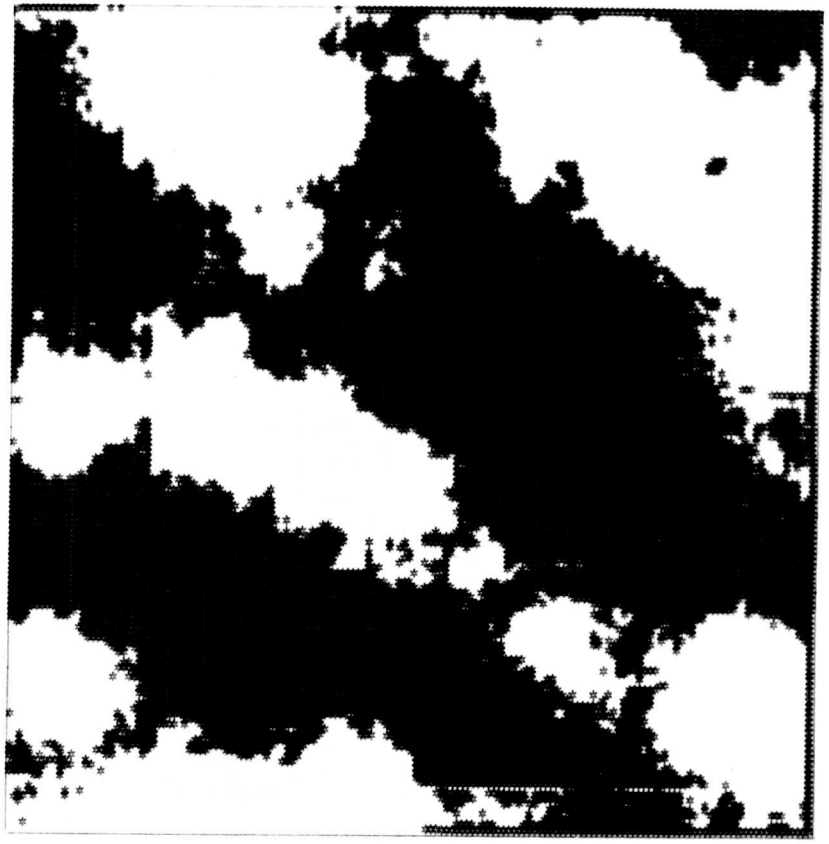

FRAME 14

CLIPPED AT 20 GRADIENT IN UPPER .750

Fig. 10 (Continued)

Frame:	14
Gradient:	over .750
Clipped:	at 20

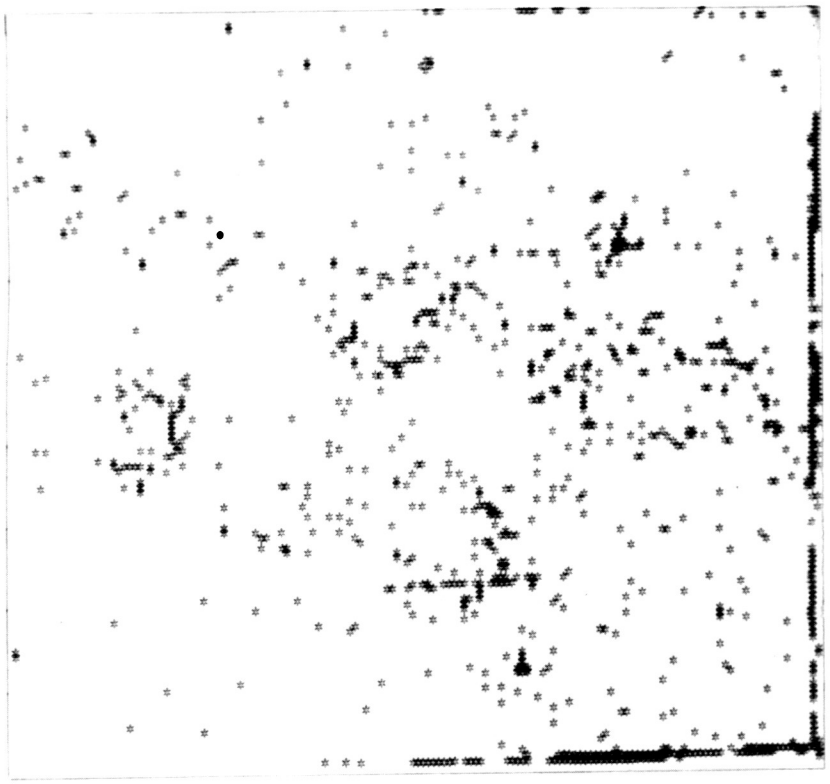

STRATOCUMULUS STREETS, STRAIGHT FR 50

GRADIENT OVER 5 UPPER .937

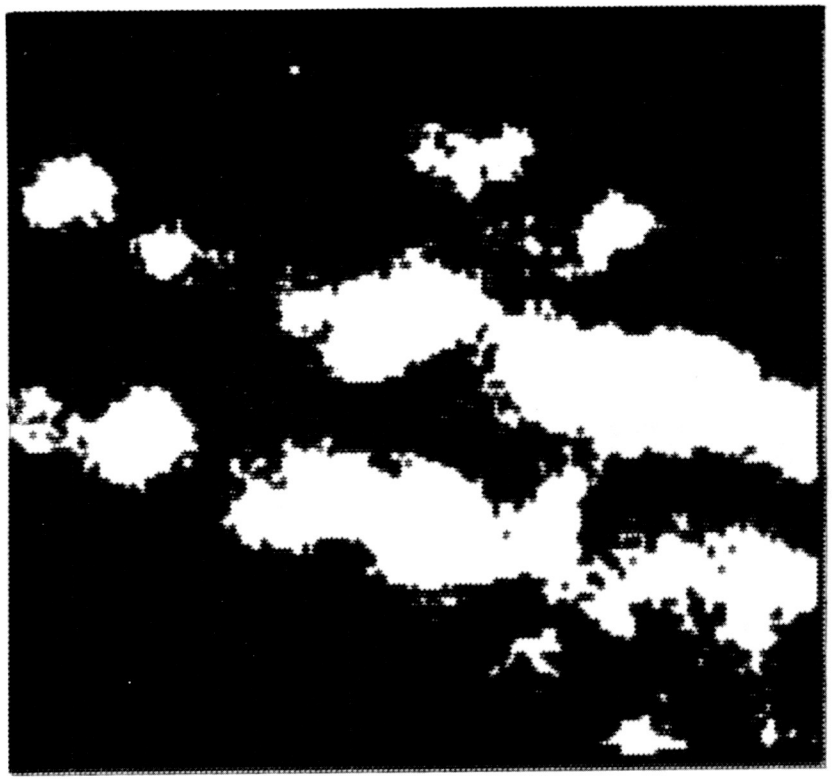

STRATOCUMULUS STREETS, STRAIGHT FR 50

CLIPPED AT 15 GRADIENT IN UPPER .937

Fig. 10 (Continued)

Frame:	50
Gradient:	over .937
Clipped:	at 15

STRATOCUMULUS STREETS, STRAIGHT FR 50

GRADIENT OVER 4 UPPER .875

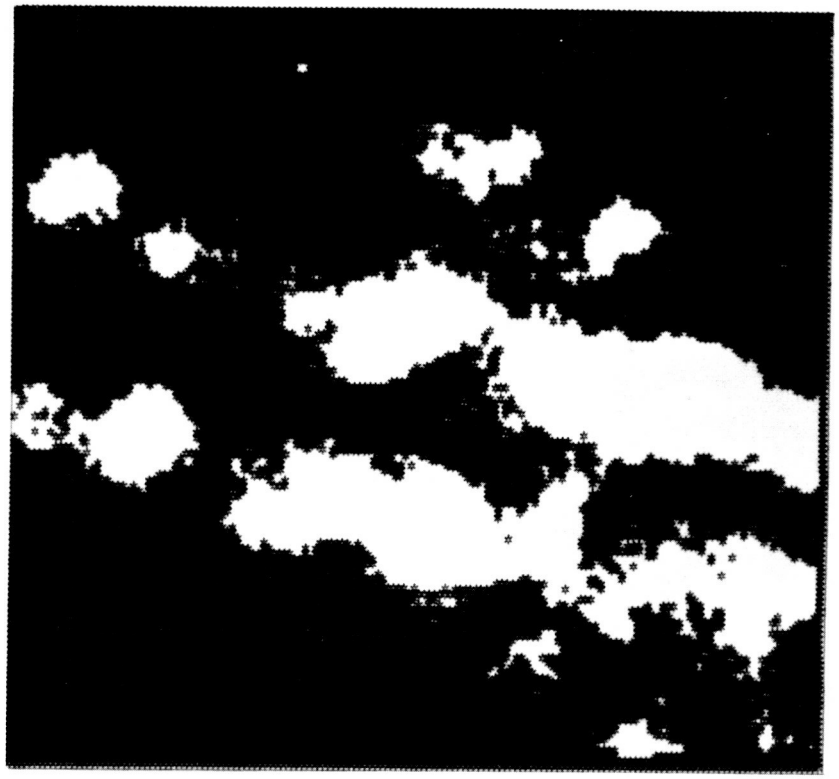

STRATOCUMULUS STREETS, STRAIGHT FR 50

CLIPPED AT 15 GRADIENT IN UPPER .875

Fig. 10 (Continued)

Frame:	50
Gradient:	over .875
Clipped:	at 15

STRATOCUMULUS STREETS, STRAIGHT FR 50

GRADIENT OVER 3 UPPER .750

STRATOCUMULUS STREETS, STRAIGHT FR 50

CLIPPED AT 14 GRADIENT IN UPPER .750

Fig. 10 (Continued)

Frame:	50
Gradient:	over .750
Clipped:	at 14

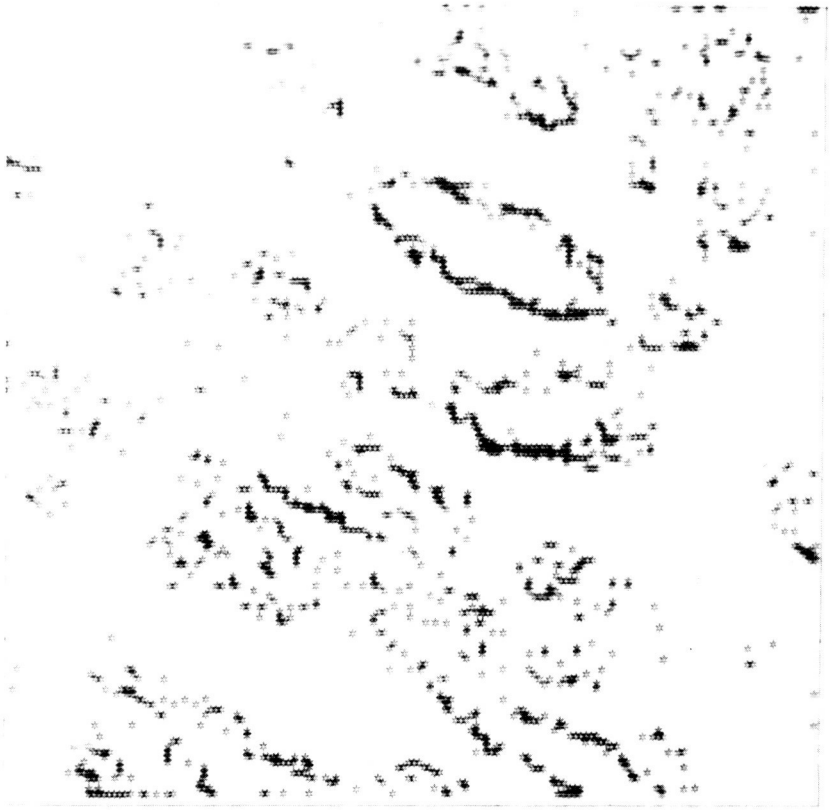

STRATOCUMULUS STREETS. STRAIGHT FR 63

GRADIENT OVER 7 UPPER .937

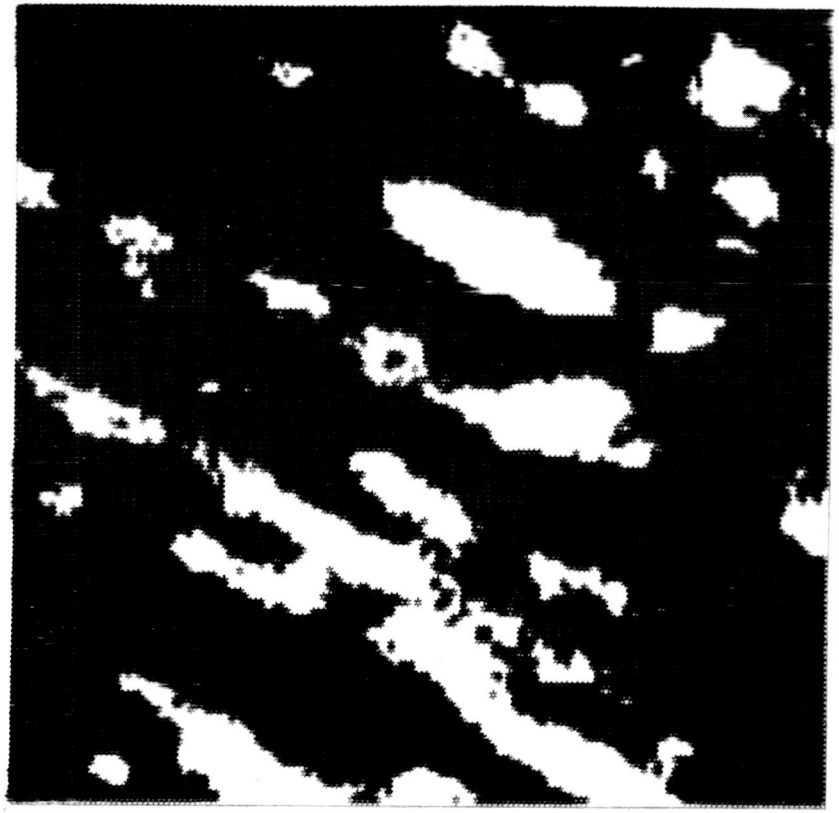

STRATOCUMULUS STREETS- STRAIGHT FR 63

CLIPPED AT 20 GRADIENT IN UPPER .937

Fig. 10 (Continued)

Frame:	63
Gradient:	over .937
Clipped:	at 20

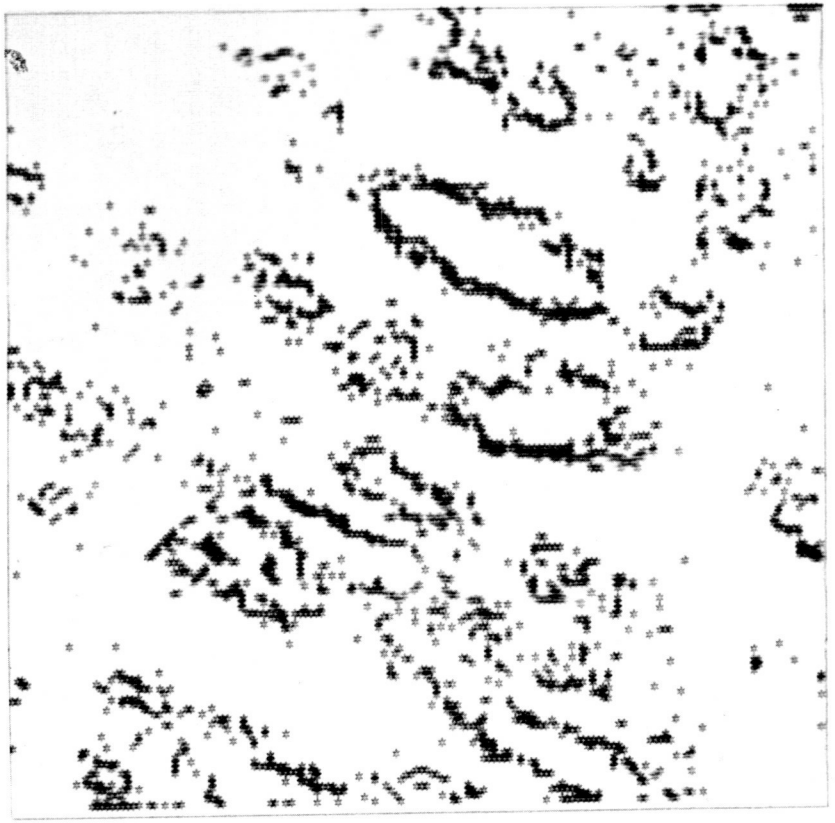

STRATOCUMULUS STREETS. STRAIGHT FR 63

GRADIENT OVER 6 UPPER .875

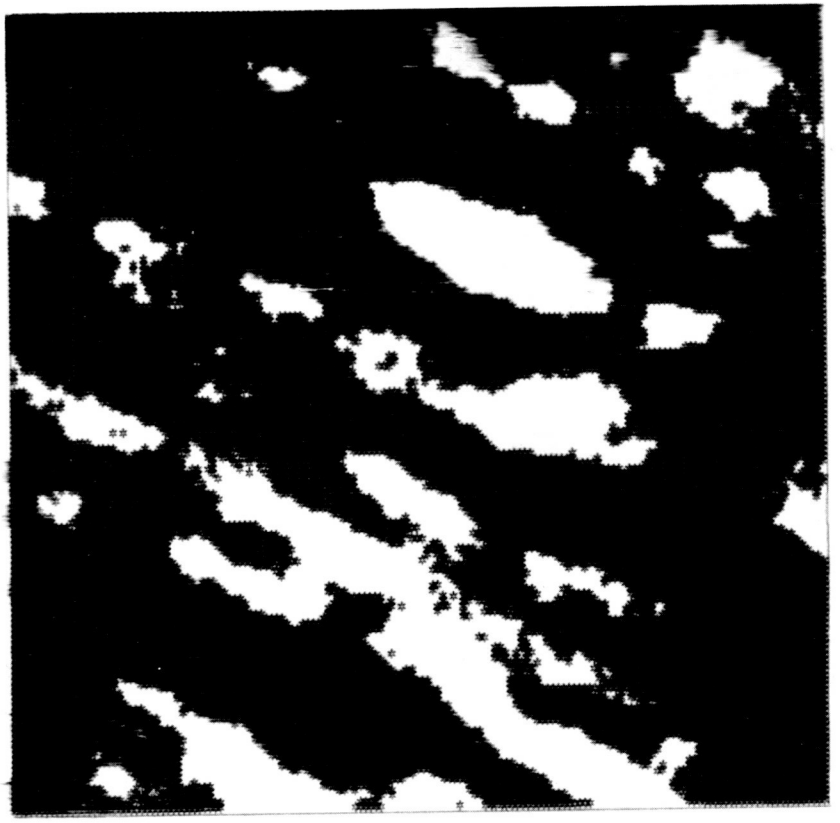

STRATOCUMULUS STREETS. STRAIGHT FR 63

CLIPPED AT 19 GRADIENT IN UPPER .875

Fig. 10 (Continued)

Frame:	63
Gradient:	over .875
Clipped:	at 19

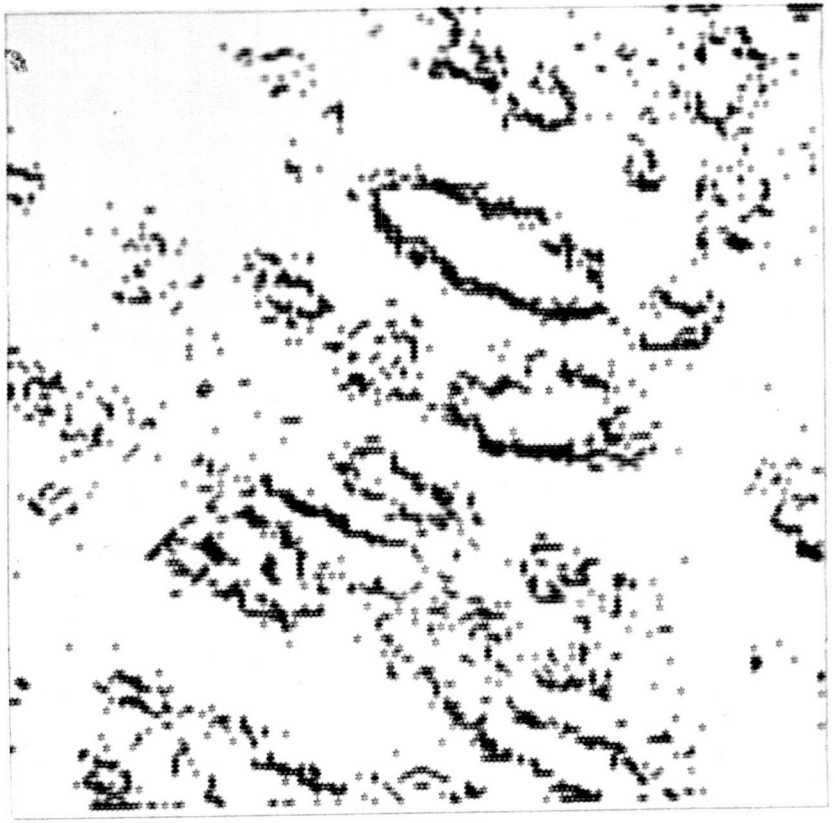

STRATOCUMULUS STREETS. STRAIGHT FR 63

GRADIENT OVER 6 UPPER .875

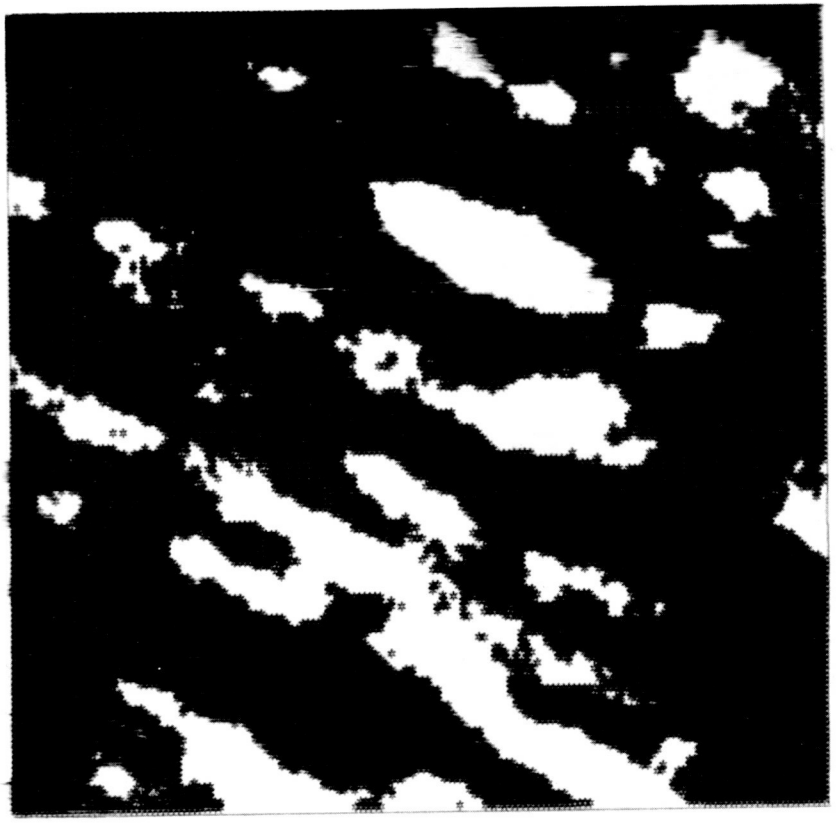

STRATOCUMULUS STREETS. STRAIGHT FR 63

CLIPPED AT 19 GRADIENT IN UPPER .875

Fig. 10 (Continued)

Frame:	63
Gradient:	over .875
Clipped:	at 19

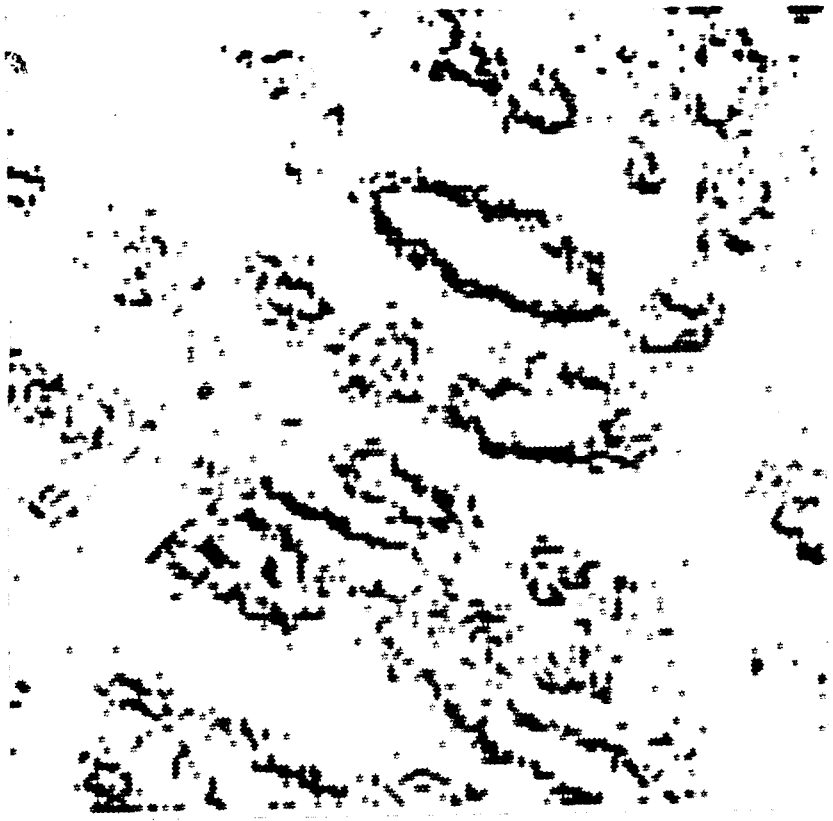

STRATOCUMULUS STREETS. STRAIGHT FR 63

GRADIENT OVER 6 UPPER .875

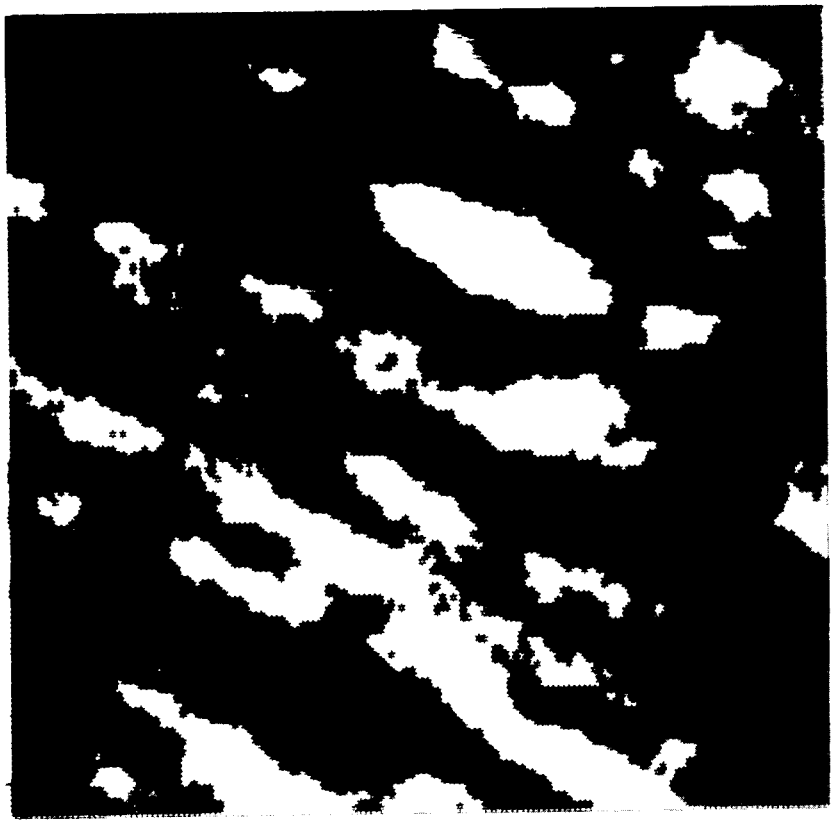

STRATOCUMULUS STREETS. STRAIGHT FR 63

CLIPPED AT 19 GRADIENT IN UPPER .875

Fig. 10 (Continued)

Frame:		63
Gradient:	over	.875
Clipped:	at	19

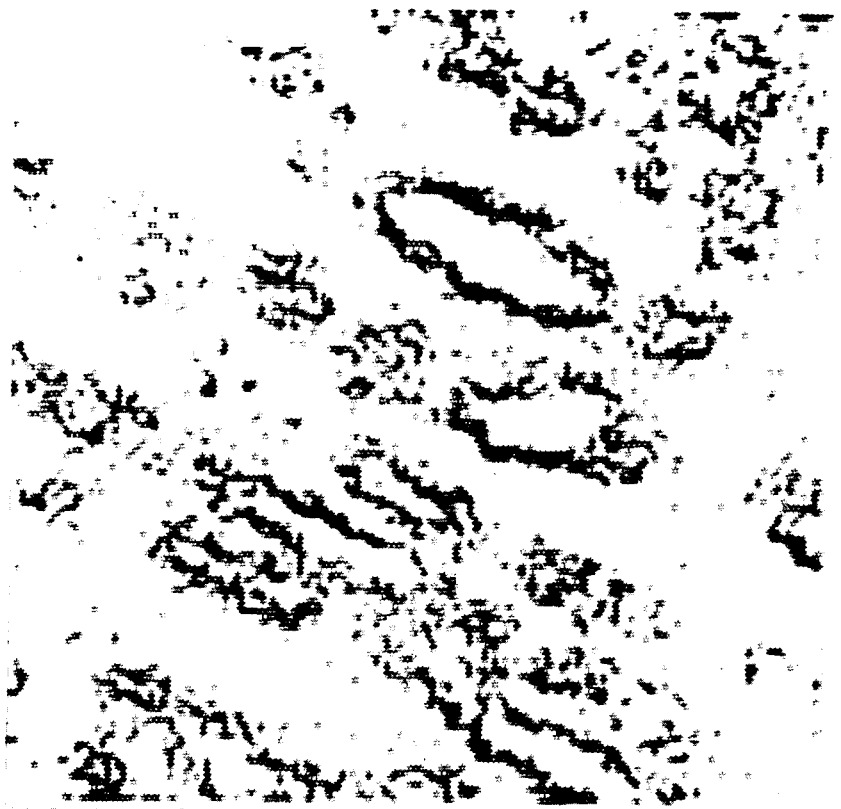

STRATOCUMULUS STREETS, STRAIGHT FR 63

GRADIENT OVER 5 UPPER .750

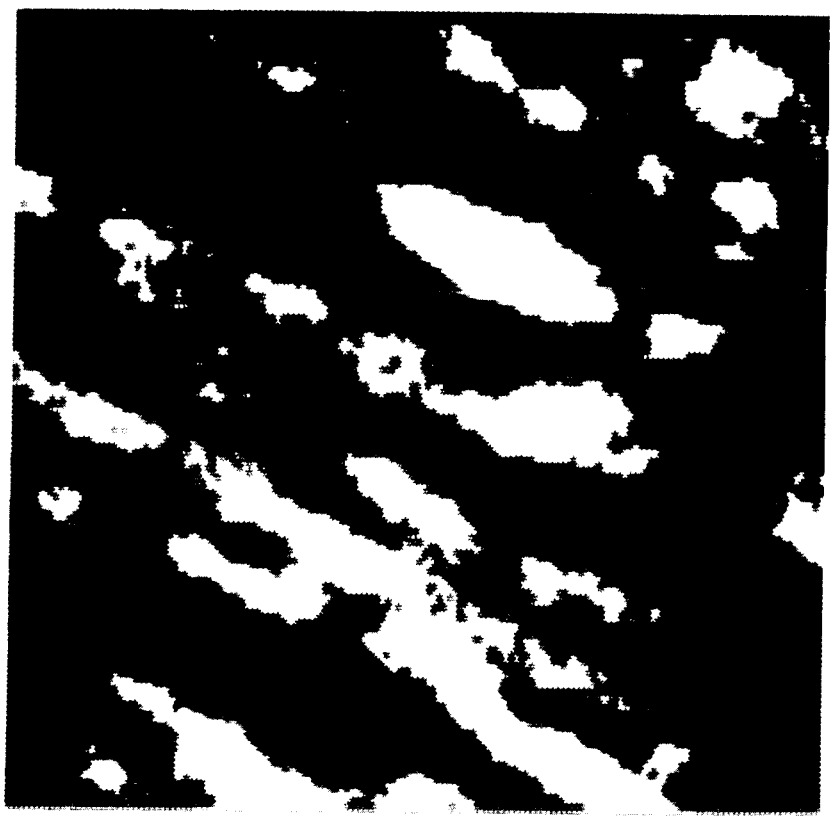

STRATOCUMULUS STREETS, STRAIGHT FR 63

CLIPPED AT 19 GRADIENT IN UPPER .750

Fig. 10 (Continued)

Frame:	63
Gradient:	over .750
Clipped:	at 19

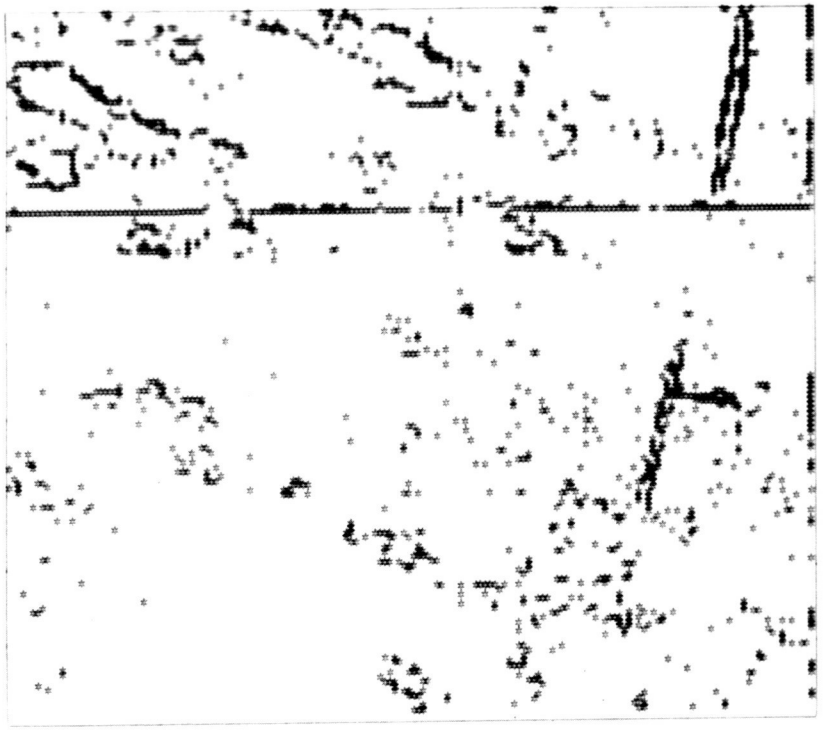

STRATOCUMULUS STREETS, STRAIGHT FR 64

GRADIENT OVER 8 UPPER .937

STRATOCUMULUS STREETS, STRAIGHT FR 64

CLIPPED AT 21 GRADIENT IN UPPER .937

Fig. 10 (Continued)

Frame:		64
Gradient:	over	.937
Clipped:	at	21

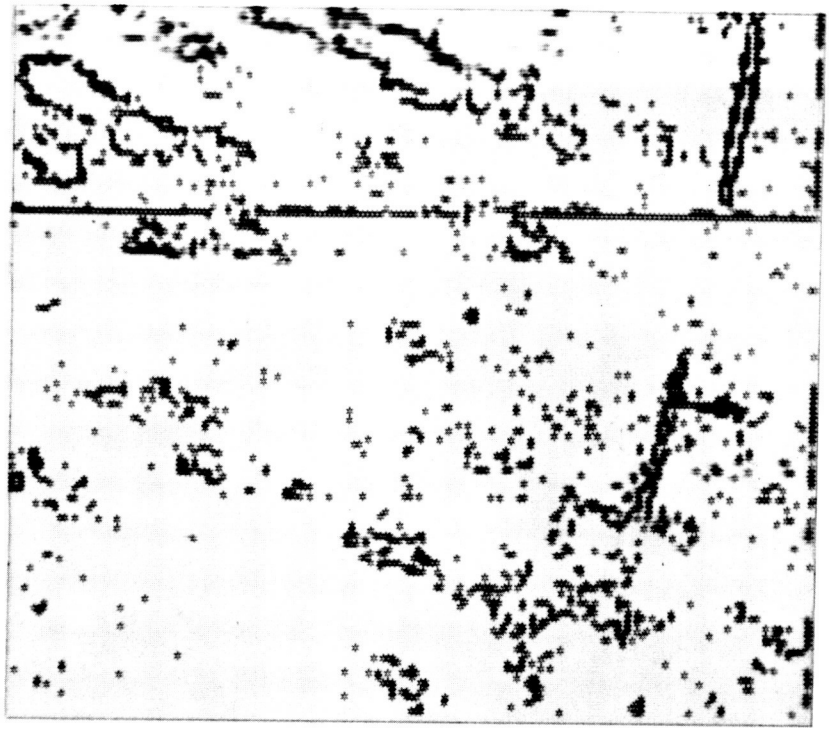

STRATOCUMULUS STREETS, STRAIGHT FR 64

GRADIENT OVER 7 UPPER .875

STRATOCUMULUS STREETS, STRAIGHT FR 64

CLIPPED AT 20 GRADIENT IN UPPER .875

Fig. 10 (Continued)

Frame:		64
Gradient:	over	.875
Clipped:	at	20

STRATOCUMULUS STREETS, STRAIGHT FR 64

GRADIENT OVER 5 UPPER .750

STRATOCUMULUS STREETS, STRAIGHT FR 64

CLIPPED AT 19 GRADIENT IN UPPER .750

Fig. 10 (Continued)

Frame:	64
Gradient:	over .750
Clipped:	at 19

02CUCL

Tens	Units 0	1	2	3	4	5	6	7	8	9
0	0	0	0	0	0	2	9	39	90	110
1	112	94	74	57	47	42	35	30	25	22
2	19	19	19	17	18	16	16	16	15	14
3	12	27								

Tens	Units 0	1	2	3	4	5	6	7	8	9
0	0	0	0	0	0	2	11	50	140	251
1	363	457	532	589	636	678	714	744	769	791
2	810	828	847	864	882	898	914	930	945	959
3	972	998								

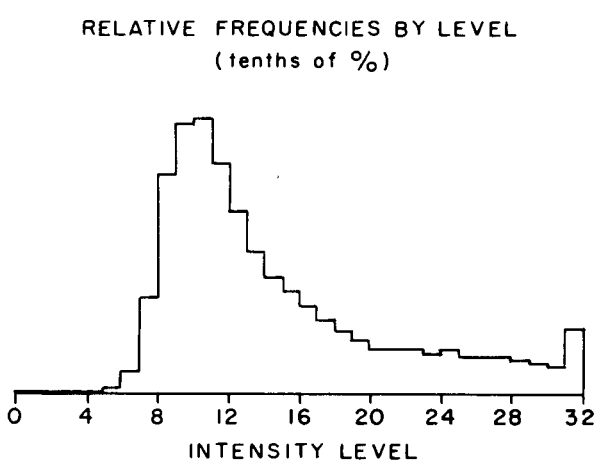

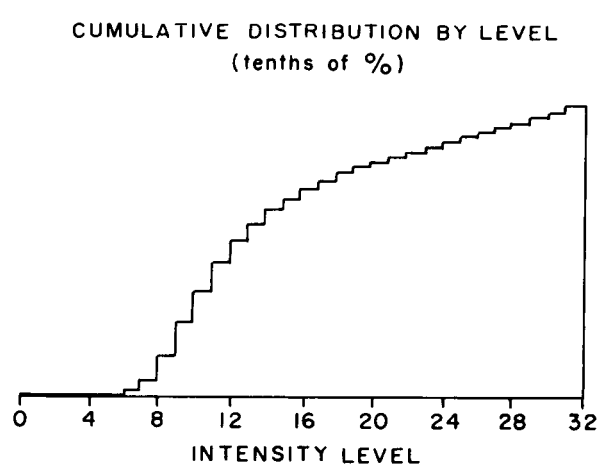

Fig. 11 Intensity distribution from SC 4020 display for frame 02

The figures are meant to be illustrative only, and the reader is reminded that the approach that yielded the pictures is an exploratory one only. Arguments as to the p that best fits the original image (our personal choice is p = upper 1/8) cannot be pursued too far. One should remember that the real cloud scene is neither fully nor accurately portrayed by television images. Clouds (as well as noncloud areas) with dimensions smaller than the resolution limit of the system automatically "disappear" completely or become incorporated with the background scene to produce something that is either difficult or impossible to interpret, let alone detect.

VI. CONCLUDING REMARKS

In this report, we have put forth some ideas and discussed some techniques for the data reduction of satellite-generated cloud photography, using both general-purpose digital computer programming and analog devices. In doing so, we believe we have made a real contribution towards the eventual solution of some of the difficult identification, recognition and classification problems in meteorological satellite research and also the data storage and retrieval aspects of the data-handling problem. We have shown that without specially constructed computers, data reduction time can be drastically cut. We have shown that a meaningful parameter can be derived automatically that will describe the degree and direction of alignment of striated clouds. The promising results from our attack on the problem of automatically assessing the amount of cloud cover from satellite photography portends well. Other techniques for possible feature extraction from cloud patterns have been suggested here, and these may prove useful for further research in pattern recognition.

It is not necessary for automatic systems to match fully the capabilities of the meteorological analyst or interpreter at all levels of sophistication. Done automatically, the economical and reliable performance of a limited number of selected tasks should allow a substantial reduction in the mass of the pictorial data that must be collected and processed in space, transmitted over limited bandwidths to the ground, further processed by humans on the ground, and retransmitted to users along further narrowed communication channels. In particular, the development of recognition techniques by analog and digital means not only promises to write "finis" to much of the drudgery (and many of the errors) of present-day visual determinations, but it may also lead to new and more objective and quantitative standards for describing and classifying cloud images from photography in relation to their meteorological significance.

Looking ahead a number of years, it appears possible that methods can be developed and devices built that will automatically heighten distinctive photographic features of clouds and their patterns, and limit the bulk of photography that must now be analyzed and interpreted by reducing the amount of information that is both redundant and of no potential meteorological value. Specific patterns and features will also be extracted and identified, thus providing invaluable interpretation aids to the meteorologist.

Appendix

SOME DATA HANDLING SCHEMES AND ROUTINES USEFUL FOR PICTURE PROCESSING

Because several groups seem to be working with digital picture processing on IBM 7090 series machines, it seems worthwhile to describe storage schemes and routines that have been found fast, efficient and reasonably flexible.

These schemes and routines are based on careful adaptation to particular characteristics of the computer. Though this approach runs counter to modern abstract fashions, it is the only way to achieve acceptable speed now.

PICTURE DATA HANDLING

Data Storage

The amount of core storage available is one of the most immediately obvious constraints to be considered. (The idea of keeping the whole image on tape, with only a portion of it in fast storage at any instant, was not pursued.) For some purposes it is convenient to have two different versions of the image available at once. Therefore, in a 32 k machine the practical limit is about 10,000 36-bit words for one digital representation of the picture.

Since cloud images can be (and practically often are) represented on a fairly limited intensity scale, one 36-bit word will store several picture-intensity measurements. The obvious choice for the IBM machines is six, since the very useful convert instructions handle data in 6-bit bites. This choice permits processing of images containing some 60,000 resolvable elements or the equivalent of a 300 by 200 element picture (almost as many elements as are exhibited on an average TV screen).

However, for most purposes a 5-bit range is preferable to 6 because some operations require that data be summed, the extra bit at the left of each character being needed to accommodate overflows. Raw data can be 6-bits per character, but will ordinarily be rescaled to the intensity range $0 \leq x \leq 31$ before further processing.

Since the picture is a rectangular array of intensity measurements, whereas machine storage is a linear string, an arrangement is needed to relate picture coordinates to storage locations. Pictures come in various proportions and sizes. To allow data always to be stored compactly and efficiently, it was decided not to store the picture in an arbitrary rectangular array of fixed dimensions. The picture is always stored as a one-dimensional array, with its upper left-hand corner at a location P(1) near the upper limit of storage (in FORTRAN common). Successive lines of the picture, traced from left to right and top to bottom, as in a TV scan, are stored in successively lower storage positions. Two variables, NW and NR, describe the current picture dimensions and are kept in the common region for the use of all routines. NR is the number of rows (horizontal lines) in the picture. NW is the number of words, each containing six data items, that make up a row. Thus, the data fill the array solidly, and the parameters describe its proportions.

Data Card Format

As long as digitalized pictures are stored on magnetic tape, input and output are straightforward; in fact, using our arrangement, a picture could be represented on tape by a parameter record, giving its dimensions and identification, and one long record for the picture itself. This arrangement would make input very fast and simple.

Unfortunately, conditions did not favor the use of tape, so another scheme using cards has provided the main input, output, and storage media. This scheme involves reading and punching special, column binary, data cards. The reason for a special card format is obvious. The data to be saved are 6-bit items. An absolute column binary card has space available for 22 words of 36 bits each and will therefore hold 132 data items. The 300 by 200 picture mentioned earlier would fit onto some 450 cards. If one has several dozen pictures, the resulting pile of cards will be large; however, the convenience of being able to load exactly those pictures to be processed on a given run compensates somewhat for the bulk. The arrangement of data on these cards is described in terms of 36-bit words with bits numbered from 0 to 35.

Word 1 contains data needed by the loading routine.

Bits 0 to 5: number of words of data on this card

Bits 6 to 11: column binary indicator bits (05)

Bits 12 to 23: x-coordinate of first data word

Bits 24 to 35: y-coordinate of first data word

Word 2 contains a logical 36-bit check sum.

Words 3 through 24 may contain 6 data items each, representing the picture intensities as integers in the range (0,63). The remaining space (columns 73 through 78) contains hollerith identification for the picture.

The x and y coordinates mentioned above are the coordinates of word locations with x increasing from left to right and y from top to bottom of the picture. The picture is built of "bricks" (words) 1 data item high by 6 long. Each data card contains a string of words that runs to the right across the picture, starting at the word whose coordinates are (x,y). The program (PATIN) that reads these special data cards puts the data from each card into the picture at the location specified by the x,y on that card; therefore, cards need not be kept in order. Figure 12 illustrates the arrangement. The upper leftmost word of the picture has word coordinates NXA, NYA and is stored in P(1).

Pattern Input from Special Data Cards -- PATIN

To read in a pattern, stored in a deck of the special column binary data cards described in the previous section, set the parameters NXA, NYA and NW (ordinarily by reading a hollerith data card) and then CALL PATIN. The routine, PATIN, expects to find the values of NXA, NYA, NW at fixed locations in FORTRAN common. It reads the system's peripheral input tape in the binary mode, storing the contents of each card in its marked place in the picture-storage array. If NX, NY are the word coordinates on a data card, the contents of the card are stored in LOC = P - (NX - NXA) - NW (NY - NYA), LOC - 1, LOC - 2 and so on. PATIN continues reading until it encounters either a special column binary card with a zero word count or a hollerith card.

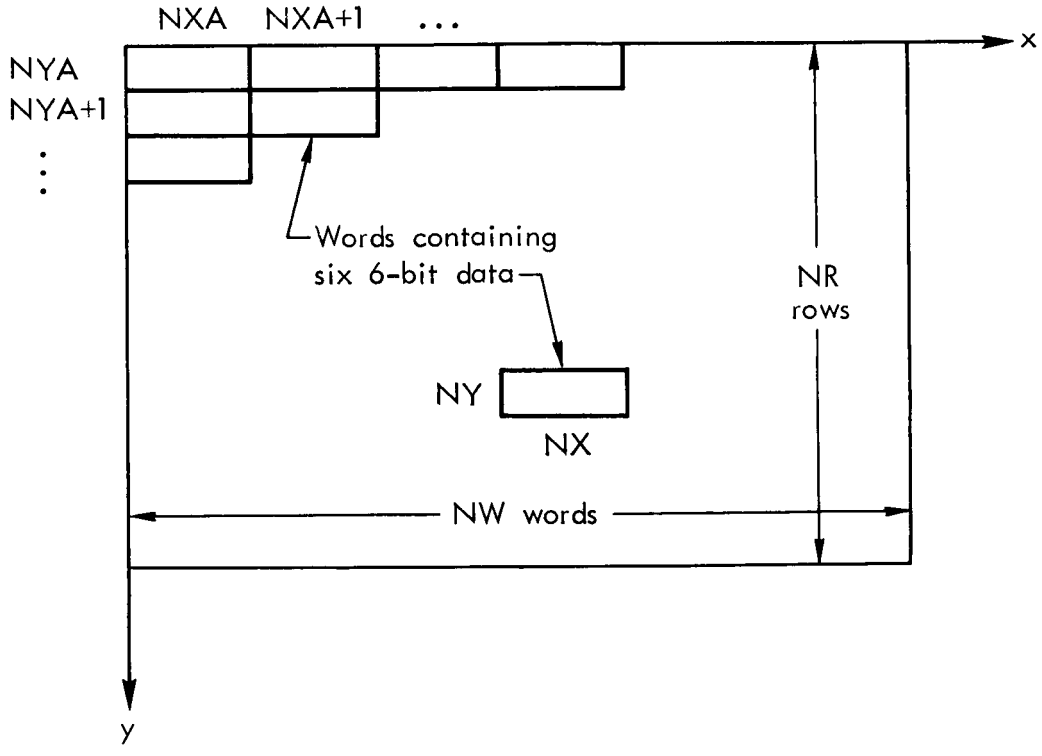

Fig. 12 Picture layout

Although PATIN gives its own data selects and channel instructions, it makes use of the standard FORTRAN library routine (IOS) and is properly integrated with normal FORTRAN tape reading except for one SCHA instruction (which can lead to trouble only if SYSPIT is on channel B and a bad tape record is encountered). PATIN overlaps checking and data storage with tape moving so that only the latter determines time comsumption.

Since there is no restriction on pattern size, some protection is necessary so that picture data will not be read in over the program. PATIN takes care of this by checking the data addresses against the upper limit of program storage; it expects the system to have space for this check remaining in the decrement of location 99.

Pattern Output onto Special Data Cards -- SPEBN

After an image has been read and modified, it may be desirable to repunch all or part of it onto new data cards in the special binary format. This is handled by combination of obvious FORTRAN programming and a FAP-coded subroutine, SPEBN. If the statement CALL SPEBN (LOC, NUM, NX, NY) is used, the NUM words stored at LOC, LOC - 1, LOC - 2,..., LOC - NUM + 1 are punched onto a special column binary data card with the picture location NX, NY of the leftmost word included. The NUM words must all be on the same line to the right of the first word. Appropriate binary records are written by SPEBN on the system's output tape; the systems's off-line peripheral program is expected to turn these into cards.

PICTURE MODIFICATIONS

Rescaling Intensities

To get from possible 6-bit raw data to 5-bit data, the picture intensities must be rescaled to the range (0,31). To retain a scale with more value than a mere halving might give, an arrangement based on the actual distribution of picture intensities has been adopted. Roughly speaking, the range of intensities, in each case, that contains most of the data can be linearly transformed to the range (0,31). The

process is naturally divided into two stages, getting the distribution and doing the scaling.

To determine the distribution, write CALL DISTR(ND), where ND is the name of an array of dimension 64 (intensities). The routine, DISTR, sets ND(I) = 16384 times (probability that intensity is I-1), where I runs from 1 to 64. It incidentally also sets up two conversion tables used for printing crude representations of the picture in type symbols; these tables are automatically adjusted to divide the distribution into two and four approximately equal parts.

In order to do the scaling, two significance parameters, NCLB and NCLT, must first be set. NCLB = 16384 times the fraction of low intensities to be forced to zero. NCLT = 16384 - 16384 times the fraction of high intensities to be forced to 31. Writing CALL SCA31, then, has an effect that is most easily appreciated by examining Fig. 13. If a picture is fogged, for example, there may be a long, insignificant region at the high-intensity end that might as well all be set to 31, while at the low end the fog level might as well be reset to zero. Of course, the facility need not be used; if the two fractions mentioned are taken to be zero, then the data will simply be divided by 2 when the routine SCA31 is called.

Both DISTR and SCA31 make (very simple) use of the convert instructions to save time. DISTR must be called before SCA31. Each of these routines uses about 80 words and a 64-word table.

Picture Smoothing

When CALL FILTR is written, the entire picture is replaced by a new picture, each point of which is an average of four points of the old picture. The impulse response of FILTR is

$$\frac{1}{4}\begin{vmatrix} 1 & 1 \\ 1 & 1 \end{vmatrix} .$$

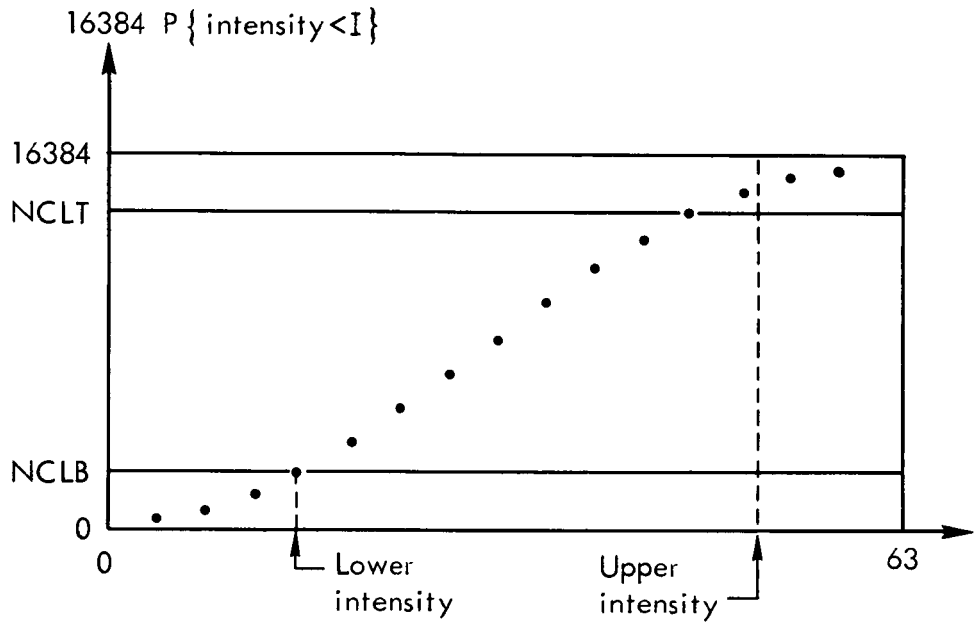

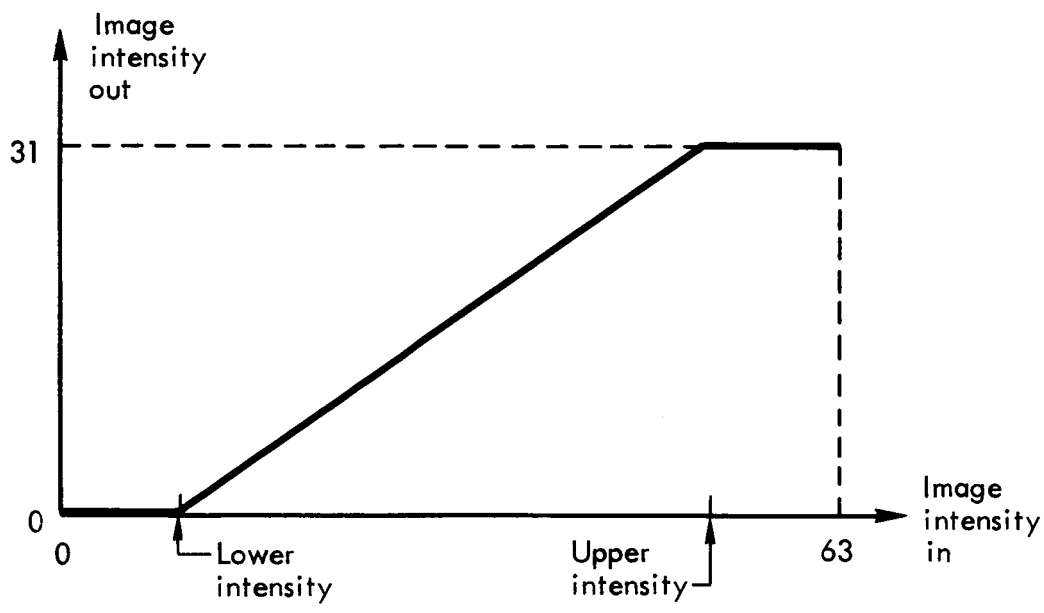

Fig. 13 Input-data distribution (upper)
the data transformation (lower)

To obtain greater smoothing this routine is simply called as often as desired. The first two iterations give the impulse responses

$$\frac{1}{16}\begin{vmatrix} 1 & 2 & 1 \\ 2 & 4 & 2 \\ 1 & 2 & 1 \end{vmatrix}$$

and

$$\frac{1}{64}\begin{vmatrix} 1 & 3 & 3 & 1 \\ 3 & 9 & 9 & 3 \\ 3 & 9 & 9 & 3 \\ 1 & 3 & 3 & 1 \end{vmatrix} .$$

Data to be operated on must lie in the range (0,31); thus SCA31 must be used before filtering if data have intensities over 31. FILTR handles data 6 at a time, with the 6th place in each bite, or character, providing room for overflow.

FILTR occupies about 60 words of storage.

REFERENCES

1. Unger, S. H., "Pattern Detection and Recognition," Proc. IRE, Vol. 47, No. 10, October 1959, pp. 1737-1752.

2. Bomba, J. S., "Alpha-Numeric Character Recognition Using Local Operations," Proc. Eastern Joint Computer Conference, Boston, Massachusetts, December 1959, pp. 218-224.

3. Elias, P., D. S. Grey, and D. Z. Robinson, "Fourier Treatment of Optical Processes," J. Opt. Soc. Amer., Vol. 42, No. 2, February 1952, pp. 127-134.

4. Horwitz, L. P., and G. L. Shelton, Jr., "Pattern Recognition Using Autocorrelation," Proc. IRE, Vol. 49, No. 1, January 1961, pp. 175-185.

5. Doyle, W., "Operations Useful for Similarity-Invariant Pattern Recognition," J. Assoc. Comput. Machinery, Vol. 9, No. 2, April 1962, pp. 259-267.

6. Kovásznay, L. S. G., and A. Arman, "Optical Autocorrelation Measurements of Two-Dimensional Random Patterns," Rev. Sci. Instruments, Vol. 28, No. 10, October 1957, pp. 793-797.

7. Blum H., An Associative Machine for Dealing With the Visual Field and Some of Its Biological Implications, Report 62-62, Air Force Cambridge Research Laboratories, Bedford, Massachusetts, February 1962.

8. Leese, J. A., and E. S. Epstein, "Application of Two-Dimensional Spectral Analysis to the Quantification of Satellite Cloud Photographs," J. Appl. Meteor., Vol. 2, No. 5, October 1963, pp. 629-644.

9. Cramér, H., Mathematical Methods of Statistics, Princeton University Press, Princeton, New Jersey, 1946.

10. Arking, A., "Latitudinal Distribution of Cloud Cover from Tiros III Photographs," Science, Vol. 143, No. 3606, February 7, 1964, pp. 569-572.